

# Summary of Professional Accomplishments

Dr Kamil Korzekwa

July 21, 2022

## Contents

<b>1</b>	<b>Name and surname</b>	<b>2</b>
<b>2</b>	<b>Diplomas and degrees</b>	<b>2</b>
<b>3</b>	<b>Previous employment in scientific institutions</b>	<b>2</b>
<b>4</b>	<b>Description of the achievements</b>	<b>2</b>
4.1	Formal statement of the achievements	2
4.2	Overview of the series <i>Optimizing quantum information processing under constraints</i>	4
4.2.1	Introduction	4
4.2.2	Motivation and scientific goals	5
4.2.3	Summary of results	8
4.3	Results on thermodynamic constraints	10
4.3.1	Optimal processing beyond the thermodynamic limit	10
4.3.2	Thermodynamic consequences of the superposition principle	18
4.4	Results on memory constraints	21
4.4.1	Optimal thermodynamic processing without memory	21
4.4.2	Quantum advantage for memoryless processes	27
4.5	Results on symmetry constraints	30
4.5.1	Optimal processes under time-translation and rotational symmetries	30
4.5.2	Optimal encoding of information into asymmetry	35
4.6	Results on classicality constraints	37
4.6.1	Minimising irreversibility of a random process	37
4.6.2	Structural differences between classical and quantum randomness	42
<b>5</b>	<b>Presentation of significant scientific activity</b>	<b>47</b>
5.1	Scientific activity at academic institutions	47
5.2	Scientific papers not included in the habilitation series	47
5.3	Local and international collaborations	48
5.4	Talks at conferences and seminars	50
5.5	Bibliometric data	52
<b>6</b>	<b>Teaching, organizational and ‘popularization of science’ achievements</b>	<b>53</b>
6.1	Teaching achievements	53
6.2	Organisational achievements	54
6.3	Popularisation of science achievements	54
<b>7</b>	<b>Other scientific achievements</b>	<b>55</b>
7.1	Awards and scholarships	55
7.2	Distinguished papers	55

# 1 Name and surname

Kamil Korzekwa

## 2 Diplomas and degrees

- **PhD in Physics** – December, 2016  
University: Imperial College London, UK  
Supervisors: Dr David Jennings, Prof. Terry Rudolph  
PhD Thesis: *Quantum coherence, thermodynamics and uncertainty relations*
- **MRes in Physics** – September, 2013  
University: Imperial College London, UK  
Supervisors: Dr David Jennings, Prof. Terry Rudolph  
MRes Thesis: *Resource Theory of Asymmetry*
- **MSc in Physics (specialisation: Nanoengineering)** – July, 2012  
University: Wrocław University of Science and Technology, Poland  
Supervisor: Prof. Paweł Machnikowski  
MSc Thesis: *Magneto-optical Kerr effect and resonant spin amplification*
- **BSc in Physics** – July, 2010  
University: Wrocław University of Science and Technology, Poland  
Supervisor: Prof. Paweł Machnikowski

## 3 Previous employment in scientific institutions

- **Junior Group Leader (Adiunkt)** – October, 2019 - present  
Quantum Resources Group  
Faculty of Physics, Astronomy and Applied Computer Science  
Jagiellonian University, Poland
- **Postdoctoral Research Fellow (Adiunkt)** – June, 2019 - December, 2019  
New Quantum Resources Group  
International Centre for the Theory of Quantum Technologies  
University of Gdańsk, Poland
- **Postdoctoral Research Fellow** – January, 2017 - May, 2019  
Quantum Science Group  
School of Physics  
University of Sydney, Australia

## 4 Description of the achievements

### 4.1 Formal statement of the achievements

Achievements, set out in art. 219 para 1 point 2 of the Higher Education and Science Act dated 20 July 2018, are given by a single-themed series of publications entitled:

*Optimizing quantum information processing under constraints.*

The series consists of the following 15 publications:

1. [H15] *Optimizing thermalizations*  
Kamil Korzekwa, Matteo Lostaglio  
*Phys. Rev. Lett.* **129**, 040602 (2022) [arXiv:2202.12616]  
Pages: 6+3, Points awarded by Ministry of Science and Education: 200, Impact factor: 8.385

2. [H14] *Continuous thermomajorization and a complete set of laws for Markovian thermal processes*  
Matteo Lostaglio, Kamil Korzekwa  
[Phys. Rev. A \*\*106\*\*, 012426 \(2022\) \[arXiv:2111.12130\]](#)  
Pages: 18, Points awarded by Ministry of Science and Education: 100, Impact factor: 2.777
3. [H13] *Encoding classical information into quantum resources*  
Kamil Korzekwa, Zbigniew Puchała, Marco Tomamichel, Karol Życzkowski  
[IEEE Trans. Inf. Theory \*\*68\*\*, 4518 \(2022\) \[arXiv:1911.12373\]](#)  
Pages: 13, Points awarded by Ministry of Science and Education: 200, Impact factor: 2.501
4. [H12] *Fluctuation-dissipation relations for thermodynamic distillation processes*  
Tanmoy Biswas, A. de Oliveira Junior, Michał Horodecki, Kamil Korzekwa  
[Phys. Rev. E \*\*105\*\*, 054127 \(2022\) \[arXiv:2105.11759\]](#)  
Pages: 30, Points awarded by Ministry of Science and Education: 140, Impact factor: 2.296
5. [H11] *Algebraic and geometric structures inside the Birkhoff polytope*  
Grzegorz Rajchel-Mieldzióć, Kamil Korzekwa, Zbigniew Puchała, Karol Życzkowski  
[J. Math. Phys. \*\*63\*\*, 012202 \(2022\) \[arXiv:2101.11288\]](#)  
Pages: 18, Points awarded by Ministry of Science and Education: 70, Impact factor: 1.488
6. [H10] *Dephasing superchannels*  
Zbigniew Puchała, Kamil Korzekwa, Roberto Salazar, Paweł Horodecki, Karol Życzkowski  
[Phys. Rev. A \*\*104\*\*, 052611 \(2021\) \[arXiv:2107.06585\]](#)  
Pages: 12, Points awarded by Ministry of Science and Education: 100, Impact factor: 2.777
7. [H9] *Quantum advantage in simulating stochastic processes*  
Kamil Korzekwa, Matteo Lostaglio  
[Phys. Rev. X \*\*11\*\*, 021019 \(2021\) \[arXiv:2005.02403\]](#)  
Pages: 20, Points awarded by Ministry of Science and Education: 200, Impact factor: 12.577
8. [H8] *Robustness of Noether's principle: Maximal disconnects between conservation laws and symmetries in quantum theory*  
Cristina Cirstoiu, Kamil Korzekwa, David Jennings  
[Phys. Rev. X \*\*10\*\*, 041035 \(2020\) \[arXiv:1908.04254\]](#)  
Pages: 41, Points awarded by Ministry of Science and Education: 200, Impact factor: 12.577
9. [H7] *Distinguishing classically indistinguishable states and channels*  
Kamil Korzekwa, Stanisław Czachórski, Zbigniew Puchała, Karol Życzkowski  
[J. Phys. A: Math. Theor. \*\*52\*\*, 475303 \(2019\) \[arXiv:1812.09083\]](#)  
Pages: 43, Points awarded by Ministry of Science and Education: 70, Impact factor: 2.110
10. [H6] *Avoiding irreversibility: engineering resonant conversions of quantum resources*  
Kamil Korzekwa, Christopher T. Chubb, Marco Tomamichel  
[Phys. Rev. Lett. \*\*122\*\*, 110403 \(2019\) \[arXiv:1810.02366\]](#)  
Pages: 6+1, Points awarded by Ministry of Science and Education: 200, Impact factor: 8.385
11. [H5] *Moderate deviation analysis of majorisation-based resource interconversion*  
Christopher T. Chubb, Marco Tomamichel, Kamil Korzekwa  
[Phys. Rev. A \*\*99\*\*, 032332 \(2019\) \[arXiv:1809.07778\]](#)  
Pages: 14, Points awarded by Ministry of Science and Education: 100, Impact factor: 2.777
12. [H4] *Beyond the thermodynamic limit: finite-size corrections to state interconversion rates*  
Christopher T. Chubb, Marco Tomamichel, Kamil Korzekwa  
[Quantum \*\*2\*\*, 108 \(2018\) \[arXiv:1711.01193\]](#)  
Pages: 32, Points awarded by Ministry of Science and Education: 140, Impact factor: 5.381
13. [H3] *Coherifying quantum channels*  
Kamil Korzekwa, Stanisław Czachórski, Zbigniew Puchała, Karol Życzkowski

New J. Phys. **20**, 043028 (2018) [arXiv:1710.04228]

Pages: 27, Points awarded by Ministry of Science and Education: 140, Impact factor: 3.539

14. [H2] *Markovian evolution of quantum coherence under symmetric dynamics*

Matteo Lostaglio, Kamil Korzekwa, Antony Milne

Phys. Rev. A **96**, 032109 (2017) [arXiv:1703.01826]

Pages: 20, Points awarded by Ministry of Science and Education: 100, Impact factor: 2.777

15. [H1] *Structure of the thermodynamic arrow of time in classical and quantum theories*

Kamil Korzekwa

Phys. Rev. A **95**, 052318 (2017) [arXiv:1609.05910]

Pages: 13, Points awarded by Ministry of Science and Education: 100, Impact factor: 2.777

The other major scientific achievement lies in forming and leading the research of Quantum Resources Group, established at the Jagiellonian University in January 2020 and consisting of the group leader, three post-doctoral researchers and one PhD student. During the first 2.5 years of its operation, the members of the group have published 16 papers in peer-reviewed journals (plus 3 arXiv pre-prints currently undergoing review), and gave 22 oral and 9 poster presentations at conferences and seminars. The full details of the group's work can be found at the official website [quantum-resources.com](http://quantum-resources.com).

## 4.2 Overview of the series *Optimizing quantum information processing under constraints*

### 4.2.1 Introduction

The role of physics is to describe our reality by telling us which things can and which cannot happen. In a sense, we can think of the laws of physics as constraining the infinite set of potentialities to the one true reality. For example, the law of gravity constrains possible movements of objects: if you drop a ball on Earth, it will fall down and not fly away to the Moon. By discovering and studying fundamental constraints, such as the law of energy conservation (energy cannot be created from nothing) or the ultimate speed limit (nothing can travel faster than light), we gain a better understanding of the world, allowing us to predict the future and infer the past based on the present.

But in order to improve this understanding, the investigated constraints need not to be *a priori* fundamental, and may as well arise from practical reasons. A prime example is given by the 19th century efforts on understanding the optimal design of heat engines, where the aim was to construct the most efficient machine performing mechanical work under the constraint that its sole source of energy is heat. Despite no apparent universality, the answer to this question nevertheless provided us with a hint on the nature of reality in the form of the second law of thermodynamics, so fundamental that Eddington once said [1]

*“If someone points out to you that your pet theory of the universe is in disagreement with Maxwell’s equations — then so much the worse for Maxwell’s equations. If it is found to be contradicted by observation — well, these experimentalists do bungle things sometimes. But if your theory is found to be against the second law of thermodynamics I can give you no hope; there is nothing for it but to collapse in deepest humiliation.”*

It is important to note that the first rigorous statements of the second law, due to Clausius in 1850 and Kelvin in 1851, were also explicitly expressed as constraints on possible physical processes [2]. The first one wrote:

*“There exists no thermodynamic transformation whose sole effect is to extract a quantity of heat from a colder reservoir and to deliver it to a hotter reservoir.”*,

while the second one said

*“There exists no thermodynamic transformation whose sole effect is to extract a quantity of heat from a given heat reservoir and to convert it entirely to work.”*

Much more recently, at the end of 20th century, investigating communication scenarios with constrained control allowed physicists to shed light on one of the most mysterious aspects of physics – the phenomenon of quantum entanglement [3]. Until then, this stronger than classical correlation between separated parties that haunted Einstein (he famously called it “spooky action at a distance”) could only be investigated qualitatively, because the standard formalism of quantum mechanics did not provide physicists with a recipe to quantify entanglement. To remedy this, the authors of the ground-breaking Ref. [4] decided to study how two parties can process a bipartite quantum state shared between them under the constraint of local operations and classical communication (LOCC in short). Since LOCC cannot create entanglement, this allowed them to partially order all bipartite quantum states according to how strongly entangled they are<sup>1</sup>: a state  $\psi$  that can be transformed to  $\phi$  by LOCC must be more entangled than  $\phi$ . This led to the introduction of quantitative measures of entanglement and transformed the once abstract concept into an almost tangible object, e.g. physicists could now investigate how much entanglement (measured in ebits) is present in a given state, or how much of it is needed to perform a given task like quantum teleportation [6, 7].

Investigating such constrained scenarios proved to be very fruitful not only for understanding entanglement, but also for the whole new emerging field of physics called quantum information science. It has long been understood that information and physics are subtly intertwined: starting with a concept of the Maxwell’s demon (that used information to reduce entropy [8]), through the thought experiments with the Szilard’s engine (that converted information into mechanical work [9]), all the way to Landauer’s principle (which yields a lower limit on the amount of energy needed to erase a bit of information [10]). The picture became even more complicated when scientists started considering physical systems that are carriers of information to obey the laws of quantum mechanics. The basic building blocks of information – bits that could take a value either 0 or 1 – had to be replaced by qubits that could be in any superposition of 0 and 1 (plus different qubits could also be entangled with one another). At the same time, the development of novel quantum cryptographic protocols (like BB84 [11] and E91 [12]) and algorithms (like Shor’s factoring algorithm [13] and Grover’s search algorithm [14]) strongly suggested that this new quantum way of processing information may lead to significant advantages over classical information processing. Thus, a new theoretical framework was needed that would allow one to quantitatively investigate potential benefits coming from the quantumness of nature.

#### 4.2.2 Motivation and scientific goals

For over a decade now, scientists around the world have been developing such a framework under the name of quantum resource theories [15, 16]. The works in the series *Optimizing quantum information processing under constraints* significantly contribute to these efforts and share the same motivation, i.e.,

- To understand which ingredients (e.g., coherence, entanglement, etc.) in a particular information processing setting (e.g., communication between spatially separated parties, limited access to energy, etc.) form “quantum resources” that allow one to beat the limits set by classical physics.
- To characterize allowed resource transformations in different regimes and to identify how to optimally exploit them.
- To find optimal ways to implement protocols exhibiting quantum advantage, while taking into account realistic constraints.

More generally, the aim of the series is to broaden our understanding of nature by analysing constrained information processing scenarios, with the constraints arising due to both fundamental reasons (like the second law of thermodynamics) and more practical ones (like the limited access to memory).

The above aims are pursued in the series on four overlapping fronts characterised by the type of investigated constraint (see Fig. 1):

1. **Thermodynamic constraints.** In this setting, one investigates how the state of a quantum system can be processed, when the system is only allowed to interact with a heat bath at thermal equilibrium with some fixed temperature  $T$  [17, 18]. The total energy conservation and the thermality of the bath then constrain the possible final states of the system given its initial state. Any sources of ordered

---

<sup>1</sup>The exact details of this partial order were only later derived by Nielsen [5].

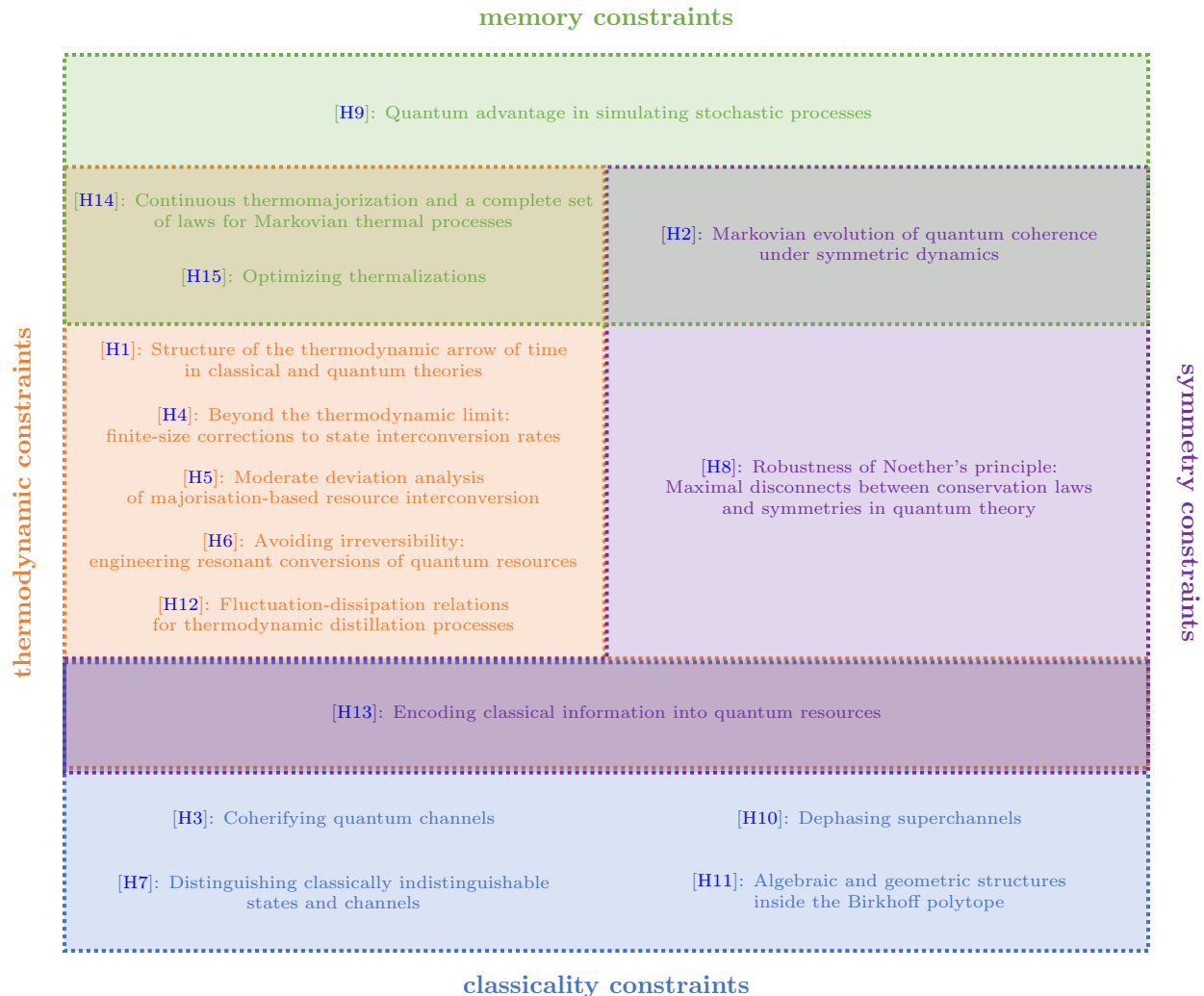


Figure 1: **Map of the series.** The series *Optimizing quantum information processing under constraints* focuses on four different kind of constraints: thermodynamic, memory, symmetry and classicality. The above graph represents which of the works in the series addressed which constraints.

energy or sinks of entropy can be also modelled, but must be explicitly introduced in the form of ancillary quantum systems (e.g. a battery system that acts as a source of work). This way, general thermodynamic processing can be investigated, while rigorously book keeping all the resources used. My main scientific goals related to quantum information processing under thermodynamic constraints were as follows:

- (a) To understand how optimal thermodynamic processing is affected when one goes beyond the thermodynamic limit, i.e., when one considers only a small number of systems to be processed. The theory of thermodynamics is traditionally constrained to the study of macroscopic systems whose energy fluctuations are negligible compared to their average energy [2]. However, the thermodynamics of a few quantum systems (e.g., a gas of a dozen particles) does not satisfy the macroscopicity conditions, and I aimed at capturing the consequences of this.
- (b) To understand how optimal thermodynamic processing is affected by the superposition principle, i.e., when the processed quantum systems are prepared in a coherent superposition of different energy states. Macroscopic thermodynamics assumes that the phases between different energy states of the system are randomised, and so one deals with an incoherent mixture of states [2].

However, in extremely well controlled experiments, a few quantum systems can preserve their relative phases, allowing them to constructively and destructively interfere during the thermodynamic process. I aimed at describing the consequences of this for the processing of quantum information.

2. **Memory constraints.** In this setting, one investigates what kind of quantum information processing is allowed when the processed system can only interact with its environment in a memoryless (Markovian) way [19, 20], i.e., the transformation of the system at each given moment in time depends only on the present state of the system (and not on states it evolved through). On the one hand, the interaction of small quantum systems with their macroscopic environment usually leads to memoryless processes [21]. Thus, investigating such scenarios, one can describe how the environmental noise deteriorates quantum information encoded in the system or, alternatively, one can characterise allowed processing of quantum information under control limited to macroscopic systems. On the other hand, by explicitly modelling memory through the use of auxiliary systems, one can assess and quantify the role played by memory in achieving optimal quantum information processing. My main scientific goals related to memory constraints were as follows:

- (a) To understand the limitations of memoryless processes for thermodynamic tasks, i.e., to assess the role played by memory in the performance of thermodynamic protocols. Standard results on optimal thermodynamic processing of information (e.g., on the maximal conversion rate of bits of information into mechanical work) assume that the second law of thermodynamics is the only constraint [17, 22]. However, in realistic experimental setups, one's control over the system-bath interactions and system-bath correlations is limited, which can be effectively modelled by having access only to memoryless processes. I aimed at describing the consequences of this for the optimal thermodynamic processes.
- (b) To understand how memoryless processing of classical information is modified when the information carriers obey the rules of quantum mechanics. The superposition principle then enlarges the state space of the information carrying system to not only include incoherent mixtures of distinguishable states, but also their coherent superpositions. This enlarged space may potentially act as an effective internal memory of the system leading, e.g., to the existence of quantum memoryless processes that cannot be performed classically without memory. I aimed at exploring this potential of quantum advantage for the processing of classical information.

3. **Symmetry constraints.** In this setting, one investigates what kind of quantum information processing is allowed when the processes are forced to obey some symmetry (e.g., if we are constrained only to rotationally invariant processes) or are given by symmetry operations themselves (e.g., if we are allowed only to rotate the processed system). In the first case, symmetry constraints can be related to conservation laws through the Noether's theorem [23]. Thus, investigating such scenarios, one can characterise allowed processing of quantum information in the presence of conserved charges. In the second case, one can quantitatively study the asymmetry of quantum states, and how to employ it in order to securely encode information [24]. My main scientific goals related to symmetry constraints were as follows:

- (a) To understand the limitations of processing quantum information encoded in the degrees of freedom corresponding to conserved charges. Typical quantum information approach abstracts away from the physical details of the information carrier, focusing only on the fact that it can be in one of many perfectly distinguishable states. However, information is physical, i.e., it is the physical objects that carry information and this information is encoded in the physical properties of the system, such as energy or angular momentum. The existence of a conservation law for a given property then constrains the way it can be transformed (e.g., energy cannot be created from nothing and must flow to the system from its environment), and I aimed at describing how this affects quantum information processing.
- (b) To understand the optimal way of using asymmetry of quantum states for secure communication of classical information [25]. When two communicating parties share a reference frame (e.g. they agree on the directions of a Cartesian reference frame) that is kept secret from the outside world, they can securely encode information into the degrees of freedom that breaks the corresponding

symmetry (e.g., in the direction of a spin coherent state that breaks the rotational symmetry). The reasons for the security are two-fold: first, the eavesdropper lacks a reference frame (and so does not know what measurement to perform on the intercepted information carrier); and second, quantum systems get disturbed by a measurement process (and so the wrong choice of a measurement erases the information originally encoded in the system). I aimed at describing the ultimate limits of secure communication based on the amount of asymmetry at the disposal of the two communicating parties.

4. **Classicality constraints.** In this setting one investigates possible quantum information processing under the constraint that it has to perform a fixed transformation of classical information. In other words, one wants to characterise families of quantum information processes that look identical from the classical perspective, i.e., when one has no access to phase information between probability amplitudes of a quantum system, but only to probabilities of outcomes of a given observable. My main scientific goals related to quantum information processing under classicality constraints were as follows:

- (a) To understand how much the randomness of a classical process can be reduced by embedding it into a quantum process. Random processes are ubiquitous in both classical and quantum physics; however, the nature of randomness in these two regimes differs significantly. On the one hand, classical random evolution is necessarily irreversible. On the other hand, quantum evolution may be completely deterministic (and thus reversible if no measurement is performed), but nevertheless lead to random measurement outcomes of a given observable by transforming a system into a coherent superposition of eigenstates of this observable. When probing the dynamics of the system one can therefore observe the same random transitions, irrespectively of whether the evolution is coherent or incoherent. I aimed at addressing the following questions: to what extent an observed random transformation can be explained via the underlying deterministic and coherent process, and how much unavoidable classical randomness must be involved in it?
- (b) To understand how much richer the set of quantum information processes is as compared to its classical counterpart. More precisely, to characterise how many distinct (i.e. fully distinguishable) quantum processes there are that classically correspond to the same process. I aimed at finding this characterisation and employing it to identify processes that optimally preserve quantum information content of the system while performing a given classical transformation.

### 4.2.3 Summary of results

#### 1. Results on thermodynamic constraints:

- (a) I<sup>2</sup> developed a mathematical framework allowing one to push the thermodynamic description beyond macroscopic systems [H4, H12]. More precisely, I introduced the concept of free energy random variable, whose average corresponds to the value of free energy functional for the system, but which also contains information about higher moments, which can be interpreted as fluctuations of the free energy content of the system. Incorporating information about such fluctuations into the framework allowed me to investigate thermodynamic transformations between small number of systems, when fluctuations are no longer negligible compared to averages. As a result, I was able to find necessary and sufficient conditions for the existence of a thermodynamic transformation between different non-equilibrium states of a few-particle systems. The macroscopic condition of non-increasing free energy was thus refined to the following statement: in order to achieve the thermodynamic transformation with a given precision, the free energy of the system has to decrease at least by  $x$ , where  $x$  is an explicit function of the precision and the free energy fluctuations of the initial and final states.
- (b) Since I concluded that processes beyond the thermodynamic limit are generally irreversible and consume free energy (e.g., thermodynamic cycles must be supplied with additional work source), I analysed the consequences of this fact for the optimal performance of thermodynamic protocols (such as work extraction, information erasure, or thermodynamically free communication) [H4, H12].

---

<sup>2</sup>Here and later in the text, by “I” it is of course meant “I and my collaborators”.

- (c) I interpreted the obtained results as a new version of the famous fluctuation-dissipation theorem, as they link the minimal amount of free energy dissipated in the process to the amount of fluctuations present in the state of the system [H12].
- (d) An important discovery of resource resonance was made [H6] – namely, when the free energy fluctuations of the initial and final states are properly tuned, the dissipation becomes significantly reduced.
- (e) Interestingly, due to mathematical similarities between the frameworks describing thermodynamic and LOCC transformations, the phenomenon of resource resonance was also predicted and numerically verified for transformations between pure bipartite entangled states [H5].
- (f) I analysed how the result on dissipation and fluctuations of free energy is affected when one allows the initial state of the system to be prepared in superposition of different energy eigenstates [H12]. Since the entropic contribution to free energy fluctuations then decreases, using states with coherence generally allows one to decrease the dissipation of free energy.
- (g) I investigated the effect quantum coherence has on the thermodynamic ordering of states in the single-shot regime. In particular, I showed that it is responsible for providing the thermodynamic arrow of time with additional lattice structure and, as a result, that quantum coherence is a necessary resource for implementing an optimal history erasure process [H1].

## 2. Results on memory constraints:

- (a) I introduced a novel concept of continuous thermomajorisation that allowed me to investigate the possible thermodynamic processing of quantum states under memoryless dynamics [H14]. Employing this concept, I derived fundamental constraints on transforming energy population of quantum systems generated by all memoryless thermal processes, i.e., given the initial population of the system in the energy eigenbasis, I stated the necessary and sufficient conditions for the existence of a memoryless thermal process that transforms the system into a state with a given final population. This provided an exhaustive H-type theorem in terms of a continuous family of entropic functions that need to monotonically increase during the dynamics.
- (b) I developed an algorithm that in a finite number of steps allows one to construct the full cone of population vectors achievable by memoryless thermal processes from a given initial state, and I demonstrated that all such vectors can be obtained from the initial state by a universal set of elementary thermal controls given by two-level partial thermalisations [H14].
- (c) The obtained results were used to investigate optimal work extraction and cooling processes, illustrating the role that memory effects play in thermodynamic protocols [H15].
- (d) The memory constraint was also investigated from the perspective of potential quantum advantage. More precisely, I proved that quantum memoryless dynamics can simulate classical processes that necessarily require memory [H9].
- (e) By extending the notion of space-time cost of a stochastic process to the quantum domain, I proved an advantage of the quantum cost of simulating a given stochastic process over the classical cost [H9].
- (f) I demonstrated that the set of classical states accessible via Markovian master equations with quantum controls is larger than the set of those accessible with classical controls, leading, e.g., to a potential advantage in cooling protocols [H9].

## 3. Results on symmetry constraints:

- (a) I analysed how time-translation symmetry, arising from energy conservation, constrains possible transformations of coherence between different energy states [H2]. The central result that was proven was a theorem bounding the minimum amount of decoherence compatible with time-translation symmetry for a given population dynamics. This theorem can be seen as a generalization to higher-dimensional systems of the famous relation  $T_2 \leq 2T_1$  for qubit decoherence time  $T_2$  and relaxation time  $T_1$ .

- (b) I showed how the obtained minimal decoherence theorem enables one to witness and assess the role of non-Markovianity as a resource for coherence preservation and transfer [H2].
- (c) I performed the analysis of the convex structure and extremal points of the set of quantum channels symmetric under the action of a general Lie group  $G$  [H8]. This allowed me to quantify the degree to which imposing a symmetry constraint on quantum channels implies a conservation law, i.e., I derived bounds on the deviation from conservation laws under any symmetric quantum channel in terms of the deviation from closed dynamics.
- (d) For the  $SU(2)$  symmetry, related to angular momentum conservation law, I provided fundamental limits on how much a spin- $j_A$  system can be used to polarize a larger spin- $j_B$  system, and on how much one can invert spin polarization using a rotationally symmetric operation [H8].
- (e) I investigated the problem of optimal communication between two parties with the encodings restricted to symmetry operations for some symmetry group  $G$  [H13]. This setting corresponds to encoding information into asymmetry of a given quantum state with respect to  $G$ , and provides a secure communication scheme with a shared reference frame corresponding to  $G$ . I derived the optimal communication rates in the single-shot and asymptotic regimes, and discussed how they can be applied to study a variety of constrained communication scenarios, e.g., when information can be encoded only in coherences of a quantum state, or when one is constrained to local operations and wants to investigate the limits of super-dense coding.

#### 4. Results on classicality constraints:

- (a) I introduced the novel concept of quantum coherifications of a classical channel, i.e., a set of quantum channels that induce the same classical transitions, but may differ in how they process quantum coherences [H3]. I showed that the classical irreversible transition matrix  $T$  can be coherified to reversible unitary dynamics if and only if  $T$  is unistochastic. Otherwise, all coherifications must necessarily be irreversible, and in order to assess the extent to which an optimal process is indeterministic, I found explicit bounds on the entropy and purity of coherified channels.
- (b) Optimal coherifications for several classes of channels, including all one-qubit channels, were found, as well as the non-optimal coherification procedure that works for an arbitrary qudit channels [H3].
- (c) In order to quantify how many distinct quantum processes exist that are consistent with given classical transitions, a collection of results on both necessary and sufficient conditions for the existence of  $M$  perfectly distinguishable coherifications of a given classical channel was obtained [H7].
- (d) Since only the set of unistochastic matrices can be fully coherified, I also investigated the properties of this set by introducing and analysing its particular superset of bracelet matrices [H11]. Algebraic and geometric properties of this set were described, including its star-shapedness, closure under multiplication by factorisable matrices, and the behaviour of the spectra of its elements. As a result, unistochastic matrices for small dimensions were fully characterised.
- (e) Beyond the concept of coherification, the classicality constraint was also investigated by introducing and characterising a class of environmental noises called dephasing superchannels, which decrease coherent properties of quantum channels, but do not affect the classical transitions they induce [H10]. I found a general mathematical description of such superchannels, showed how they can be physically realised, and characterised the possible effects on the coherent properties of channels they act upon.

### 4.3 Results on thermodynamic constraints

#### 4.3.1 Optimal processing beyond the thermodynamic limit

**Thermodynamic setting.** In the emerging field of quantum thermodynamics (see Ref. [26] and references therein) a focus is placed on possible transformations of small quantum systems interacting with a thermal environment. The investigated system is described by a Hamiltonian  $H = \sum_i E_i |E_i\rangle\langle E_i|$  and its initial state

by a general density matrix  $\rho$ , whereas the state of the bath, described by a Hamiltonian  $H_B$ , is given by a thermal equilibrium density matrix,

$$\gamma_B = \frac{e^{-\beta H_B}}{\text{Tr}(e^{-\beta H_B})}, \quad (1)$$

where  $\beta = 1/k_B T$  is the inverse temperature with  $k_B$  denoting the Boltzmann constant. The evolution of the joint system is assumed to be closed, so that it is described by a unitary operator  $U$ , which additionally conserves the total energy,

$$[U, H \otimes \mathbb{1}_B + \mathbb{1} \otimes H_B] = 0. \quad (2)$$

The central question now is about the interconversion problem: what are the possible final states that a given initial state  $\rho$  can be transformed into? More formally, one defines the set of *thermal operations* [17, 27], which describes all possible transformations of the system that can be performed without the use of additional resources (beyond the single heat bath). The set of thermal operations for a given fixed inverse temperature  $\beta$  consists of all completely positive trace-preserving (CPTP) maps  $\{\mathcal{E}^\beta\}$  that act on a system in state  $\rho$  with Hamiltonian  $H$  as

$$\mathcal{E}^\beta(\rho) = \text{Tr}_{B'}(U(\rho \otimes \gamma_B)U^\dagger), \quad (3)$$

with  $U$  satisfying Eq. (2),  $\gamma_B$  given by Eq. (1),  $H_B$  being arbitrary, and  $B'$  denoting any subsystem of the joint system. Note that energy conservation condition, Eq. (2), can be interpreted as encoding the first law of thermodynamics; whereas the fact that the bath is in thermal equilibrium leads to  $\mathcal{E}^\beta(\gamma) = \gamma$ , with  $\gamma$  being the thermal Gibbs state of the system (i.e., given by Eq. (1) with  $H_B$  replaced by  $H$ ), thus encoding the second law.

**Thermodynamic limit and beyond.** An important variant of the interconversion problem is the asymptotic state interconversion, where one considers transforming arbitrarily many copies of the initial state and asks for the maximal conversion rate at which it is possible to transform instances of one state to another with asymptotically vanishing error. Physically, this corresponds to macroscopic systems composed of  $n \rightarrow \infty$  particles, in the so-called thermodynamic limit when energy fluctuations are much smaller than the average energy. It was found that the asymptotic conversion rate is given by the ratio of non-equilibrium free energies of the initial and target states [18], resulting in transformations being fully reversible in this regime. However, for finite  $n$  the macroscopic results do not hold any more, and transformations may become irreversible. Although the necessity to go beyond classical thermodynamics is mostly motivated by the fact that at the nanoscale quantum effects, like coherence [28–31] [KK10, KK11] and entanglement [32–34], start playing an important role, in the quantum regime one also deals with systems composed of a finite number  $n$  of particles. Hence, thermodynamic transformations of such systems are affected by the effective irreversibility and one of my goals was to rigorously address this problem. My works [H4–H6, H12] provide a bridge between the extreme case of single-shot thermodynamics with  $n = 1$  [17] and the asymptotic limit of  $n \rightarrow \infty$  [18], allowing one to study the irreversibility of thermodynamic processes in the intermediate regime of large but finite  $n$ .

**Optimal incoherent interconversion rate.** Work [H4] focuses on a system comprised of a finite number  $n$  of non-interacting subsystems (each governed by the same Hamiltonian  $H$ ) and considers a pair of initial and target subsystem states  $\rho$  and  $\sigma$  that both commute with  $H$  (i.e., energy-incoherent states). The aim is to find the maximal rate  $R$  for which there exists a thermal operation  $\mathcal{E}^\beta$  such that  $\mathcal{E}^\beta(\rho^{\otimes n}) = \tilde{\sigma}$  for some state  $\tilde{\sigma}$  on  $Rn$  subsystems that is sufficiently close to  $\sigma^{\otimes Rn}$ . In other words, the problem of optimal thermodynamic state interconversion between a finite number of instances of states  $\rho$  and  $\sigma$  is investigated for a fixed inverse temperature  $\beta$  of the background bath and allowed constant transformation error  $\epsilon$ . The error is quantified by the proximity of two quantum states measured using infidelity, i.e. it is required that  $F(\sigma^{\otimes Rn}, \tilde{\sigma}) \geq 1 - \epsilon$  for some accuracy parameter  $\epsilon \in (0, 1)$ , where  $F(\cdot, \cdot)$  denotes Uhlmann’s fidelity [35],

$$F(\rho, \sigma) := \left( \text{Tr} \left( \sqrt{\sqrt{\rho}\sigma\sqrt{\rho}} \right) \right)^2. \quad (4)$$

The maximal conversion rate  $R = R(\rho, \sigma, n, \epsilon)$  depends on the initial and target states,  $\rho$  and  $\sigma$ , as well as the number of subsystems  $n$  and the accuracy  $\epsilon$ . The results are expressed in terms of two information

quantities: the relative entropy [36] with the Gibbs state,  $D(\cdot\|\gamma)$ , and the relative entropy variance [37, 38] with the Gibbs state,  $V(\cdot\|\gamma)$ , which are defined by

$$D(\rho\|\gamma) := \text{Tr}(\rho(\log \rho - \log \gamma)), \quad V(\rho\|\gamma) := \text{Tr}(\rho(\log \rho - \log \gamma)^2) - D(\rho\|\gamma)^2. \quad (5)$$

These quantities can also be interpreted thermodynamically:  $D(\rho\|\gamma)/\beta$  is the difference between the generalised free energies of  $\rho$  and  $\gamma$  [18], while  $V(\rho\|\gamma)$  is proportional to a generalised heat capacity of the system [H4]. Also, note that  $D(\rho\|\gamma)$  vanishes if and only if  $\rho = \gamma$ , whereas  $V(\rho\|\gamma)$  vanishes whenever  $\rho$  is proportional to the Gibbs state on the support of  $\rho$ , e.g., when  $\rho$  is pure. It is assumed that neither the initial state  $\rho$  nor the target state  $\sigma$  are the thermal state  $\gamma$ , as otherwise the interconversion problem is trivial. The optimal interconversion rate is then proved to be given by

$$R(\rho, \sigma, n, \epsilon) \simeq \frac{D(\rho\|\gamma)}{D(\sigma\|\gamma)} \left( 1 + \sqrt{\frac{V(\rho\|\gamma)}{n D(\rho\|\gamma)^2}} Z_{1/\nu}^{-1}(\epsilon) \right) \quad (6a)$$

$$\simeq \frac{D(\rho\|\gamma)}{D(\sigma\|\gamma)} \left( 1 + \sqrt{\frac{V(\sigma\|\gamma)}{n D(\rho\|\gamma) D(\sigma\|\gamma)}} Z_{\nu}^{-1}(\epsilon) \right), \quad (6b)$$

where  $Z_{\nu}^{-1}$  is the inverse of the cumulative function of Rayleigh-normal distribution  $Z_{\nu}$  introduced in Ref. [39] with  $\nu$  given by

$$\nu = \frac{V(\rho\|\gamma)/D(\rho\|\gamma)}{V(\sigma\|\gamma)/D(\sigma\|\gamma)}, \quad (7)$$

and  $\simeq$  denotes equality up to terms of order  $o(1/\sqrt{n})$ . Note that  $Z_0 = \Phi$  is the cumulative normal distribution function and  $Z_1$  is the cumulative Rayleigh distribution function. The inverse of the cumulative Rayleigh-normal distribution is typically negative for small values of  $\epsilon$  (unless  $\nu = 1$ ), and thus the finite-size correction term that scales as  $1/\sqrt{n}$  is generally negative. The reason to state both formulas, Eqs. (6a)-(6b), is that this way one covers each of the special cases,  $V(\rho\|\gamma) = 0$  and  $V(\sigma\|\gamma) = 0$ , avoiding the use of  $Z_{\infty}^{-1}$ , which is undefined. The special case when both relative entropy variances vanish is covered separately by the following exact expression for  $R$ :

$$R = \frac{1}{n} \left\lfloor \frac{nD(\rho\|\gamma) - \log(1 - \epsilon)}{D(\sigma\|\gamma)} \right\rfloor \simeq \frac{D(\rho\|\gamma)}{D(\sigma\|\gamma)}. \quad (8)$$

Finally, using results originally derived in Ref. [40], one can numerically evaluate the optimal interconversion rates for small  $n$  and compare the above second-order expansion to the exact interconversion rates. As shown in Fig. 2, even for relatively small system sizes, the second-order asymptotic expansion gives a remarkably good approximation to the optimal interconversion rates, especially when compared to the first-order asymptotics.

**Finite-size irreversibility effects.** Although studying general state interconversion rates may seem to be a rather abstract problem, the formalism can be applied to study more familiar thermodynamic scenarios. Since asymptotic conversion rates allow for reversible interconversion cycles and the results of Ref. [H4] describe finite-size corrections to these rates, the main effect that will be discussed is irreversibility. The first indicator of irreversibility can be captured by calculating the rate at which  $n$  copies of a system can be transformed from initial state  $\rho$ , through  $\sigma$ , and back to  $\rho$ :

$$\rho^{\otimes n} \xrightarrow{\epsilon_1} \sigma^{\otimes Rn} \xrightarrow{\epsilon_2} \rho^{\otimes R'Rn}, \quad (9)$$

which is illustrated in Fig. 3a. Without the second-order asymptotic corrections derived in Ref. [H4], the reversibility rate  $R_r := RR'$  is equal to 1, and Eq. (9) describes a perfect cyclic process. However, including the derived finite-size corrections, one obtains

$$R_r \simeq 1 + \sqrt{\frac{V(\rho\|\gamma)}{n D(\rho\|\gamma)^2}} \left( Z_{1/\nu}^{-1}(\epsilon_1) + Z_{1/\nu}^{-1}(\epsilon_2) \right). \quad (10)$$

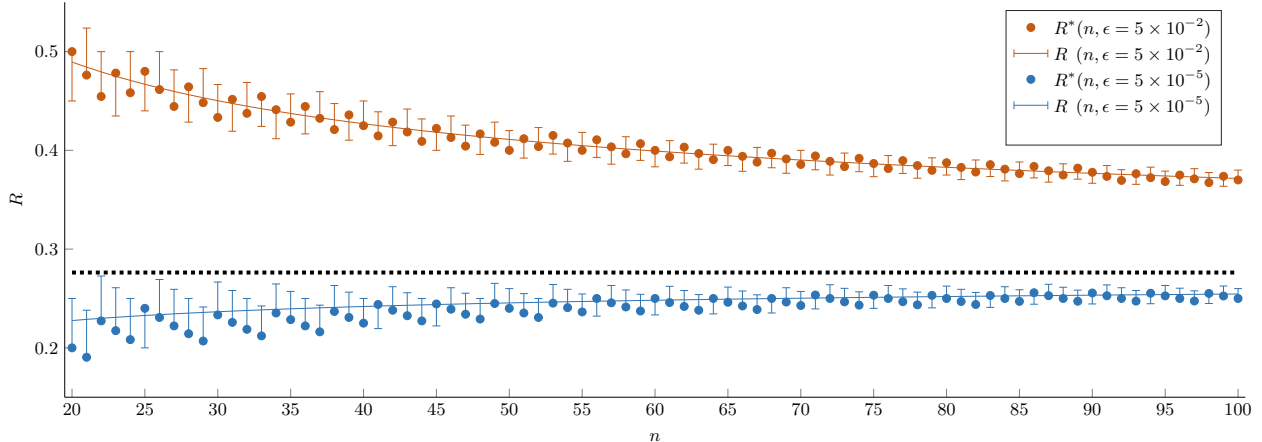


Figure 2: **Optimal interconversion rates.** Comparison between the second-order approximation  $R$  and exact thermal interconversion rates  $R^*$ , when converting from  $\rho = \frac{7}{10} |0\rangle\langle 0| + \frac{3}{10} |1\rangle\langle 1|$  to  $\sigma = \frac{8}{10} |0\rangle\langle 0| + \frac{2}{10} |1\rangle\langle 1|$ , with Hamiltonian  $H = |1\rangle\langle 1|$  and access to a thermal bath at temperature  $1/\beta = 3$ . The circles indicate exact conversion rates, and the lines the second-order approximation given by Eq. (6a). As the exact interconversion rate is always a multiple of  $1/n$ , the rounding of the second-order approximation to the nearest multiples of  $1/n$  is also indicated with error bars. The colours encode the infidelity tolerance, with  $\epsilon = 5 \times 10^{-2}$  for red and  $\epsilon = 10^{-5}$  for blue. The dotted line corresponds to the asymptotic interconversion rate.

The error is accumulated during both transformations appearing in Eq. (9), and the total error  $\epsilon$  can be bounded as

$$\epsilon \leq \left( \sqrt{\epsilon_1(1-\epsilon_2)} + \sqrt{\epsilon_2(1-\epsilon_1)} \right)^2. \quad (11)$$

Now, requiring that the number of systems  $n$  stays constant at all times (i.e., enforcing  $R = R' = 1$ ) implies

$$\epsilon_1 = \epsilon_2 = Z_{1/\nu}(0), \quad (12)$$

and the total error  $\epsilon$  can then be bounded by

$$\epsilon \leq 4Z_\nu(0)(1 - Z_\nu(0)), \quad (13)$$

where the duality property of Rayleigh-normal distribution,  $Z_{1/\nu}(\mu) = Z_\nu(\sqrt{\nu}\mu)$ , has been used. Since the right hand side of the above has a single minimum at  $\nu = 1$ , the parameter  $\nu$  can be interpreted as reversibility parameter that quantifies the compatibility of two states. In other words, the closer  $\nu$  is to 1, the less error will be induced while performing a thermodynamic transformation  $\rho^{\otimes n} \rightarrow \sigma^{\otimes n} \rightarrow \rho^{\otimes n}$  (i.e., the more reversible the process will be).

Another important consequence of irreversibility is the difference between distillable work and work of formation [17]. These quantify the amount of thermodynamically relevant resources that can be distilled from, or are needed to form, a given state. Similarly to the resource theory of entanglement, where Bell states act as standard units of entanglement resource [3], also within the resource theory of thermodynamics there are states acting as “gold standards” for measuring the amount of resources present in a state. These are given by pure energy eigenstates which, having zero entropy, have a clear energetic interpretation. The transformation requiring a change of an ancillary battery state  $|w\rangle$ , with energy  $w$ , into a state  $|0\rangle$ , with zero energy, is thus interpreted as performing work  $w$ ; and a transformation allowing for an opposite change corresponds to extracting work  $w$ . Hence, in order to assess the thermodynamic resourcefulness of  $n$  copies of a given energy-incoherent state,  $\rho^{\otimes n}$ , one can investigate how much the energy of a pure battery system has to decrease per copy of  $\rho$  to construct  $\rho^{\otimes n}$  from a thermal equilibrium state, and how much can it increase per copy of  $\rho$  while transforming  $\rho^{\otimes n}$  to a thermal state. Using Eq. (6b), one can arrive at the following

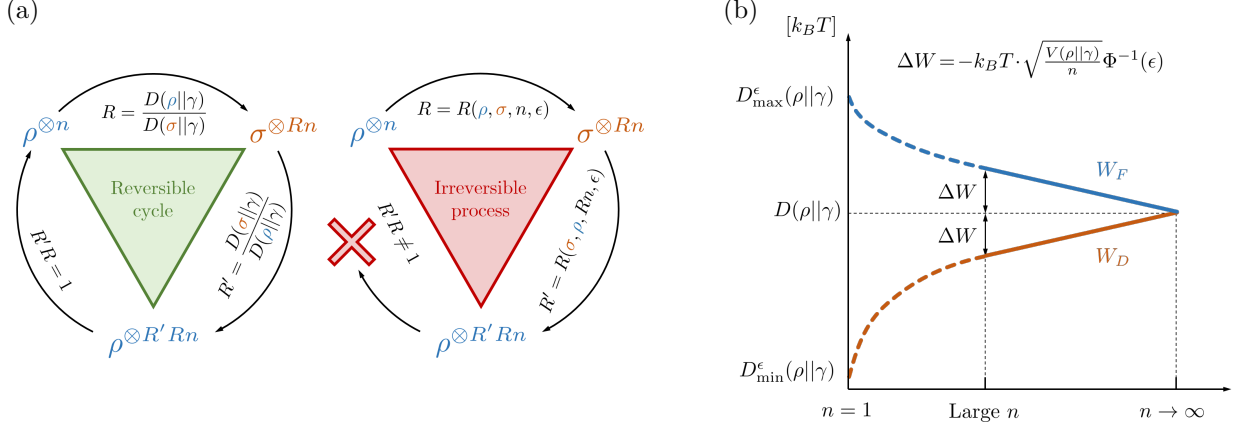


Figure 3: **(a) Finite-size irreversibility.** Left: in the asymptotic limit,  $n \rightarrow \infty$ , the optimal conversion rate from  $\rho$  to  $\sigma$  is equal to the inverse of the conversion rate from  $\sigma$  to  $\rho$ . Therefore, reversible cycles can be performed. Right: in general, finite  $n$  corrections to conversion rates for near-perfect interconversion are negative, leading to irreversibility with  $R'R < 1$ . **(b) Work gap.** The behaviour of distillable work  $W_D$  and work of formation  $W_F$  varies in different regimes. In single-shot scenarios they are proportional to min- and max-relative entropies [17]. In the intermediate regime of large but finite  $n$  studied in Ref. [H4], the values of  $W_D$  and  $W_F$  lie symmetrically around the value achieved in the asymptotic limit, where  $W_D$  and  $W_F$  coincide and are equal to the non-equilibrium generalisation of free energy. Note that the  $y$  axis above is in the units of  $k_B T$ .

second order asymptotic expressions for the work of distillation  $W_D$  and work of formation  $W_F$ :

$$W_D \simeq \frac{1}{\beta} \left( D(\rho||\gamma) + \sqrt{\frac{V(\rho||\gamma)}{n}} \Phi^{-1}(\epsilon) \right), \quad W_F \simeq \frac{1}{\beta} \left( D(\rho||\gamma) - \sqrt{\frac{V(\rho||\gamma)}{n}} \Phi^{-1}(\epsilon) \right), \quad (14)$$

with  $\Phi^{-1}$  being the inverse of the cumulative normal Gaussian distribution. Note that the obtained values of  $W_D$  and  $W_F$  lie symmetrically around the asymptotic value  $W = D(\rho||\gamma)/\beta$ ,

$$W_D \simeq W - \Delta W, \quad W_F \simeq W + \Delta W, \quad \text{with} \quad \Delta W := -\frac{1}{\beta} \sqrt{\frac{V(\rho||\gamma)}{n}} \Phi^{-1}(\epsilon), \quad (15)$$

and that the correction term  $\Delta W$  is positive for small values of infidelity  $\epsilon$ . Thus, the resource cost of near-perfect formation of a state is always larger than the amount of resources than can be distilled from it, indicating irreversibility. This symmetric gap that opens for finite  $n$  is illustrated in Fig. 3b, where it is also compared with the values of  $W_D$  and  $W_F$  for the single-shot scenario  $n = 1$  (where  $W_D$  and  $W_F$  generally lie asymmetrically around the asymptotic value  $W$ ). Finally, in Ref. [H4], it is also explained how the performance of heat engines gets affected by finite-size working body. In particular, it is shown that finite-size effects prevent the possibility of perfect work extraction with Carnot efficiency.

**Extension to moderate-deviation regime.** The results of Ref. [H4] concerned the second-order corrections to the asymptotic rate in the so-called *small deviation* regime [41], where the conversion rate approaches the asymptotic one for  $n \rightarrow \infty$ , but the transformation is realised with a constant error. In Ref. [H5] the issue of constant error was solved by deriving corrections to the asymptotic rate in the *moderate deviation* regime [42], where the correction term still vanishes as  $n \rightarrow \infty$ , but also the transformation is asymptotically error-free. To formally state the main result of Ref. [H5], the following notion is needed: a sequence of real numbers  $\{t_n\}_n$  is a *moderate sequence* if its scaling is strictly between  $1/\sqrt{n}$  and 1, meaning that  $t_n \rightarrow 0$  and  $\sqrt{n}t_n \rightarrow +\infty$  as  $n \rightarrow \infty$ . Note that an important family of moderate sequences is given by  $t_n \sim n^{-\alpha}$  for  $\alpha \in (0, 1/2)$ , which can be used to obtain a particularly simple version of the results. For any moderate sequence  $t_n$  and the accepted error level (quantified by either the infidelity,  $1 - F$ , or total variation distance  $\delta$ )

of

$$\epsilon_n = e^{-nt_n^2}, \quad (16)$$

the asymptotic expansion of the optimal conversion rate  $R(\rho, \sigma, n, \epsilon_n)$  is given by

$$R(\rho, \sigma, n, \epsilon_n) \simeq \frac{D(\rho||\gamma)}{D(\sigma||\gamma)} - \sqrt{\frac{2V(\rho||\gamma)}{D(\sigma||\gamma)^2}} |1 - 1/\sqrt{\nu}| t_n, \quad (17)$$

where  $\nu$  is the reversibility parameter given by Eq. (7) and  $\simeq$  here denotes equality up to terms of order  $o(t_n)$ . Note that when  $V(\rho||\gamma) = 0$ , resulting in  $1/\sqrt{\nu}$  diverging to infinity and the apparent multiplication of zero times infinity, one can simply use the definition of  $\nu$  to replace Eq. (17) with

$$R(\rho, \sigma, n, \epsilon_n) \simeq \frac{D(\rho||\gamma)}{D(\sigma||\gamma)} - \sqrt{\frac{2V(\sigma||\gamma)D(\rho||\gamma)}{D(\sigma||\gamma)^3}} t_n. \quad (18)$$

**Extension to other resource theories.** Somewhat surprisingly, the statements concerning moderate deviation expansion of the interconversion rate under thermal operations can be rather straightforwardly translated to two other prominent examples of resource theories: that of entanglement [3] and that of coherence [43]. This is because they are formally very strongly related, as single-shot interconversion in these two theories (i.e., with transformations constrained to local operations and classical communication, LOCC, and to incoherent operations) is ruled by a majorization partial order [5, 44], while in thermodynamics it is its variant known as thermomajorization [17]. This not only allows for a unified treatment, but also for a simplified representation of initial and target quantum states,  $\rho$  and  $\sigma$ , as probability distributions,  $\mathbf{p}$  and  $\mathbf{q}$ . More precisely, for entanglement theory, the initial and target pure bipartite states,  $\rho = |\Psi\rangle\langle\Psi|$  and  $\sigma = |\Phi\rangle\langle\Phi|$ , with the Schmidt decomposition given by  $|\Psi\rangle = \sum_i \sqrt{p_i} |\psi_i\rangle \otimes |\psi'_i\rangle$  and  $|\Phi\rangle = \sum_i \sqrt{q_i} |\phi_i\rangle \otimes |\phi'_i\rangle$ , can be represented by  $\mathbf{p}$  and  $\mathbf{q}$ . Analogously, for coherence theory with respect to a fixed basis  $\{|i\rangle\}$ , one can represent pure initial and target states,  $\rho = |\psi\rangle\langle\psi|$  and  $\sigma = |\phi\rangle\langle\phi|$ , using  $p_i = |\langle i|\psi\rangle|^2$  and  $q_i = |\langle i|\phi\rangle|^2$ . Then, it was proven in Ref. [H5] that the asymptotic expansion of the optimal conversion rate between states represented by  $\mathbf{p}$  and  $\mathbf{q}$ ,  $r(\mathbf{p}, \mathbf{q}, n, \epsilon_n)$ , for both entanglement and coherence transformations is given by

$$r(\mathbf{p}, \mathbf{q}, n, \epsilon_n) \simeq \frac{H(\mathbf{p})}{H(\mathbf{q})} - \sqrt{\frac{2V(\mathbf{p})}{D(\mathbf{q})^2}} |1 - 1/\sqrt{\nu'}| t_n, \quad (19)$$

where  $t_n$  is an arbitrary moderate sequence,  $\nu'$  is given by [39]

$$\nu' = \frac{V(\mathbf{p})/H(\mathbf{p})}{V(\mathbf{q})/H(\mathbf{q})}, \quad (20)$$

with  $H$  denoting the Shannon entropy and  $V$  the corresponding entropy variance [41, 45],

$$H(\mathbf{p}) = -\sum_i p_i \log p_i, \quad V(\mathbf{p}) = \sum_i p_i (\log p_i + H(\mathbf{p}))^2. \quad (21)$$

Note that when  $V(\mathbf{p}) = 0$ , resulting in  $1/\sqrt{\nu'}$  diverging to infinity and the apparent multiplication of zero times infinity, one can simply use the definition of  $\nu'$  to replace Eq. (19) with

$$r(\mathbf{p}, \mathbf{q}, n, \epsilon_n) \simeq \frac{H(\mathbf{p})}{H(\mathbf{q})} - \sqrt{\frac{2V(\mathbf{q})H(\mathbf{p})}{H(\mathbf{q})^3}} t_n. \quad (22)$$

**Resource resonance.** As we have just seen, for transformations in resource theories of thermodynamics, entanglement and coherence, when the initial and target states satisfy  $\nu = 1$  (or  $\nu' = 1$ ), the optimal conversion rate in the regime of vanishing error is given by the asymptotic rate with no corrections. This means that, up to terms of order  $o(t_n)$ , such transformations are reversible even for finite  $n$ . As a result, a novel *resource resonance* phenomenon was discovered and discussed in Ref. [H6]. Note that since the free energy  $D(\cdot||\gamma)$  (or the Shannon entropy  $H(\cdot)$ ) quantifies the average (asymptotic) resource content of a state,

free energy variance  $V(\cdot||\gamma)$  (or the entropy variance  $V(\cdot)$ ) can be understood as quantifying its fluctuations. Hence, the ratio  $V/D$  (or  $V/H$ ) tells us about relative strength of resource fluctuations in a single copy of a given state, and so the resonance condition  $\nu = 1$  (or  $\nu' = 1$ ) is satisfied for pairs of states with equal relative resource fluctuations. Here, this general phenomenon will be illustrated with two particular examples.

First, consider a heat engine, with a finite-size working body consisting of  $n = 200$  non-interacting two-level systems and operating between two thermal baths at temperatures  $T_h > T_c$ , performing work on a battery system initially in the ground state. Such a process can be elegantly phrased as an interconversion problem within the resource theory of thermodynamics, with the working body at cold temperature  $T_c$  acting as a non-equilibrium resource in the presence of a hot bath at temperature  $T_h$ . While the working body heats up from  $T_c$  to  $T_{c'}$ , part of its resource content can be converted into work by exciting the battery system. Now, a perfect engine with an infinite working body,  $n \rightarrow \infty$ , and constantly operating at the Carnot efficiency would extract the amount of work  $nW_C$  equal to the free energy change of the working body. However, since  $n$  is small, the energy fluctuations of the working body are not negligible compared to the average energy, and thus the engine operates beyond the thermodynamic limit. One can then expect two kinds of effects. On the one hand, the quality of work [46, 47] will not be perfect, as some of the energy fluctuations will be transferred to the battery. In the left panel of Fig. 4a, the optimal work quality as a function of  $T_c$  and  $T_{c'}$  is presented for an engine extracting  $W = 0.95W_C$  per qubit of the working body. On the other hand, if one demands the work quality to be above some threshold level, the optimal efficiency of the engine may be affected so that it cannot achieve the Carnot limit. In the right panel of Fig. 4a, the optimal fraction of  $W_C$  that can be extracted when its quality is bounded by a constant is plotted, again as a function of  $T_c$  and  $T_{c'}$ . In both plots one can see clear resonant lines (corresponding precisely to the resonant condition  $\nu = 1$ ), indicating near-perfect quality and near-Carnot efficiency corresponding to reversible (and thus dissipationless) processes, obtained while operating well outside the asymptotic regime with a finite-size working body.

Second, imagine one has access to  $n$  bipartite and pure entangled systems, each initially in a state  $\rho_1$  or  $\rho_2$ , and wants to transform them to a target state  $\sigma$ . Moreover, assume that the asymptotic resource values of  $\rho_1$  and  $\rho_2$  are equal, i.e., asymptotically one can obtain the same number of copies of  $\sigma$  from either  $n$  copies of  $\rho_1$  or  $n$  copies of  $\rho_2$ . One can achieve this asymptotic conversion rate also for finite  $n$ , but for the price of error  $\epsilon$ . This error depends on the reversibility parameter  $\nu'$ , and thus for finite  $n$  the states  $\rho_1$  and  $\rho_2$  no longer have the same value. Crucially, however, it may happen that they are incompatible with  $\sigma$  in opposite ways, such that the reversibility parameter for  $\rho_1$  and  $\sigma$  is smaller than 1, while for  $\rho_2$  and  $\sigma$  it is larger than 1. Thus, by taking  $\lambda n$  copies of  $\rho_1$  and  $(1 - \lambda)n$  copies of  $\rho_2$  one can tune the initial state to be in resonance with the target state, i.e., to have reversibility parameter close to 1. In the left panel of Fig. 4b, one can see how such tuning can reduce the infidelity of entanglement transformation by several orders of magnitude. Note that this effect is much stronger than the increase in fidelity due to the increased number  $n$  of processed states that can be observed for  $\lambda \in \{0, 1\}$ . Instead of demanding conversion at the asymptotic rate, one can enforce the error to be below some fixed threshold value  $\epsilon$ . Again, one can focus on a set of initial states  $\{\rho_i\}$  that are asymptotically equivalent and ask how many copies of the target state  $\sigma$  can be obtained from  $\rho_i^{\otimes n}$  with error not exceeding  $\epsilon$ . Based on Eq. (19), the conversion rate  $r$  should grow with  $n$  approaching the asymptotic value quicker for states  $\rho_i$  that are closer to resonance with  $\sigma$ . Indeed, this is the case, as the numerical results presented in the right panel of Fig. 4b confirm.

**Links with fluctuation-dissipation relation.** The fluctuation-dissipation theorem is a fundamental result in statistical physics that establishes a connection between the response of a system subject to a perturbation and the fluctuations associated with observables in equilibrium [48, 49]. In Ref. [H12], I derived its version within a resource-theoretic framework, where one investigates optimal quantum state transitions under thermodynamic constraints. This was achieved by investigating thermodynamic distillation processes in which the initial system consisting of asymptotically many non-interacting subsystems is transformed via thermal operations, with some transformation error, to a pure energy eigenstate of the final system. Within this setting, which is analogous to the one from Refs. [H4–H6], the main results of Ref. [H12] are given by two theorems. The first one yields the optimal transformation error  $\epsilon$  as a function of the free energy difference  $\Delta F$  (measured by relative entropy  $D(\cdot||\gamma)$ ) between the initial and target states, and the free energy

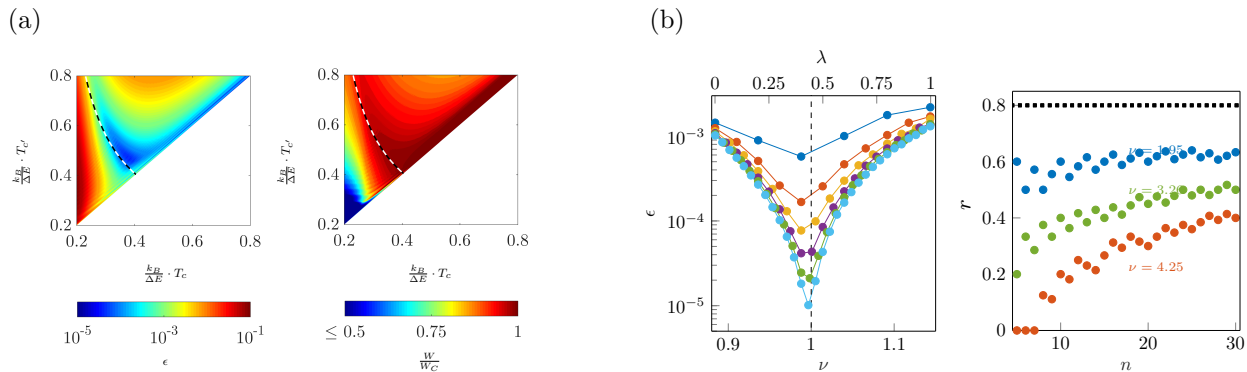


Figure 4: **(a) Resonance in work extraction.** Performance of the heat engine with a working body consisting of  $n = 200$  non-interacting qubits, each with energy gap  $\Delta E$ . Hot bath temperature is set by  $k_B T_h = 10\Delta E$ , the working body is initially at cold bath temperature  $T_c$  and heats up to  $T_c'$  in the process. Left: the optimal quality of work, measured by the infidelity  $\epsilon$  between the final and excited battery state, while extracting  $W = 0.95W_C$  per qubit. Right: the optimal fraction of  $W_C$  that can be extracted per qubit when the quality of work is bounded by  $\epsilon < 10^{-3}$ . The dashed line in both plots indicates the position of the resonance predicted by setting  $\nu = 1$  in Eq. (7). **(b) Tuning resources to resonance.** State interconversion under LOCC for a bipartite system consisting of  $n$  pairs of qutrits. Left: the infidelity  $\epsilon$  between the target state  $|\Phi\rangle^{\otimes n}$  and the optimal final state obtained from  $|\Psi_1\rangle^{\otimes \lambda n} \otimes |\Psi_2\rangle^{\otimes (1-\lambda)n}$ . Different plots correspond to varying numbers of interconverted states  $n \in \{5, 10, \dots, 30\}$ , from top to bottom. The location of the resonant mixing factor  $\lambda_*$  (dashed line) can be found using Eq. (20). Right: The optimal conversion rate  $r$  between the initial state  $|\Psi_i\rangle^{\otimes n}$  and the target state  $|\Phi\rangle^{\otimes rn}$  with transformation infidelity bounded by  $\epsilon < 0.01$ . Different plots correspond to initial states with equal asymptotic conversion rate (dashed line), but varying reversibility parameters  $\nu'$ .

fluctuations  $\sigma(F)$  (measured by relative entropy variance  $V(\cdot||\gamma)$ ) in the initial state:

$$\epsilon = \Phi\left(-\frac{\Delta F}{\sigma(F)}\right), \quad (23)$$

where  $\Phi(x)$ , as before, is the Gaussian cumulative distribution function. This statement was proven for many independent initial systems in arbitrary incoherent states, as well as for many independent and identical systems in the same pure state. The second theorem (that employs the first one as a building block) provides a precise relation between the free energy fluctuations  $\sigma(F)$  of the initial state and the minimal amount of free energy  $F_{\text{diss}}$  dissipated in the optimal thermodynamic distillation process (i.e., the difference between the initial and final free energy of the system):

$$F_{\text{diss}} = a(\epsilon) \sigma(F) \quad (24)$$

where

$$a(\epsilon) = -\Phi^{-1}(\epsilon)(1 - \epsilon) + \frac{\exp\left(\frac{-(\Phi^{-1}(\epsilon))^2}{2}\right)}{\sqrt{2\pi}}. \quad (25)$$

This statement was proven for many independent systems in identical incoherent states, while for many independent systems in identical pure states it was proven that the right hand side of Eq. (24) is a lower bound for  $F_{\text{diss}}$ . The physical interpretation of this result is clear and in direct correspondence with the original fluctuation-dissipation relation: whenever the system is dragged out of its initial (not necessarily equilibrium) state to some final state, the amount of free energy dissipated in this process is exactly proportional to the amount of free energy fluctuations present in the initial state. In other words, it is these fluctuations that are responsible for dissipation, as in the original works of Einstein and Smoluchowski on Brownian motion [50, 51]. Recall that there an object moving through a fluid experiences resistance that dissipates energy, with the source of resistance (i.e., many small fluid molecules bumping into the investigated object) being the same as the source of random position fluctuations of the object at equilibrium.

### 4.3.2 Thermodynamic consequences of the superposition principle

**Optimal processing of states with coherence.** The results obtained in Ref. [H12] were also used to refine the known results on the performance of important thermodynamic protocols. Most importantly, by extending the analysis to arbitrary pure initial states, not only the effect of thermal fluctuations could be studied, but also of quantum fluctuations that arise due to the superposition principle. To be more precise, the optimal amount of extractable work and the optimal thermodynamically-free communication rate were calculated for initial states consisting of  $n$  identical pure states,  $|\psi\rangle^{\otimes n}$ . Despite the completely different nature of such states as compared to energy-incoherent states, the derived formulas up to second order asymptotic terms (i.e., the values for  $n \rightarrow \infty$  with a correction term scaling as  $1/\sqrt{n}$ ) had the same form. The only change needed in the formulas was to replace the free energy and free energy fluctuations with average energy  $\langle E \rangle$  and energy fluctuations  $\sigma(E)$ , where

$$\langle E \rangle = N \langle \psi | H | \psi \rangle, \quad \sigma(E) = \sqrt{N} \left( \langle \psi | H^2 | \psi \rangle - \langle \psi | H | \psi \rangle^2 \right). \quad (26)$$

In conclusion, it was shown that in the regime of many processed systems, the analysis of the thermodynamic transformations of states with coherence is similar in spirit to energy-incoherent states.

**Structure of the thermodynamic partial order.** Work [H1] investigates the structure of the thermodynamic ordering of non-equilibrium states that emerges when the set of thermodynamic transformations is defined by the largest set of quantum operations that do not allow one to construct a perpetuum mobile. These are given by transformations  $\mathcal{E}$  that leave the thermal equilibrium state unchanged, the so-called *Gibbs-preserving* (GP) operations satisfying  $\mathcal{E}(\gamma) = \gamma$ , and form a superset of the previously discussed thermal operations. These operations encode the structure of the *thermodynamic arrow of time* by telling one which states can be reached from a given state (and which states can evolve into it) in accordance with the laws of thermodynamics. In other words, whenever a state  $\rho$  can freely, i.e., without using any extra thermodynamic resources, evolve to a state  $\sigma$ , then  $\rho$  precedes  $\sigma$  in a thermodynamic partial order. Instead of studying the ordering induced by Gibbs-preserving operations between particular states, the focus in Ref. [H1] is on the global properties of the thermodynamic arrow of time. More precisely, a partial order is a very general structure, studied within the field of mathematics known as order theory [52], with three defining properties: reflexivity, transitivity and antisymmetry. Being such a broad and general concept, it seems natural to ask whether the thermodynamic ordering has a more rigid and specific structure. Inspired by order-theoretic studies, Ref. [H1] focuses on a special kind of partial order known as a *lattice*, interprets it from a thermodynamic perspective, and provides evidence that the superposition principle brings additional structure to the thermodynamic arrow of time.

**Thermodynamic lattice.** In order to investigate the thermodynamic ordering of states encoded by Gibbs-preserving maps, it is useful to introduce the notion of *thermal cones* (see Fig. 5a). The set of states  $\mathcal{T}_+(\rho)$  that a quantum state  $\rho$  can be mapped to via GP quantum channels is called the *future thermal cone* of  $\rho$ . Analogously, the set of states  $\mathcal{T}_-(\rho)$  that can be mapped to  $\rho$  via GP quantum channels is called the *past thermal cone* of  $\rho$ . Next, for any two states  $\rho$  and  $\sigma$ , define a set of states  $\mathcal{T}_-(\rho, \sigma) = \mathcal{T}_-(\rho) \cap \mathcal{T}_-(\sigma)$ , i.e., the set of all states whose future thermal cones contain both  $\rho$  and  $\sigma$ . The thermodynamic interpretation of  $\mathcal{T}_-(\rho, \sigma)$  is that of a set of states in the past that are allowed by the thermodynamic arrow of time to evolve both into  $\rho$  and  $\sigma$  at present. Analogously, define a set of states  $\mathcal{T}_+(\rho, \sigma) = \mathcal{T}_+(\rho) \cap \mathcal{T}_+(\sigma)$ , i.e., the set of all states whose past thermal cones contain both  $\rho$  and  $\sigma$ . Thermodynamically  $\mathcal{T}_+(\rho, \sigma)$  is the set of states in the future that are allowed by the thermodynamic arrow of time to be reached from both  $\rho$  and  $\sigma$  at present. Now, if there exists  $\tau_- \in \mathcal{T}_-(\rho, \sigma)$  such that for all  $\tau \in \mathcal{T}_-(\rho, \sigma)$  we have  $\tau_- \in \mathcal{T}_+(\tau)$  then  $\tau_-$  is called the *join* of  $\rho$  and  $\sigma$  and is usually denoted by  $\rho \vee \sigma$  (see Fig. 5b). The notation is justified by the fact that  $\mathcal{T}_+(\tau_-)$  is the smallest thermal cone that contains  $\mathcal{T}_+(\rho) \cup \mathcal{T}_+(\sigma)$ . Thermodynamically we can interpret the join of  $\rho$  and  $\sigma$  as the unique state<sup>3</sup> in the past that is consistent both with  $\rho$  and  $\sigma$  at present, as well as with all possible joint pasts of  $\rho$  and  $\sigma$ . The join can also be seen as the extremal moment in the past evolution, at which the system has to “decide” whether to evolve into  $\rho$  or  $\sigma$ . Analogously, if there exists  $\tau_+ \in \mathcal{T}_+(\rho, \sigma)$

<sup>3</sup>To be precise, the “unique state” actually means a state that is unique up to equivalence relation given by states that are reversibly interconvertible under GP operations.

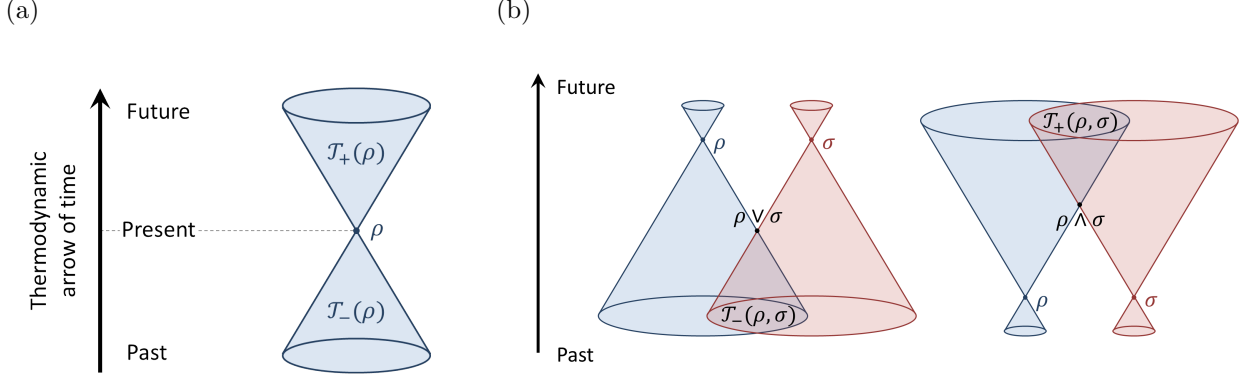


Figure 5: **(a) Thermal cones.** The reachability of one state from another via a GP map introduces the ordering of states along the thermodynamic arrow of time. States that can be reached from a given state  $\rho$  form its future thermal cone  $\mathcal{T}_+(\rho)$ , whereas states that can be transformed into  $\rho$  form its past thermal cone  $\mathcal{T}_-(\rho)$ . **(b) Visualising the join and meet.** Left: the intersection of past thermal cones of  $\rho$  and  $\sigma$ , denoted by  $\mathcal{T}_-(\rho, \sigma)$ , is a set of states that can thermodynamically evolve to both  $\rho$  and  $\sigma$ . The join  $\rho \vee \sigma$  is the unique state belonging to  $\mathcal{T}_-(\rho, \sigma)$  that can be thermodynamically reached from all states in  $\mathcal{T}_-(\rho, \sigma)$ . Right: the intersection of future thermal cones of  $\rho$  and  $\sigma$ , denoted by  $\mathcal{T}_+(\rho, \sigma)$ , is a set of states that can be thermodynamically reached from both  $\rho$  and  $\sigma$ . The meet  $\rho \wedge \sigma$  is the unique state belonging to  $\mathcal{T}_+(\rho, \sigma)$  that can thermodynamically evolve to all states in  $\mathcal{T}_+(\rho, \sigma)$ .

such that for all  $\tau \in \mathcal{T}_+(\rho, \sigma)$  we have  $\tau_+ \in \mathcal{T}_-(\tau)$ , then  $\tau_+$  is called the *meet* of  $\rho$  and  $\sigma$  and is usually denoted by  $\rho \wedge \sigma$  (see Fig. 5b). Again, the notation is justified by the fact that  $\mathcal{T}_+(\tau_+)$  is the biggest thermal cone that is contained in  $\mathcal{T}_+(\rho) \cap \mathcal{T}_+(\sigma)$ . Thermodynamically the meet of  $\rho$  and  $\sigma$  is the unique state in the future that is consistent both with  $\rho$  and  $\sigma$  at present, as well as with all possible joint futures of  $\rho$  and  $\sigma$ . The meet can also be seen as the extremal moment in the future evolution, after which the system “forgets” whether it evolved from  $\rho$  or  $\sigma$ , as its state is consistent with both pasts.

In Ref. [H1], I point out that in the infinite-temperature limit the thermodynamic arrow of time actually reflects the structure of a lattice, and I provide explicit expressions for the join and meet of any two states. Crucially, the lattice structure is still preserved if one limits considerations to the subset of classical states, i.e. states incoherent in the energy eigenbasis that can be represented by probability distributions over their energy levels. Thus, when  $T \rightarrow \infty$ , both classical and quantum thermodynamic arrows of time have a lattice structure. However, I show that this structure is lost in the classical regime at finite temperatures. Surprisingly, however, I prove that the lattice structure may be preserved at finite temperatures when considering the full set of quantum states, suggesting that coherence can play a role in providing structure to the thermodynamic arrow of time. This is achieved by studying the simplest quantum scenario of a two-dimensional system, fully solving state interconversion problem under GP quantum channels, and showing that the resulting ordering forms a lattice. First, the future thermal cone  $\mathcal{T}_+(\rho)$  is obtained for all qubit states  $\rho$ . In the Bloch sphere, it is given by the region obtained from revolving the intersection of two disks,  $D_1(\rho) \cap D_2(\rho)$ , around the  $z$  axis (see Fig. 6a), with  $D_1$  and  $D_2$  defined as follows. Recall the Bloch sphere representation of a qubit state  $\rho$ ,

$$\rho = \frac{\mathbb{1} + \mathbf{r}_\rho \cdot \boldsymbol{\sigma}}{2}, \quad (27)$$

where  $\boldsymbol{\sigma} = (\sigma_x, \sigma_y, \sigma_z)$  denotes the vector of Pauli matrices. Next, orient the Bloch sphere so that the Bloch vectors of the considered state  $\rho$  and the thermal state  $\gamma$  are given by  $\mathbf{r}_\rho = (x, 0, z)$  and  $\mathbf{r}_\gamma = (0, 0, \zeta)$ , respectively. The two disks,  $D_1(\rho)$  and  $D_2(\rho)$ , then have radii

$$R_1(\rho) = \frac{R_-(\rho) + \zeta^2}{1 - \zeta^2}, \quad R_2(\rho) = \frac{R_+(\rho) - \zeta^2}{1 - \zeta^2}, \quad (28)$$

and are centred at

$$\mathbf{z}_1(\rho) = [0, 0, \zeta(1 + R_1(\rho))], \quad \mathbf{z}_2(\rho) = [0, 0, \zeta(1 - R_2(\rho))], \quad (29)$$

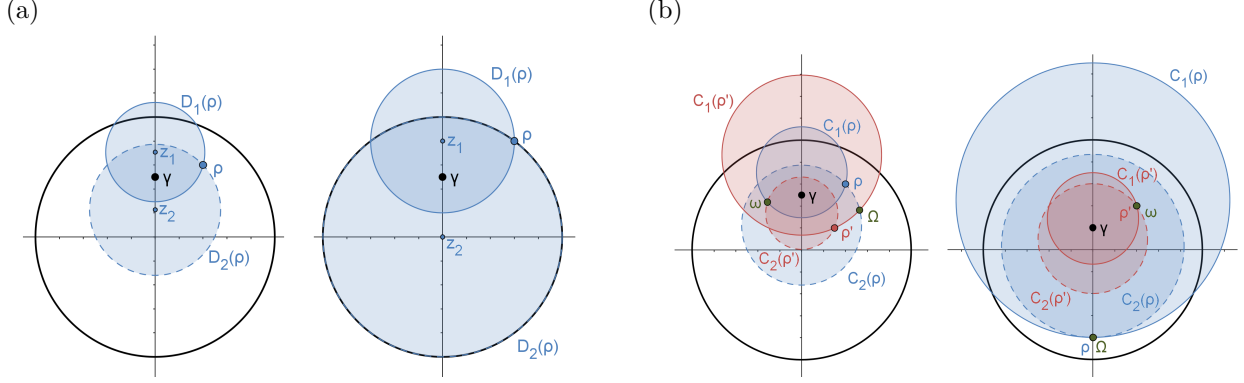


Figure 6: **(a) Future thermal cones for qubits (GP operations).** A general qubit state  $\rho$  and a thermal state  $\gamma$  with  $\mathbf{r}_\gamma = (0, 0, 0.5)$  presented in the Bloch sphere. The disk  $D_1(\rho)$  corresponds to a set of states  $\{\sigma\}$  with  $R_-(\sigma) \leq R_-(\rho)$ , whereas the disk  $D_2(\rho)$  corresponds to a set  $\{\sigma\}$  with  $R_+(\sigma) \leq R_+(\rho)$ . The equalities are obtained at the edges of the disks. The set of states  $\rho$  can be mapped to via GP quantum channels is given by the intersection  $D_1(\rho) \cap D_2(\rho)$  (which can also be freely revolved around the  $z$  axis). Left: a mixed initial state with  $\mathbf{r}_\rho = (0.4, 0, 0.6)$ . Right: a pure initial state with  $\mathbf{r}_\rho = (0.6, 0, 0.8)$ . **(b) Thermodynamic lattice for qubits.** A thermal state  $\gamma$  and two states  $\rho$  and  $\rho'$  presented in the Bloch sphere. Left: states described by  $\mathbf{r}_\rho = (0.4, 0, 0.6)$ ,  $\mathbf{r}_{\rho'} = (0.3, 0, 0.2)$ ,  $\mathbf{r}_\gamma = (0, 0, 0.5)$ . The join  $\Omega$  of  $\rho$  and  $\rho'$  lies at the intersection of circles  $C_i$  defining  $D_1(\rho')$  and  $D_2(\rho)$ , whereas their meet  $\omega$  lies at the intersection of circles  $C_i$  defining  $D_1(\rho)$  and  $D_2(\rho')$ . Right: states described by  $\mathbf{r}_\rho = (0, 0, -0.8)$ ,  $\mathbf{r}_{\rho'} = (0.4, 0, 0.4)$ ,  $\mathbf{r}_\gamma = (0, 0, 0.2)$ . The join  $\Omega$  of  $\rho$  and  $\rho'$  lies at the intersection of circles  $C_i$  defining  $D_1(\rho)$  and  $D_2(\rho)$  (which coincides with  $\rho$ ), whereas their meet  $\omega$  lies at the intersection of circles  $C_i$  defining  $D_1(\rho')$  and  $D_2(\rho')$  (which coincides with  $\rho'$ ).

where

$$R_\pm(\rho) = \sqrt{(z - \zeta)^2 + x^2(1 - \zeta^2)} \pm \zeta z. \quad (30)$$

Now, the join and meet of  $\rho$  and  $\rho'$  are defined using

$$\rho_m^{\max} = \arg \max\{R_m(\rho), R_m(\rho')\}, \quad \rho_m^{\min} = \arg \min\{R_m(\rho), R_m(\rho')\}, \quad (31)$$

for  $m \in \{1, 2\}$ : the join is given by a state lying in the Bloch sphere at the intersection of two circles defining  $D_1(\rho_1^{\max})$  and  $D_2(\rho_2^{\max})$ , and the meet is defined analogously by replacing  $\max$  with  $\min$  (see Fig. 6b).

Finally, it is important to emphasize that the existence of a thermodynamic lattice would not only bring a new understanding of the thermodynamic arrow of time (with a unique consistent future and past for each subset of states), but could also allow us to use new algebraic tools to study thermodynamics. Namely, if thermodynamic partial order forms a lattice, then it can be fully described as an algebraic structure consisting of a set of quantum states and two binary operations  $\vee$  and  $\wedge$  satisfying the following axioms for all states  $\rho, \sigma, \tau$ :

$$\rho \vee \sigma = \sigma \vee \rho, \quad \rho \vee (\sigma \vee \tau) = (\rho \vee \sigma) \vee \tau, \quad \rho \vee (\rho \wedge \sigma) = \rho, \quad (32)$$

and another three obtained from the above by exchanging  $\vee$  with  $\wedge$ .

**History erasure process.** In order to provide a physical interpretation of the above results and to highlight the differences between the infinite- and finite-temperature cases (as well as between classical and quantum scenarios), the *history erasure process* was introduced and analysed in Ref. [H1]. Imagine that two possible events may have happened “in the past”: the system could have been prepared either in the state  $\rho$  or in the state  $\sigma$ . It then evolved along the thermodynamic arrow of time into a state  $\tau$ , i.e., a GP quantum channel transformed the system state into  $\tau$ . Now ask: can one infer the past of the system, i.e., whether it was initially prepared in a state  $\rho$  or  $\sigma$ , based on the present state  $\tau$ ? If both  $\rho$  and  $\sigma$  belong to the past thermal cone  $\mathcal{T}_-(\tau)$  then it is impossible, and one says that the  $(\rho, \sigma)$ -history has been erased during the evolution. Clearly, any history can be erased by evolution that brings the system to the thermal equilibrium state  $\gamma$ . However, it may not be necessary for the system to evolve all the way to  $\gamma$  in order to erase its

history. Therefore, the question is as follows: how far along the thermodynamic arrow of time does a system have to evolve for its state to be consistent with both possible pasts, specified by states  $\rho$  and  $\sigma$ ? To make the notion of “far” precise one may ask: how much the free energy (entropy) of the system has to decrease (increase) in order to erase its  $(\rho, \sigma)$ -history. The simplest scenario happens when the two possible pasts are thermodynamically ordered, say that  $\rho$  lies in the past thermal cone of  $\sigma$ . Then, if the system were prepared in the state  $\sigma$ , it would not need to evolve at all (so its free energy would not need to decrease) in order to achieve history erasure. Indeed, observing the state  $\sigma$  one cannot tell whether the system started in  $\rho$  and thermalised towards  $\sigma$ , or if it was prepared in  $\sigma$  and did not evolve at all (recall that the identity map is a free thermodynamic operation). A more interesting scenario arises when  $\rho$  and  $\sigma$  are not ordered. Then, in general, there may be many optimal states  $\tau$  which lead to history erasure, i.e., states that lie in the future thermal cones of both  $\rho$  and  $\sigma$ , but whose past thermal cones contain no states with that property. However, if the thermodynamic order has a lattice structure, there is a unique optimal state  $\tau$ , given by the meet  $\rho \wedge \sigma$ , that leads to  $(\rho, \sigma)$ -history erasure. The fact that in the infinite temperature limit one deals with a lattice means that when information is the only thermodynamic resource (in the sense that it does not matter which energy states are occupied, and the only important thing is how “sharp” the distribution is), there exists a unique optimal history erasure process. In other words, there is a well-defined way to erase the history while decreasing all thermodynamic monotones (in particular, increasing entropy) in a minimal way. On the other hand, in the classical regime at finite temperatures, there does not exist a single unique optimal history erasure process, but rather many inequivalent ones, each optimising a different monotone. However, for two-level systems, if one is not restricted to classical states, there is an optimal way of erasing  $(\rho, \sigma)$ -history, given by the meet of  $\rho$  and  $\sigma$ . Note that, for two classical states, their meet is given by a state with coherence. One thus sees that for  $d = 2$  coherence is necessary for the existence of an optimal history erasure process at finite temperatures, and so exploiting coherence one can erase the classical history of a system using less free energy.

## 4.4 Results on memory constraints

### 4.4.1 Optimal thermodynamic processing without memory

**Markovian thermal processes.** The aim of work [H14] was to capture the laws governing possible thermodynamic transformations under the assumption that the system interacts with a thermal bath at an inverse temperature  $\beta$  in a memoryless (Markovian) way. The Markovianity condition typically arises in the microscopic derivations employing the assumption of a large bath and the weak coupling limit [21, 53, 54]. More formally, the evolution of a state  $\rho$  of a quantum system is then governed by a master equation with the general form [19, 20]:

$$\frac{d\rho(t)}{dt} = \mathcal{H}(\rho(t)) + \mathcal{L}_t(\rho(t)). \quad (33)$$

The first term,  $\mathcal{H}$ , is the generator of a closed (reversible) quantum dynamics,

$$\mathcal{H}(\rho) = -i[H, \rho], \quad (34)$$

with  $[\cdot, \cdot]$  denoting the commutator,  $[A, B] = AB - BA$ , and  $H$  being the (dressed) Hamiltonian of the system, which is assumed here to be time-independent. The second term,  $\mathcal{L}_t$ , is known as the *Lindbladian* or *dissipator* and generates an open (irreversible) quantum dynamics. It has the following general form:

$$\mathcal{L}_t(\rho) = \sum_i r_i(t) \left( L_i(t)\rho L_i(t)^\dagger - \frac{1}{2} \{L_i(t)^\dagger L_i(t), \rho\} \right), \quad (35)$$

with  $\{\cdot, \cdot\}$  denoting the anticommutator,  $\{A, B\} = AB + BA$ ,  $L_i(t)$  being time-dependent *jump operators*, and  $r_i(t)$  being time-dependent non-negative *jump rates*. While a general Lindbladian only requires the rates  $r_i$  to be non-negative, Lindbladians arising from the interaction of a quantum system with a large heat bath have two standard properties [21, 53, 54]:

(P1) **Stationary thermal state.** The Gibbs thermal state  $\gamma$  of the system (recall Eq. (1)) is a stationary solution of the dynamics, i.e.,

$$\forall t : \quad \mathcal{L}_t \gamma = 0. \quad (36)$$

(P2) **Covariance.** The Lindbladian  $\mathcal{L}_t$  commutes with the generator of the Hamiltonian dynamics  $\mathcal{H}$  at all times  $t$ , i.e.,

$$\forall \rho: \quad \mathcal{L}_t(\mathcal{H}(\rho)) = \mathcal{H}(\mathcal{L}_t(\rho)). \quad (37)$$

Quantum dynamics generated by master equations in the form of Eq. (33) and satisfying properties (P1)-(P2) are called *Markovian thermal processes*. In other words, a quantum channel  $\mathcal{E}$  is a Markovian thermal process (MTP) if it results from integrating the Markovian master equation, Eq. (33), between time 0 and  $t_f \in [0, +\infty]$ , where the Lindbladian  $\mathcal{L}_t$  satisfies properties (P1)-(P2). These form a standard description of thermalization in the field of quantum thermodynamics and beyond (see, e.g., Sec. 3.1 of Ref. [54]) and are the main focus of Ref. [H14].

While it is not straightforward to characterize *all* physical setups modelled via MTPs, they are commonplace. A crucial observation to be kept in mind is the following: MTPs constitute an *effective model* that emerges after common approximations (such as the secular approximation, ignoring the Lamb shift) and in an appropriate frame (in general, a rotating frame). For a concrete example of such an emergence after relevant approximations, consider a typical setup of discrete quantum heat engines in the weak coupling regime. There, one assumes that the dissipators only operate for a given amount of time, and they are then suddenly switched to new ones according to some schedule. This is a special case of Eq. (35) where  $L_i(t) \equiv L_i$ ,  $r_i(t)$  are taken to be appropriate step functions and  $H$  is (approximatively) constant after ignoring a small Lamb shift. These are not only a nice class of examples: as was shown in Ref. [H14], these controls are sufficient to realize every transformation that can be achieved by a generic MTP. Thus, any model that can be formally written as Eq. (33) with properties (P1)-(P2) (with or without time-dependence on  $\mathcal{L}_t$ ) falls within the scope of work [H14]. These include incoherent noise in quantum computers and effective models describing fluorescence and other non-radiative decay channels in atoms, molecules and nanostructures [55]. The formal equivalence between thermodynamic and other models of dissipation is well-known and it is in fact leveraged as a standard technique to realize effective heat baths [56]. In quantum information terms, depolarization and amplitude damping can be seen as limiting cases of Markovian thermal processes when  $\beta \rightarrow 0$  and  $\beta \rightarrow \infty$ , respectively. This means that, in principle, the results of Ref. [H14] that will be summarised in the following paragraphs, apply well-beyond the obvious thermodynamic scenarios.

**Complete set of laws.** The central question that I investigated in work [H14] is: what final states  $\rho(t_f)$  are accessible from an initial state  $\rho(0)$  by means of Markovian thermal processes? When such a process transforming  $\rho(0)$  into  $\rho(t_f)$  exists, it is denoted by

$$\rho(0) \xrightarrow{\text{MTP}} \rho(t_f). \quad (38)$$

The main contribution of Ref. [H14] is to find a complete set of conditions to answer this question when  $\rho(t_f)$  is block-diagonal in the energy basis (i.e., when it is energy-incoherent). Due to property (P2), the problem is reduced to the one involving energy distributions ('populations')

$$\mathbf{p}(0) \xrightarrow{\text{MTP}} \mathbf{p}(t_f). \quad (39)$$

It is crucial to highlight that the obtained solution satisfies two desiderata:

(D1) **Finite verifiability.** One can verify in a finite number of steps whether  $\mathbf{p}(0) \xrightarrow{\text{MTP}} \mathbf{p}(t_f)$  holds for any given initial and final states.

(D2) **Constructability.** Whenever  $\mathbf{p}(0) \xrightarrow{\text{MTP}} \mathbf{p}(t_f)$  holds, one can explicitly construct a Markovian thermal process realizing this transition through a sequence of elementary controls.

These are central requirements for the applicability of the framework and in typical resource theory approaches these are not both satisfied.

**Continuous thermomajorization.** The first step towards finding the complete set of laws governing transformations by MTPs, was to introduce a generalised version of the well-known thermomajorisation ordering  $\succ_\gamma$  [17, 27]. A probability distribution  $\mathbf{p}$  is said to *continuously thermomajorize*  $\mathbf{q}$ , denoted  $\mathbf{p} \succ_\gamma \mathbf{q}$ , if there exists a continuous path of probability distributions  $\mathbf{r}(t)$  for  $t \in [0, t_f)$  such that

1.  $\mathbf{r}(0) = \mathbf{p}$ ,
2.  $\forall t_1, t_2 \in [0, t_f] : t_1 \leq t_2 \Rightarrow \mathbf{r}(t_1) \succ_\gamma \mathbf{r}(t_2)$ ,
3.  $\mathbf{r}(t_f) = \mathbf{q}$ .

The family of probability distributions  $\mathbf{r}(t)$  satisfying the above is called a *thermomajorizing trajectory* from  $\mathbf{p}$  to  $\mathbf{q}$ . The importance of continuous thermomajorization for transformations under MTPs is captured by the following result established in Ref. [H14]:

$$\mathbf{p}(0) \xrightarrow{\text{MTP}} \mathbf{p}(t_f) \iff \mathbf{p}(0) \succ_\gamma \mathbf{p}(t_f). \quad (40)$$

**Universality of elementary thermalizations.** The second step was to establish the existence of a particularly simple thermomajorizing trajectory for every pair of probability distributions satisfying  $\mathbf{p}(0) \succ_\gamma \mathbf{p}(t_f)$ . This is achieved through *elementary thermalizations*, each of which acts only on two energy levels  $(i, j)$  and is represented by an extremely simple reset Markovian master equation

$$\frac{dp_i}{dt} = \frac{1}{\tau} \left( \frac{\gamma_i}{\gamma_i + \gamma_j} (p_i + p_j) - p_i \right), \quad \frac{dp_j}{dt} = -\frac{dp_i}{dt}.$$

which describes an exponential relaxation to equilibrium:

$$\mathbf{p}^{i,j}(t) = e^{-t/\tau} \mathbf{p}^{i,j}(0) + N_{ij}(0)(1 - e^{-t/\tau}) \boldsymbol{\gamma}^{i,j}. \quad (42)$$

Above,  $\mathbf{x}^{i,j}(t) := (x_i(t), x_j(t))$  and  $N_{ij} = p_i(0) + p_j(0)$ . Formally, this can be represented by a matrix equation

$$\mathbf{p}^{i,j}(t) = T^{i,j}(\lambda_t) \mathbf{p}^{i,j}(0) \quad (43)$$

with  $\lambda_t = 1 - e^{-t/\tau}$  and

$$T^{i,j}(\lambda) = \begin{bmatrix} (1 - \lambda) + \frac{\lambda \gamma_i}{\gamma_i + \gamma_j} & \lambda \frac{\gamma_i}{\gamma_i + \gamma_j} \\ \lambda \frac{\gamma_j}{\gamma_i + \gamma_j} & (1 - \lambda) + \frac{\lambda \gamma_j}{\gamma_i + \gamma_j} \end{bmatrix}. \quad (44)$$

These transformations stand out for their formal simplicity – they are the stochastic processes with thermal fixed point on two states that can be realized by a Markovian master equation. But they also arise naturally in rather diverse approaches to quantum thermodynamics [57–59], where they are often used as building blocks for more complex protocols [60–62]. The importance of elementary thermalizations for transformations under MTPs was established in Ref. [H14] via the following result:

$$\mathbf{p}(0) \succ_\gamma \mathbf{p}(t_f) \iff \mathbf{p}(t_f) = T^{i_f, j_f}(\lambda_f) \dots T^{i_1, j_1}(\lambda_1) \mathbf{p}(0), \quad (45)$$

i.e., elementary thermalizations form universal thermodynamic control in the sense that whenever there exists some thermomajorizing trajectory connecting  $\mathbf{p}(0)$  and  $\mathbf{p}(t_f)$ , then there also exists such a path defined via elementary thermalizations.

**Second laws in the Markovian regime.** Combining the results from Eq. (40) and Eq. (45), one can establish equivalence between the existence of a Markovian thermal channel between two block-diagonal quantum states described by probability distributions  $\mathbf{p}$  and  $\mathbf{q}$ , and the existence of a finite sequence of elementary thermalizations between these two distributions:

$$\mathbf{p}(0) \xrightarrow{\text{MTP}} \mathbf{p}(t_f) \iff \mathbf{p}(t_f) = T^{i_f, j_f}(\lambda_f) \dots T^{i_1, j_1}(\lambda_1) \mathbf{p}(0). \quad (46)$$

Finally, in Ref. [H14], it was shown how, without loss of generality, one can restrict most of the above elementary thermalizations to a finite class of full thermalizations with  $\lambda = 1$ . As a result, one ends up with a finite number of conditions to be verified, so (D1) is satisfied. Moreover, whenever these are satisfied, one also knows exactly how to construct an MTP from  $\mathbf{p}(0)$  to  $\mathbf{p}(t_f)$  using elementary thermalizations, so (D2) is satisfied. To state these conditions, one needs to introduce the following two notions. First, a  $\gamma$ -ordering  $\boldsymbol{\pi}(\mathbf{p})$  of a given vector  $\mathbf{p}$  is the reordering of  $\{1, \dots, d\}$  that sorts  $p_i/\gamma_i$  in a non-increasing order. Second, a

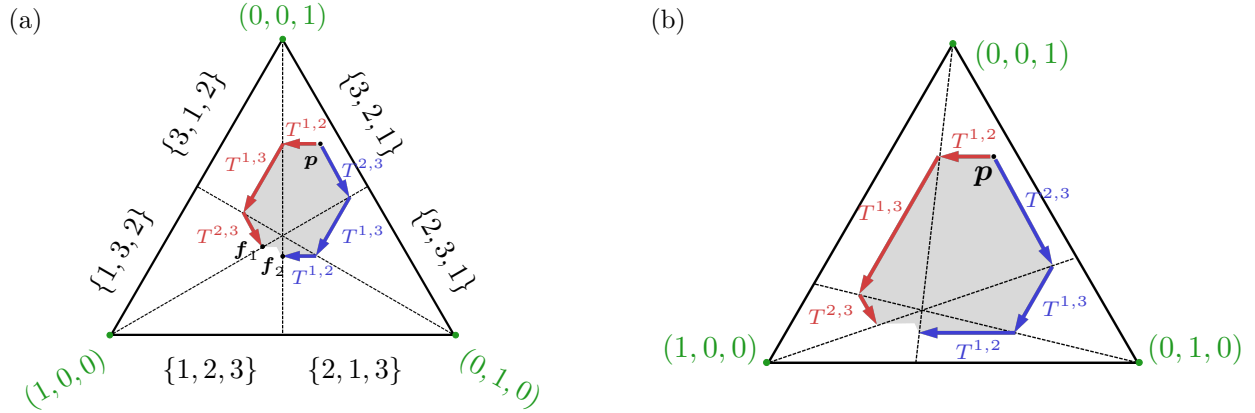


Figure 7: **States achievable via MTP for  $d = 3$ .** (a) Simplex representing the state space of all 3-dimensional probability distributions with regions of fixed  $\gamma$ -orderings indicated by  $\{.,.,.\}$ . The optimal paths connecting a state  $\mathbf{p}(0)$  with  $\gamma$ -ordering  $\{3, 2, 1\}$  to states  $\mathbf{f}_1, \mathbf{f}_2$  of  $\gamma$ -ordering  $\{1, 2, 3\}$  are realized by elementary thermalizations  $T^{i,j}$  (indicated by red and blue arrows). The set of states with  $\gamma$ -ordering  $\{1, 2, 3\}$  achievable from  $\mathbf{p}(0)$  by Markovian thermal processes is finally obtained as the union of the set of  $\mathbf{q}$  thermomajorized by  $\mathbf{f}_1$  and the set of  $\mathbf{q}$  thermomajorized by  $\mathbf{f}_2$ . Here the thermal state was chosen to be  $\gamma = [1/3, 1/3, 1/3]$ , which corresponds to the infinite temperature limit. (b) The grey area denotes the set of achievable states from  $\mathbf{p}$  under arbitrary Markovian thermal processes when the thermal state is  $\gamma = [1/2, 1/3, 1/6]$ . The elementary thermalizations  $T^{i,j}$ , which fully thermalize the pair of levels  $i$  and  $j$  and whose action is indicated by red and blue arrows, play a central role in the sequence of required controls.

sequence of  $\gamma$ -ordering vectors  $\{\pi^k\}$  is canonical when  $\pi^k$  and  $\pi^{k+1}$  differ only by a transposition of adjacent elements, and each  $\gamma$ -ordering appears at most once in the sequence. The central result of Ref. [H14] is then as follows. Given  $\mathbf{p}$  and  $\mathbf{q}$ , enumerate all canonical sequences  $\{\pi^k\}_{k=1}^N$  with  $\pi^1 = \pi(\mathbf{p})$  and  $\pi^N = \pi(\mathbf{q})$ . For each sequence, construct the state

$$\mathbf{f} := \prod_{k=1}^{N-1} T^{i_k, j_k}(1)\mathbf{p}, \quad (47)$$

where  $T^{i_k, j_k}(1)$  are full elementary thermalizations with  $\lambda = 1$  and the levels  $i_k, j_k$  are the labels indicating which of the elements of  $\pi^k$  and  $\pi^{k+1}$  differ. Then  $\mathbf{p} \xrightarrow{\text{MTP}} \mathbf{q}$  if and only if for at least one  $\mathbf{f}$

$$\mathbf{f} \succ_{\gamma} \mathbf{q}. \quad (48)$$

In Fig. 7, it is illustrated how to verify the above complete second laws conditions for a simple example of a system of dimension  $d = 3$ . Moreover, an explicit algorithm verifying the conditions for arbitrary  $d$  was explained in detailed in Ref. [H14] and a corresponding `Mathematica` code was provided [63].

**Optimizing thermalizations.** Work [H15] employed the mathematical tools derived in Ref. [H14] to solve optimization problems involving cooling, work extraction and catalysis, and to quantify the non-Markovianity boosts to the performance of these thermodynamic protocols. It starts by analysing an experimentally relevant setting of heat-bath algorithmic cooling (HBAC) protocols [64–68], whose aim is to achieve the largest possible cooling of a target system by means of protocols involving two main steps. First, a unitary interaction can be performed that involves the target system and some thermal ancilla qubits. Second, there is an interaction between system+ancillas and a thermal environment. The two steps are repeated several times. Experimental realizations have been demonstrated in the context of (liquid and solid) state NMR, ion traps and quantum optical setups, among others [68]. In the well-known PPA protocol [69], the interaction with the environment simply resets the ancilla qubits to a thermal state. For a long time, this was the best known scheme. More recently, the state-reset- $\Gamma$  (SR $\Gamma$ ) protocol [70] was introduced. This is based on the Nuclear Overhauser Effect, and performs a reset of the submanifold  $\{|00\dots 0\rangle, |11\dots 1\rangle\}$  of the energy levels

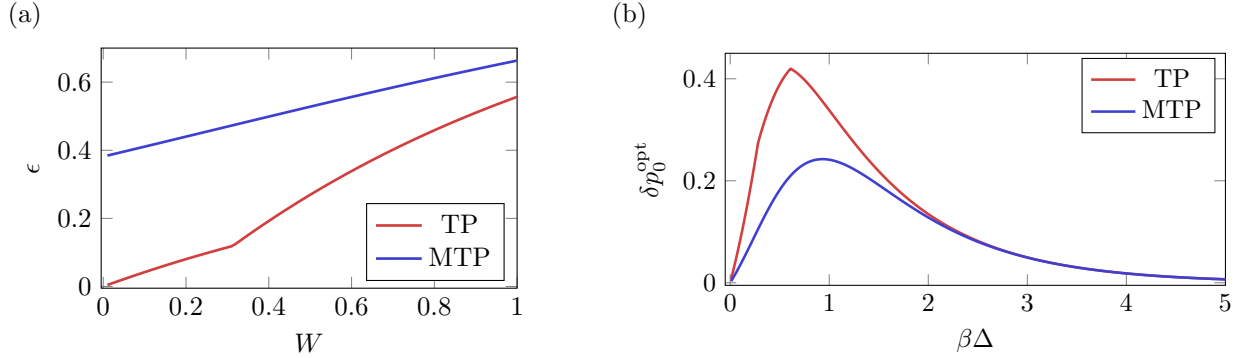


Figure 8: **(a)  $\epsilon$ -deterministic work extraction from a two-level system.** Minimal error  $\epsilon$  as a function of the work  $W$  extracted from a two-level system with energy splitting  $\Delta$  prepared in a thermal state at temperature  $1/\beta_S$  smaller than the environmental temperature  $1/\beta_E$ . System-environment interactions are modelled by TP or MTP. Parameters:  $\beta_S\Delta = 2$  and  $\beta_E\Delta = 1$ . **(b) Optimal cooling of a four-level system.** Optimal change of the ground state population  $\delta p_0^{\text{opt}}$  for a four-level quantum system initially at equilibrium with inverse temperature  $\beta$  in one round of algorithmic cooling consisting of a unitary inversion of the populations, followed by the optimal TP or MTP. The system has equidistant energy spectrum with smallest energy difference  $\Delta$ .

of system+ancillas, hence involving collective interactions which lead to better cooling. Note that in both protocols the interaction with the environment is described by an MTP. One could then ask: is the SRG optimal, or could even better cooling be achieved with similar level of control by tweaking the thermalization dynamics? In Ref. [H15], I show that the framework developed in Ref. [H14] algorithmically returns the SRG protocol as the best available algorithmic cooling protocol on a qubit target system and a qubit thermal ancilla, where the optimization is carried out over all MTPs. This is not only a previously unknown optimality result, but it also showcases how one can move from guesswork to optimization in devising cooling protocols.

Next, the fundamental protocol of work extraction is investigated in Ref. [H15]. Work in quantum thermodynamics is often treated as a random variable, but for microscopic systems its average can be of the same order of magnitude as its fluctuations [46]. Hence, much attention has been given to taming such fluctuations [17, 46, 71, 72]. Single-shot work extraction protocols guarantee to extract an amount of work  $W$  up to a failure probability  $\epsilon$ . More precisely, given an out of equilibrium system  $S$  and access to a thermal environment  $E$  at inverse temperature  $\beta$ , the task is to deterministically excite a battery system  $B$ , initially prepared in an energy eigenstate  $E_0$ , over an energy gap  $W$ . When the probability that  $B$  has energy  $E_0 + W$  is at least  $1 - \epsilon$ , one extracts  $\epsilon$ -deterministic work  $W$  [17]. The optimal extraction error under Thermal Processes (TP), i.e. all processes satisfying (P1)-(P2) but not necessarily memoryless, can be computed via the thermomajorization condition of Ref. [17]. However, when one is limited to MTPs, the optimal error  $\epsilon_{\text{MTP}}(W)$  can be computed with the algorithm of Ref. [H14]. It is observed that memory effects dramatically decrease the minimal error for given  $W$  (see Fig. 8a). Note that  $\epsilon_{\text{MTP}}(W)$  remains very high even in the  $W \rightarrow 0$  limit, showing that converting a non-equilibrium resource into deterministic work either requires control over the energy spectrum (as in Ref. [46, 60]), or otherwise relies on environmental memory effects. In a similar manner, one can provide model-independent evidence of the role played by system-environment correlations in boosting cooling processes. Consider a system initially at equilibrium with the environment at inverse temperature  $\beta$ , and the task of cooling it down by maximising its ground state occupation through a round of algorithmic cooling protocol. The first step of the protocol is to unitarily invert the occupations (while thermal occupations are monotonically decreasing with growing energy, the inverted occupations are monotonically increasing); and the second step is to optimally interact it with the bath to maximise the occupation of the ground state. Now, the interactions may be optimised over all TPs or all MTPs, and the difference in performance quantifies the boost to cooling due to memory effects. This is illustrated in Fig. 8b for a four-level system with an equidistant spectrum.

What is more, one is not only limited to investigations of the difference in performance of thermodynamic protocols with and without memory, but one can also interpolate between these two extremes. This question

relates to the well-known topic of *catalysis* in thermodynamics [73–75]. Catalysis is the phenomenon by which a certain transformation  $\mathbf{p} \mapsto \mathbf{q}$  is only possible when aided by an auxiliary system  $\mathbf{c}$  (the catalyst, playing the role of a memory), which is given back unchanged and uncorrelated at the end:  $\mathbf{p} \otimes \mathbf{c} \mapsto \mathbf{q} \otimes \mathbf{c}$ . To illustrate this, consider a two-level system initially at temperature two times higher than that of the bath. Under MTPs and with no catalyst, the system can be cooled at most to the temperature of the bath [76, 77]. The algorithm of Ref. [H14] shows that a qubit thermal catalyst already allows one to cool the original system below the bath’s temperature, highlighting how catalysis is useful not only in the abstract resource theory setting [73–75], but also in the context of Markovian master equations describing standard thermalization models. What is more, differently from previous approaches, the algorithm returns an explicit set of controls implementing the protocol. This tackles one of the main challenges that insofar prevented the general results on catalysis to impact practical protocols.

**A complete set of entropy production relations.** Finally, the results obtained in Refs. [H14, H15] also allow one to greatly strengthen the standard positive entropy production inequality,

$$\frac{d\Sigma(t)}{dt} = \frac{dS(t)}{dt} - \beta J(t) \geq 0, \quad (49)$$

where  $S(t) := -\text{Tr}(\rho(t) \log \rho(t))$  is the von Neumann entropy,  $J := \text{Tr}(Hd\rho(t)/dt)$  is the heat current flowing to the system, and  $\rho(t)$  is the state of the system interacting with a heat bath in a memoryless way. Specifically, it was shown that for any well-behaved convex function  $h : \mathbb{R} \rightarrow \mathbb{R}$ , the  $h$ -divergence defined by

$$\Sigma_h(t) = - \sum_{i=1}^d \gamma_i h \left( \frac{p_i(t)}{\gamma_i} \right), \quad (50)$$

must be monotonically non-decreasing,  $d\Sigma_h(t)/dt \geq 0$ . For each choice of  $h$ , the above qualifies as a valid *generalized entropy production* (GEP) inequality. Choosing  $h(x) = x \log(x)$ , one obtains:  $d\Sigma_d(t)/dt = dS_d(t)/dt - \beta J(t) \geq 0$ , where  $S_d(t) = -\sum_i p_i(t) \log p_i(t)$  is often referred to as the *diagonal entropy* [78]. This recovers a result recently appearing in Ref. [79], and can be used to derive the standard entropy production inequality in Eq. (49). Hence, the GEP framework implies the usual entropy production relation. Choosing  $h(x) = \text{sgn}(\alpha)x^\alpha/(\alpha - 1)$  for  $\alpha \in \mathbb{R}$ , one obtains  $d\Sigma_\alpha(t)/dt \geq 0$ , where  $\Sigma_\alpha(t) = -S_\alpha(\mathbf{p}(t)\|\boldsymbol{\gamma})$  is the relative Rényi entropy. This recovers the “second laws” of Ref. [73] in a more stringent form. In contrast to the end-point conditions of Ref. [73], constraints obtained here prescribe that all the  $\Sigma_\alpha$  must be constantly non-decreasing along the dynamical trajectory  $\mathbf{p}(t)$ . When  $\boldsymbol{\gamma}$  is a uniform distribution (infinite temperature limit) the above conditions reduce to the non-decreasing of all Rényi entropies [80]. Another relevant class of GEP inequalities can be found taking  $h_q(x) = \text{sgn}(q)(1 - x^q)/(1 - q)$ , giving  $d\Sigma_q^T(t)/dt \geq 0$ , with  $\Sigma_q^T(t) = -S_q^T(\mathbf{p}(t)\|\boldsymbol{\gamma})$  and  $S_q^T(\mathbf{p}\|\boldsymbol{\gamma}) := \text{sgn}(q)(\sum_i p_i^q \gamma_i^{1-q} - 1)/(q - 1)$  being the Tsallis relative entropy. The Tsallis entropies, well-known in non-extensive statistical mechanics and information theory [81–83], are recovered in the infinite temperature limit. This extends to arbitrary temperatures the results of Ref. [84]. Taking  $h(x) = -\log x$  we get  $-d\mathcal{V}(t)/dt \geq 0$ , with  $\mathcal{V}(t) = -S(\boldsymbol{\gamma}\|\mathbf{p}(t))$  the ‘vacancy’, found in Ref. [85] to be the central constraint at very low temperatures.

The obtained GEP inequalities encompass a wealth of disparate results as part of a unified framework. At the same time, a natural question arises: is there a family of entropic conditions that implies *all others*? The affirmative answer was found in Ref. [H14] and it can be interpreted as a sort of exhaustive  $H$ -theorem. Namely, all GEP inequalities are implied by the non-decreasing of

$$\Sigma_a(t) := - \sum_{i=1}^d \left| p_i(t) - a \frac{\gamma_i}{\gamma_d} \right|, \quad a \in [0, 1]. \quad (51)$$

What is more, if there exists a trajectory connecting  $\mathbf{p}(0)$  and  $\mathbf{p}(t_f)$  along which all  $\Sigma_a$  do not decrease, then there exists an MTP transforming  $\mathbf{p}(0)$  into  $\mathbf{p}(t_f)$ . Not only  $\Sigma_a$  are a complete set of GEP, but they even guarantee the existence of a physical realization. In contrast, to satisfy the standard entropy production relation along a trajectory does not ensure the existence of a physical process.

#### 4.4.2 Quantum advantage for memoryless processes

**Quantum embeddable stochastic evolutions.** While works [H14, H15] were devoted to studying the effect of memory constraints in a thermodynamic setting, in Ref. [H9] I focused on the memory constraints themselves (i.e., on evolutions described by Eq. (33), but not necessarily satisfying properties (P1)-(P2)). In particular, I compared the power of classical and quantum memoryless processes, and showed that the latter ones can simulate classical processes that necessarily require memory. Thus, I discovered a novel quantum advantage, where memory-constrained quantum dynamics is more powerful than its classical counterpart.

Recall that, in a classical setting, a state of a  $d$ -dimensional system is described by a probability distribution  $\mathbf{p}$  over states  $\{1, \dots, d\}$ . A stochastic matrix or process  $P$  is a matrix  $P_{ij}$  of transition probabilities,

$$P_{ij} \geq 0, \quad \sum_i P_{ij} = 1, \quad (52)$$

which describes the evolution of the system from one state  $\mathbf{p}$  to another  $P\mathbf{p}$ . Classically, matrices  $P$  that can be achieved without employing memory are known as *embeddable*, i.e., a stochastic matrix  $P$  is embeddable if it can be generated by a continuous Markov process [86]. This notion can be understood as a control problem involving a master equation. Namely, introducing a *rate matrix* or *generator*  $L$  as a matrix with finite entries satisfying

$$L_{ij} \geq 0 \text{ for } i \neq j, \quad \sum_i L_{ij} = 0, \quad (53)$$

a continuous one-parameter family  $L(t)$  of rate matrices generates a family of stochastic processes  $P(t)$  satisfying

$$\frac{d}{dt}P(t) = L(t)P(t), \quad P(0) = \mathbb{1}. \quad (54)$$

The aim of the control  $L(t)$  is to realize a target stochastic process  $P$  at some final time  $t_f$  as  $P = P(t_f)$ , and if this is possible for some choice of  $L(t)$ , then  $P$  is embeddable. The question of which stochastic matrices  $P$  are embeddable is a challenging open problem that has been extensively investigated for decades [86–91]. The full characterization does not go beyond  $2 \times 2$  and  $3 \times 3$  stochastic matrices, however various necessary conditions have been found. In particular, in Ref. [90] it was proven that every embeddable stochastic matrix  $P$  satisfies the following inequalities:

$$\prod_i P_{ii} \geq \det P \geq 0. \quad (55)$$

The condition  $\det P \geq 0$  is, in fact, also known to be sufficient in dimension  $d = 2$  [88], and a time-independent rate matrix  $L$  can then be found.

In a quantum setting, a state of a  $d$ -dimensional quantum system is given by a  $d \times d$  density matrix  $\rho$ , while a general evolution is described by a quantum channel  $\mathcal{E}$ . Now, focussing on the computational basis  $\{|k\rangle\}_{k=1}^d$ , suppose we input the quantum state  $\rho_{\mathbf{p}} = \sum_k p_k |k\rangle\langle k|$ , apply the channel  $\mathcal{E}$  and measure the resulting state  $\mathcal{E}(\rho_{\mathbf{p}})$  in the computational basis. The measurement outcomes will be distributed according to  $P\mathbf{p}$ , where

$$P_{ij} = \langle i | \mathcal{E}(|j\rangle\langle j|) | i \rangle. \quad (56)$$

In this way, the preparation of  $\rho_{\mathbf{p}}$ , followed by a channel  $\mathcal{E}$  and the computational basis measurement, simulates the action of a stochastic process  $P$  on the classical state  $\mathbf{p}$ . In Ref. [H9] a stochastic matrix  $P$  was defined as *quantum-embeddable* if it could be simulated by a quantum process as in Eq. (56) with  $\mathcal{E}$  a *Markovian quantum channel* [92], i.e. a channel that can result from a Markovian master equation given by Eq. (33).

**Advantages in simulations.** It is relatively straightforward to show that all classically-embeddable stochastic processes are also quantum-embeddable. However, the converse is not true. As shown in Ref. [H9], there exist many stochastic matrices  $P$  that can be generated by a quantum, but not a classical Markov process. The simplest example is given by a non-trivial permutation  $\Pi$ , satisfying

$$\det \Pi = \pm 1, \quad \prod_i \Pi_{ii} = 0. \quad (57)$$

Clearly, Eq. (55) is violated and hence  $\Pi$  is not embeddable. However, noting that every unitary channel  $U(\cdot)U^\dagger$  is Markovian, and that a permutation matrix  $\Pi$  is unitary, one concludes that every permutation  $\Pi$  is quantum-embeddable. This conclusion also proves that neither of the two conditions in Eq. (55) are necessary for quantum-embeddability. More generally, a larger class of stochastic matrices that are quantum-embeddable is given by the set of *unistochastic* matrices defined by [93, 94]

$$P_{ij} = |\langle j|U|i\rangle|^2 \quad (58)$$

for some unitary matrix  $U$ . The set of unistochastic matrices includes permutations, but also other (classically) non-embeddable stochastic matrices. As an example one can consider any  $2 \times 2$  bistochastic matrix, since in dimension  $d = 2$  every bistochastic matrix is unistochastic and so it is quantum-embeddable. In fact, in Ref. [H9], this result was strengthened, as it was proven there that all  $2 \times 2$  stochastic matrices are quantum-embeddable. Moreover, one can generate larger families of quantum embeddable stochastic matrices by employing the result of Ref. [H9] stating that quantum-embeddable stochastic matrices are closed under composition, i.e., if  $P$  and  $Q$  are quantum-embeddable, then also  $PQ$  is. Thus, for general dimension  $d$ , one can compose, e.g., classically embeddable matrices with unistochastic ones. Moreover, by composing  $2 \times 2$  stochastic matrices acting on different two-dimensional subspace, one obtains that all products of pinching matrices [95] (also known as factorisable matrices [H11]) are quantum-embeddable. In conclusion, quantum embeddings allow one to achieve many stochastic processes that necessarily require memory from a classical standpoint. As a particular example, consider  $3 \times 3$  circulant stochastic matrices, defined by

$$P = \begin{bmatrix} 1 - a - b & a & b \\ b & 1 - a - b & a \\ a & b & 1 - a - b \end{bmatrix}. \quad (59)$$

For such matrices, the necessary and sufficient conditions for classical embeddability were found in Ref. [96], and their set is illustrated by an orange region in Fig. 9a. On the other hand, as shown in Ref. [H9], quantum embeddable circulant stochastic matrices include not only classically embeddable matrices, but also their compositions with any unistochastic matrix. As a result, the quantum set is a larger blue region in Fig. 9a.

**Advantages in space-time cost.** The next step in Ref. [H9] was to go beyond the simple distinction between stochastic processes that can or cannot be simulated without memory, and take a more quantitative approach. To this end, the recent formalism of Ref. [97] was employed, which allows one to quantify the classical space-time cost of a given stochastic process, i.e., the minimal amount of memory and time-steps needed to classically implement a given process. More formally, let  $P$  be a non-embeddable stochastic matrix acting on  $d$  so-called *visible* states. One may then ask: how many additional *memory* states  $m$  are needed, in order to implement  $P$  by a classical Markov process? One thus looks for an embeddable stochastic matrix  $Q$  acting on  $d + m$  states whose restriction to the first  $d$  rows and columns is identical to  $P$ . When this happens,  $Q$  is said to *implement*  $P$  with  $m$  memory states. Following Ref. [97], one defines the *space cost* of a  $d \times d$  stochastic matrix  $P$ , denoted  $C_{\text{space}}(P)$ , as the minimum  $m$  such that there exists a  $(d + m) \times (d + m)$  embeddable matrix  $Q$  implementing  $P$ . Once a matrix  $Q$  implementing  $P$  is found, the next question may be: what is the number of time-steps required to realise  $Q$ ? The notion of a time-step is meant to capture the number of independent controls that are needed to achieve  $Q$ . Again, following Ref. [97], a stochastic matrix  $T$  is called *one-step* if it is embeddable and the controls  $L(t)$  that generate  $T$  at time  $t_f$  through Eq. (54) can be chosen such that the set of non-zero transition probabilities of  $P(t)$  is the same for all  $t \in (0, t_f)$ . The *time cost*  $C_{\text{time}}(P, m)$  of a  $d \times d$  stochastic matrix  $P$ , while allowing for  $m$  memory states, is then defined as the minimum number  $\tau$  of one-step stochastic matrices  $T^{(i)}$  of dimension  $(d + m) \times (d + m)$  such that  $Q = T^{(\tau)} \dots T^{(1)}$  implements  $P$ . Classical notions of space and time cost were extended in Ref. [H9] in a natural way to the quantum domain, i.e., a quantum space cost,  $Q_{\text{space}}(P)$ , and a quantum time cost,  $Q_{\text{time}}(P, m)$ , were introduced.

The central question in the classical setting is to find  $C_{\text{space}}(P)$  and then characterise  $C_{\text{time}}(P, m)$  for  $m \geq C_{\text{space}}(P)$ . The main result of Ref. [97] was to solve this problem for stochastic matrices  $P_f$  that are  $\{0, 1\}$ -valued or, in other words, represent a function  $f$  over the set of states  $\{1, \dots, d\}$ . More precisely, it was shown that the time cost of  $P_f$  is given by

$$C_{\text{time}}(P_f, m) = \left\lceil \frac{m + d + \max[\text{c}(f) - m, 0] - \text{fix}(f)}{m + d - |\text{img}(f)|} \right\rceil + b_f(m) \geq \left\lceil \frac{m + d - \text{fix}(f)}{m + d - |\text{img}(f)|} \right\rceil,$$

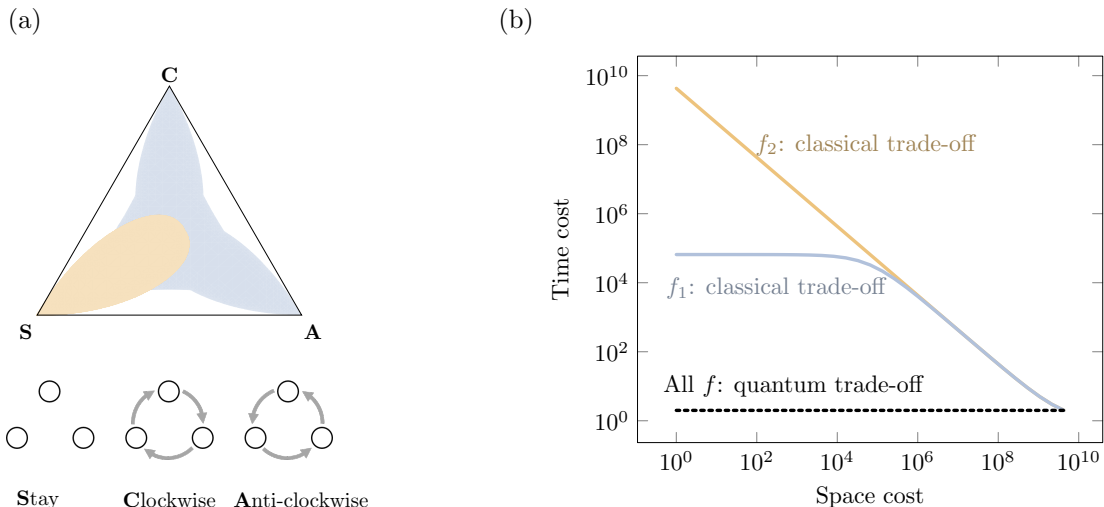


Figure 9: **(a) Embeddability of  $3 \times 3$  circulant matrices.** The vertices of the triangle correspond to deterministic processes (**S**: stay, **C**: move clockwise, **A**: move anti-clockwise) for a random walker moving between three states. Points inside the triangle correspond to probabilistic mixtures (convex combinations) of these three deterministic processes, e.g., the centre of the triangle corresponds to the maximally mixing dynamics (with **S**, **C** and **A** each happening with probability  $1/3$ ). The orange petal-shaped region contains all stochastic processes that can arise from time-continuous memoryless classical dynamics. For time-continuous memoryless quantum dynamics this set is enlarged by the remaining shaded region in blue. **(b) Classical versus quantum space-time trade-off.** The optimal trade-off between space cost and time cost of implementing stochastic matrices for a system of  $s = 32$  bits, i.e., with dimension  $d = 2^{32}$  (plotted in log-log scale). Solid coloured curves correspond to optimal trade-offs for classically implementing exemplary  $\{0, 1\}$ -valued stochastic matrices described by functions  $f_1(i) = i \oplus 1$  (addition modulo  $d$ ) and  $f_2(i) = \min\{i + 2^{s/2}, 2^s - 1\}$ , as analysed in Ref. [97]. Dashed black curve corresponds to optimal trade-offs for quantumly implementing any  $\{0, 1\}$ -valued stochastic matrix, thus illustrating a quantum advantage.

where  $\text{fix}(f)$  is the number of fixed points of  $f$ ,  $|\text{img}(f)|$  is the dimension of the image of  $f$ ,  $c(f)$  is the number of cycles of  $f$ , and  $b_f(m) = 0$  or  $1$ . For the state space given by all bit strings of length  $s$  (so  $d = 2^s$ ), the above shows that if  $|\text{img}(f)|$  is  $O(d)$ , then  $P_f$  is expensive to simulate by memoryless dynamics unless the number of fixed points is also  $O(d)$ . Since for a typical  $f$  one has  $|\text{img}(f)| = O(d)$  and  $\text{fix}(f) = O(1)$ , one concludes that typically  $C_{\text{time}}(P_f, m) = O(2^s/m)$ , i.e., an exponential number of memory states are required to have an efficient simulation in the number of time-steps. Conversely, one needs an exponential number of time-steps to have an efficient simulation for a fixed number of memory states. Analogous question concerning the space-time trade-off was asked and answered in Ref. [H9] for the quantum domain. Surprisingly, it was proven that for any  $m \geq 0$  and any function  $f$ , one has

$$Q_{\text{time}}(P_f, m) \leq 2. \quad (60)$$

Hence, one can achieve every function quantumly using zero memory states and only two time-steps, compared to the typical classical cost  $C_{\text{time}}(P_{f_1}, m) \geq d/m$ . This result, illustrated in Fig. 9b, is quantitative evidence of the power of superposition to act as effective memory.

**Advantages in control.** Finally, in Ref. [H9], I also demonstrated that the set of classical states accessible via Markovian master equations with quantum controls is larger than the set of those accessible with classical controls, leading, e.g., to a potential advantage in cooling protocols. More precisely, I proved that quantum memoryless dynamics with a given fixed point (e.g., a thermal Gibbs state), as compared to classical memoryless dynamics with the same fixed point, allow one to access a larger set of final states from any initial state. This is most evident in the case of maximally mixed fixed points, since every transformation that is classically possible with arbitrary amounts of memory can be realised in a memoryless fashion in the quantum

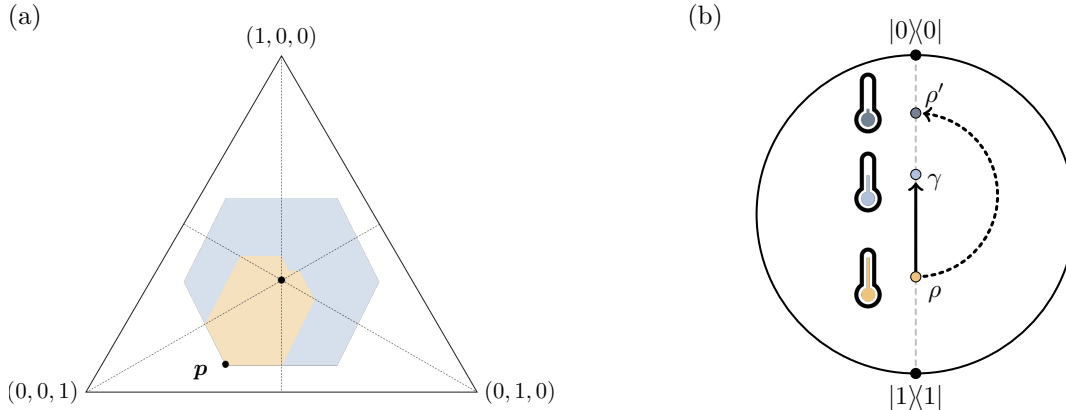


Figure 10: **(a) Quantum advantage for a uniform fixed point and  $d = 3$ .** The sets of states accessible via classical (smaller orange shape) and quantum (larger blue hexagon) memoryless dynamics with a uniform fixed point for a system of dimension  $d = 3$  and an exemplary initial state  $\mathbf{p}$  (each point inside a triangle corresponds to a probabilistic mixture of sharp distributions). The blue region coincides with the set of states achievable classically via processes employing with a uniform fixed point and employing arbitrary amounts of memory. **(b) Markovian cooling of a qubit.** Classical memoryless processes can only cool the initial state  $\rho$  of a two-dimensional system to the thermal state  $\gamma$  at the environmental temperature (path along the solid line arrow). Quantum memoryless dynamics with fixed point  $\gamma$  allows one to cool the system below that, all the way to the state  $\rho'$  with the lowest temperature achievable by classical processes with memory (path along the dotted line arrow).

domain (see Fig. 10a). For general fixed points, an analogous result was proven for systems of dimension  $d = 2$ , and it was argued that the set of accessible states is strictly larger in the quantum regime than in the classical one for all  $d$ . Since it is known that memory effects enhance cooling [76, 98], a direct consequence of the results presented in Ref. [H9] is that quantumly it is possible to bring a two-dimensional system below the environmental temperature without employing memory effects, something that is impossible classically (see Fig. 10b).

## 4.5 Results on symmetry constraints

### 4.5.1 Optimal processes under time-translation and rotational symmetries

**Time-translation covariant dynamics.** In Ref. [H2], I focused on symmetry under time translations, a property characterising dynamical evolutions whose action is insensitive to their particular timing. Such dynamics constrain possible transformations of coherence, which then becomes an essential resource in quantum information processing [99, 100]. A central question is therefore: what is the minimal amount of decoherence compatible with a given population dynamics (e.g., relaxation process)? The main technical contribution of Ref. [H2] is the minimal decoherence theorem, which gives the optimal coherence evolution consistent with a given population dynamics among all time-translation symmetric and Markovian processes. The evolution of quantum states under such processes is described by a master equation from Eq. (33), with a time-independent Lindbladian  $\mathcal{L}$  (i.e., given by Eq. (35) with constant jump rates  $r_i$  and jump operators  $L_i$ ) satisfying the covariance property from Eq. (37). Note that this property is equivalent to stating that the channel  $\mathcal{E}_t$  describing the evolution,

$$\mathcal{E}_t(\rho) := e^{(-i\mathcal{H} + \mathcal{L})t}(\rho), \quad (61)$$

is time-translation covariant:

$$\mathcal{E}_t \left( e^{-i\mathcal{H}t'}(\rho) \right) = e^{-i\mathcal{H}t'}(\mathcal{E}_t(\rho)), \quad (62)$$

where  $e^{-i\mathcal{H}t}(\rho) = e^{-i\mathcal{H}t}\rho e^{i\mathcal{H}t}$ . As a result of time-translation covariance, the evolution of populations (diagonal terms  $|x\rangle\langle x|$ ) of a density matrix  $\rho$  decouples from the evolution of coherences (off-diagonal terms  $|x\rangle\langle y|$ )

of  $\rho$ ), and the latter one can also be divided into independently evolving modes [101]. Introducing the vector of populations  $\mathbf{p}$  with components defined by  $p_x := \rho_{xx}$ , the evolution of  $\mathbf{p}(t)$  is then fully described by the *population transfer rate matrix*  $L$ ,

$$\frac{d\mathbf{p}}{dt} = L\mathbf{p}, \quad (63)$$

where the matrix elements of  $L$  are given by

$$L_{x'|x} = \langle x' | \mathcal{L}(|x\rangle\langle x|) |x'\rangle. \quad (64)$$

The significance of the symmetry captured by Eq. (62) may initially seem unclear since, despite its broad applicability, it is often referred to differently in different fields, and it is sometimes hidden within various physical approximations. Within quantum optics, time-translation symmetry is a consequence of the *rotating-wave approximation* (RWA). This corresponds to manipulating the interaction Hamiltonian by discarding the so-called counter-rotating terms, which are those which rotate with higher frequency in the interaction picture. A typical example is the Jaynes-Cummings Hamiltonian, which in the simplest case reads  $H_{JC} \propto (\sigma_+ + \sigma_-) \otimes (a + a^\dagger)$ , with  $\sigma_\pm$  denoting qubit raising/lowering operators and  $a, a^\dagger$  being bosonic annihilation and creation operators. In this case the approximation discards the terms  $\sigma_- \otimes a$  and  $\sigma_+ \otimes a^\dagger$ , which leads to a master equation satisfying Eq. (62). More generally, within the theory of open quantum systems, Eq. (62) is called the *secular approximation*, and it coincides with discarding terms in the Lindbladian that would prevent the commutation relation specified by Eq. (37) from being satisfied. It is in fact a “safer” way of implementing the RWA [102] and is broadly used in applications [21]. In quantum metrology, for the task of estimating the phase  $\phi$  of a unitary  $U_\phi$  generated by the Hamiltonian  $H$ ,  $U_\phi = e^{-iH\phi}$ , Eq. (62) identifies the set of quantum channels that degrade *any* metrological resource  $\rho$  [100]. Furthermore, in quantum information, Eq. (62) coincides with the set of channels that can be performed in the absence of a reference frame for time, or in the presence of a superselection rule for particle number [25]. A dual perspective comes from the theory of  $U(1)$ -asymmetry, which is a resource theory where Eq. (62) defines the set of free operations [24]. This is in fact a resource theory of quantum coherence in the basis defined by  $H$  [100]. Finally, time-translation covariance can also be linked to a global conservation law on energy [24, 103] and it is one of the defining properties of thermal operations [29].

**Minimal decoherence theorem.** The central result of Ref. [H2] provides a bound on the optimal amount of coherence that can be preserved in a state at time  $t$ , in terms of the entries of the population transfer rate matrix  $L$ . For notational convenience the matrix elements of a density matrix  $\rho$  in the energy eigenbasis will be parametrized in the following way:  $\rho_{xy} = |\rho_{xy}| \vartheta_{xy}$ , where  $\vartheta_{xy}$  is a phase factor,  $|\vartheta_{xy}| = 1$ . One also needs to define damping rates  $\gamma_{x'y'} := (|L_{x'|x'}| + |L_{y'|y'}|)/2$ , transport rates  $t_{y'|y}^{x'|x} := \sqrt{L_{x'|x} L_{y'|y}}$  and introduce the symbol  $\sum_{x,y}^{(\omega)}$  to indicate the sum over indices of a mode  $\omega$ , i.e.,  $x, y$  with a fixed energy difference  $E_x - E_y = \omega$ . Also, let  $\tilde{\rho}_{x'y'}(t)$  be the solution of

$$\frac{d\tilde{\rho}_{x'y'}}{dt} = -\gamma_{x'y'} \tilde{\rho}_{x'y'} + \sum_{\substack{x \neq x' \\ y \neq y'}}^{(\omega_{x'y'})} t_{y'|y}^{x'|x} \tilde{\rho}_{xy}, \quad (65)$$

with  $\tilde{\rho}_{x'y'}(0) = |\rho_{x'y'}(0)|$ . Then, if the time evolution of  $\rho$  is time-translation covariant and Markovian with population transfer rate matrix  $L$ , one has

$$|\rho_{x'y'}(t)| \leq \tilde{\rho}_{x'y'}(t), \quad (66)$$

for all  $t \geq 0$ . Moreover, the bound can be saturated for all elements of a mode  $\omega$  if for every  $x', y', x, y$  with  $E_{x'} - E_{y'} = E_x - E_y = \omega$  one has

$$\vartheta_{x'y'}(0) \vartheta_{xy}^*(0) = \vartheta_{x'x}(0) \vartheta_{y'y}^*(0). \quad (67)$$

Eq. (67) will be referred to as the *Markovian phase-matching* condition for the initial state. It is important to point out that pure states, and also mixed states for which amplitudes share a common phase (i.e.,  $\vartheta_{xy} = \vartheta$

for all  $x$  and  $y$ ), satisfy this condition for all modes. Moreover, the Markovian phase-matching condition is also satisfied independently of the initial state for modes consisting of a single element or two overlapping elements, i.e.,  $\rho_{xy}$  and  $\rho_{x'y'}$  with  $x = y'$ . Finally, it is crucial to note that the evolution of  $|\rho_{xy}|$  only depends on elements  $|\rho_{x'y'}|$  with  $E_{x'} - E_{y'} = E_x - E_y$ , which reflects the mode structure of the time-translation symmetric Lindbladian. Physically, the above result demonstrates a combination of decay and transport phenomena, corresponding to each of the two terms in Eq. (65) that contribute to the evolution of  $\rho_{x'y'}$ . The first is a *decay term*, proportional to the amount of coherence  $\rho_{x'y'}$  itself. If only this term were present then one would obtain a familiar exponential damping of coherence (with rate  $\gamma_{x'y'}$ ), due to the presence of the dissipative environment. The extra contributions to the evolution of  $\rho_{x'y'}$  are *transport terms*. Only coherence elements  $\rho_{xy}$  that rotate with the same frequency as  $\rho_{x'y'}$  (i.e., belong to the same mode of coherence) can contribute, as indicated by the restricted summation. This “selection rule” is imposed by the underlying time-translation symmetry. The transport terms themselves have a suggestive physical interpretation. Namely,  $L_{x'|x}$  is the transfer rate of the classical process that maps the energy state  $x$  into  $x'$ , so  $L_{x'|x}p_x(t)dt$  gives the population flow from  $x$  to  $x'$  between times  $t$  and  $t + dt$ . The transfer of coherence from  $\rho_{xy}$  to  $\rho_{x'y'}$  involves a superposition of *two* classical processes: the mapping of  $x$  into  $x'$  and of  $y$  into  $y'$ . The optimal transport of coherence from  $\rho_{xy}$  to  $\rho_{x'y'}$  is characterised by the geometric mean of the transition rates of these two classical processes, i.e.,  $\sqrt{L_{x'|x}L_{y'|y}}\rho_{xy}(t)dt$ .

**Applications of minimal decoherence theorem.** It is well known that a general solution of a time-translation covariant Markovian evolution of a two-level system yields [21]

$$p(t) = \pi + (p(0) - \pi)e^{-t/T_1}, \quad |c(t)| = e^{-t/T_2}|c(0)|, \quad (68)$$

where  $p(t)$  is the occupation of the ground state,  $c(t)$  is the coherence between ground and excited state,  $\pi$  is the stationary ground state population,  $T_1$  is the relaxation time, and  $T_2$  is the decoherence time. Moreover, it is known that the population relaxation process (described by  $T_1$ ) and the decoherence process (described by  $T_2$ ) are not independent and must satisfy  $T_2 \leq 2T_1$ . This constraint, together with Eq. (68), links possible evolution of coherence with the evolution of population (see Fig. 11a). Using the minimal decoherence theorem, this result was generalised in Ref. [H2] to  $d$ -dimensional quantum systems with non-degenerate Bohr spectrum, i.e., described by Hamiltonians for which all energy differences between any two levels are distinct. For such systems, the evolution of off-diagonal elements is given by

$$|\rho_{xy}(t)| = |\rho_{xy}(0)|e^{-t/T_2^{xy}}, \quad (69)$$

with  $T_2^{xy}$  denoting the decoherence time between energy levels  $x$  and  $y$ . Also, assuming that the population dynamics has a unique stationary distribution  $\boldsymbol{\pi}$  (a situation sometimes referred to as *ergodic* dynamics [58]), the evolution of diagonal elements is given by

$$\boldsymbol{p}(t) = \boldsymbol{\pi} + \sum_{x=1}^{d-1} b_x e^{-t/T_1^x} e^{i \text{Im}(\lambda_x)t} \boldsymbol{v}_x, \quad (70)$$

with  $T_1^x$  being the generalised relaxation times,  $\boldsymbol{v}_x$  denoting the eigenvectors of  $L$ ,  $\lambda_x$  its eigenvalues and  $b_x$  being constants determined by the initial conditions. Then, the following result obtained in Ref. [H2] gives a direct relation between the decoherence times  $T_2^{xy}$  and the relaxation times  $T_1^x$ :

$$\langle T_2 \rangle_h \leq \frac{d}{d-1} \langle T_1 \rangle_h, \quad (71)$$

where  $\langle \cdot \rangle_h$  denotes the harmonic mean over all decoherence times  $T_2^{xy}$  and all relaxation times  $T_1^x$ . Moreover, for general systems (not necessarily with non-degenerate Bohr spectrum), it was proven that if the population dynamics has a unique stationary distribution  $\boldsymbol{\pi}$  with  $\pi_x \neq 0$ , then all coherence term vanish as  $t \rightarrow \infty$ . This is a very strong evidence that the phenomenon of *frozen coherence* [104, 105] requires non-Markovian effects. Finally, Ref. [H2] introduced and analysed the concept of coherence-based witnessing of non-Markovianity. Assume that one knows the initial preparation  $\rho(0)$ , the final state  $\rho(t)$  at a unique time  $t > 0$ , and the fixed point of the evolution  $\rho(\infty)$ . As discussed in Ref. [H2], sometimes this knowledge is enough to deduce whether the evolution of the system is non-Markovian. This is because if the evolution was Markovian,

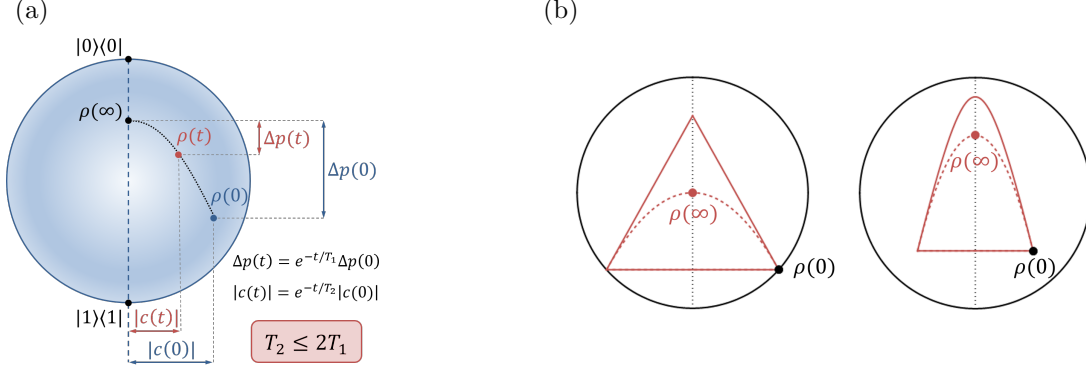


Figure 11: **(a) Relaxation and decoherence times.** The evolution of the initial qubit state  $\rho(0)$  towards the stationary state  $\rho(\infty)$  presented on the Bloch sphere. During the evolution the difference between the current population and the stationary population,  $\Delta p(t) = |p(t) - \pi|$ , must decrease. Due to a constraint linking relaxation and decoherence processes, at any time the ratio between the current and initial coherence,  $|c(t)|/|c(0)|$ , is bounded by  $\sqrt{\Delta p(t)/\Delta p(0)}$ . **(b) Qubit covariant dynamics: Markovian vs non-Markovian.** The dashed lines show the maximum coherence preservation possible with Markovian covariant dynamics with a given fixed point  $\rho(\infty)$ ; the solid lines show the maximum coherence preservation possible for general thermal operations with a thermal state given by  $\rho(\infty)$ . Left: initial state with  $p(0) = 1/6$  and  $c(0) = \sqrt{5}/6$ , and  $\rho(\infty)$  such that  $\pi = (1/2, 1/2)$ . Right: initial state with  $p(0) = 1/4$  and  $c(0) = 1/4$ , and  $\rho(\infty)$  such that  $\pi = (3/4, 1/4)$ .

the minimal decoherence theorem would hold, bounding the allowed state of the system at time  $t$ . This is illustrated in Fig. 11b, where if the observed final state  $\rho(t)$  lies outside the dashed region, one can infer that the dynamics was non-Markovian.

**Symmetry principles versus conservation laws.** Noether's theorem states that for every continuous symmetry of a closed unitary dynamics there is an associated conserved charge [23, 106, 107]. However, the most general kind of evolution of a quantum state, for relativistic or non-relativistic quantum theory, is not unitary dynamics but instead a quantum channel. This broader formalism includes both unitary evolution and open system dynamics, but also allows more general quantum operations such as state preparation or discarding of subsystems. It is therefore natural to ask about the status of Noether's principle for those quantum channels that obey a symmetry principle, and thus, in Ref. [H8], I investigated the maximal possible disconnects between symmetry principles and conservation laws. More precisely, I studied quantum channels  $\mathcal{E}$  between systems  $A$  and  $B$ , constrained to respect a symmetry described by a Lie group  $G$ , i.e.,

$$\mathcal{E}(U_A(g)\rho_A U_A^\dagger(g)) = U_B(g)\mathcal{E}(\rho_A)U_B^\dagger(g) \quad (72)$$

for all  $g \in G$ , where  $U(g)$  denotes a unitary representation of the group  $G$  on the appropriate quantum system. The main focus was on  $U(1)$  and  $SU(2)$  symmetries related to energy and angular momentum conservation laws. The first goal was to derive general bounds on possible deviations from conservation laws for symmetric dynamics. These describe the trade-off between allowed deviations and the departure from closed unitary dynamics as schematically portrayed in Fig. 12a. In order to quantify how close a channel  $\mathcal{E}$  is to a unitary dynamics, the notion of *unitarity* was employed, first introduced in Ref. [108]. It is defined as the average output purity over all pure states with the identity component subtracted, i.e.,

$$u(\mathcal{E}) := \frac{d_A}{d_A - 1} \int \text{Tr} \left( \mathcal{E} \left( \psi - \frac{\mathbb{1}_A}{d_A} \right)^2 \right) d\psi, \quad (73)$$

and satisfies  $u(\mathcal{E}) \leq 1$  with equality if and only if  $\mathcal{E}$  is a unitary channel. In order to quantify the deviations from conservation laws, the notion of *average total deviation*  $\Delta(\mathcal{E})$  from a conservation law was introduced in

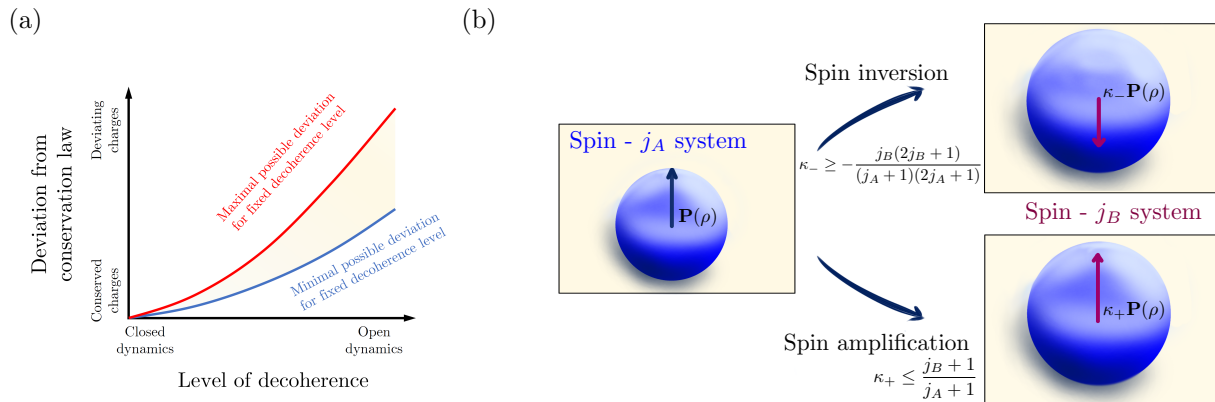


Figure 12: **(a) Robustness of Noether's principle & trade-off relations.** A qualitative description of trade-off relations between deviation from conservation laws and level of decoherence under the dynamics of a symmetric channel. While the red upper bound exists for all symmetries described by connected Lie groups, the lower bound is present when quantum systems have multiplicity-free decompositions. **(b) Spin-inversion and amplification.** There exist quantum channels that can approximately invert or amplify the polarisation of a spin system while exactly respecting  $SU(2)$  rotational symmetry. The values  $\kappa_{\pm}$  provide the ultimate limits of such processes and depend only on the dimension of the spin systems involved.

Ref. [H8]. It is defined as the average  $L_2$  norm of the difference in expectation values between  $\psi = |\psi_A\rangle\langle\psi_A|$  and  $\mathcal{E}(\psi)$  of the symmetry generators,  $\{J_A^k\}_{k=1}^n$  and  $\{J_B^k\}_{k=1}^n$ , associated with conserved charges:

$$\Delta(\mathcal{E}) := \sum_{k=1}^n \int |\text{Tr}(\mathcal{E}(\psi)J_B^k - \psi J_A^k)|^2 d\psi, \quad (74)$$

where the integration is with respect to the standard Haar measure on pure states. Now, in Ref. [H8], it is shown that given any connected compact Lie group, for a symmetric channel  $\mathcal{E}$  approximating a symmetric unitary the associated conservation laws will hold approximately. In other words, there exists an upper bound on the deviation from conservation law in terms of unitarity:

$$\Delta(\mathcal{E}) \leq M(1 - u(\mathcal{E})) \quad (75)$$

for some constant  $M > 0$  that is independent of  $\mathcal{E}$ , and depends only on the dimensions of the systems involved and the symmetry generators. Moreover, it is proven in Ref. [H8] that also the lower bound on the deviation from conservation law in terms of unitarity exists, whenever the quantum system carries a representation  $U_A$  of a Lie group  $G$  for which  $U_A \otimes U_A^*$  has a multiplicity-free decomposition. In particular, this happens in the case of spin- $j$  system with symmetry generators given by higher-dimensional spin angular momenta generating an irreducible representation of  $SU(2)$ . As a result, for a spin- $j$  system, spin angular momentum conservation laws are robust to noise described by a symmetric channel  $\mathcal{E}$  and the following bounds hold:

$$\frac{3\sqrt{2}j^{3/2}}{2j+1}(1 - u(\mathcal{E})) \geq \sqrt{\Delta(\mathcal{E})} \geq \frac{\sqrt{2}j^{1/2}}{(2j+1)^2}(1 - u(\mathcal{E})). \quad (76)$$

**Optimal spin inversion and amplification.** In Ref. [H8], I also show how the  $SU(2)$  symmetry constraints result in impossibility of perfect spin inversion or amplification, and find the optimal allowed approximations of these transformations (see Fig. 12b). The higher-dimensional spin angular momentum observables  $\mathbf{J}_A := (J_A^x, J_A^y, J_A^z)$  along the three Cartesian coordinates generate rotations corresponding to elements  $g \in SU(2)$ , which act on the system via the unitary representations  $U_A(g)$  describing the underlying symmetry principle. A channel  $\mathcal{E}$  is symmetric under rotations, or  $SU(2)$ -covariant, if it satisfies Eq. (72) for all input states  $\rho_A$  and  $g \in SU(2)$ . Now, rotational invariance ensures that the symmetric channel  $\mathcal{E}$  acts on

single spin systems isotropically. As a result, spin polarisation vector  $\mathbf{P}(\rho_A) := \text{Tr}(\mathbf{J}\rho_A)$  of an initial state  $\rho_A$  is simply scaled by the action of  $\mathcal{E}$ , i.e.,

$$\mathbf{P}(\mathcal{E}(\rho_A)) = f(\mathcal{E})\mathbf{P}(\rho_A) \quad (77)$$

for a single parameter  $f(\mathcal{E})$  that is independent of  $\rho_A$  or the spatial direction. The goal is then to determine the symmetric quantum channel  $\mathcal{S}_-$  with coefficient  $f(\mathcal{S}_-)$  that is as close as possible to  $-1$  (which can only be achieved by the unphysical spin-inversion operation). In Ref. [H8], it was proven that the optimal spin polarisation inversion channel is achieved by the extremal point of  $\text{SU}(2)$ -covariant channels with the largest dimension  $2j_A + 1$  of the environment required to implement it, and it results in an inversion factor:

$$\kappa_- := f(\mathcal{S}_-) = -\frac{j_A}{j_A + 1} = -1 + O(1/j_A). \quad (78)$$

This generalises the previous result on optimal approximations of universal-NOT under rotational symmetry, and determines a fundamental limit that quantum theory imposes on the specific task of (universally) inverting the spin of a quantum system. The higher the dimension of the system, the larger is the maximal spin-inversion factor. Specifically, the optimal channel  $\mathcal{S}_-$  in the limit  $j_A \rightarrow \infty$  approaches  $f(\mathcal{S}_-) \rightarrow -1$ . Similarly, one may ask about the maximal possible amplification of spin, i.e., the symmetric quantum channel  $\mathcal{S}_+$  with coefficient  $f(\mathcal{S}_+)$  that is as large as possible. While for  $j_A = j_B$ , it is always the case that  $f(\mathcal{E}) \leq 1$ , this no longer holds true for  $j_B > j_A$ , and the spin can be amplified under a symmetric open dynamics. The ultimate limits of this were derived in Ref. [H8], and are summarised as follows. Denote by  $\kappa_+ = \max_{\mathcal{E}} f(\mathcal{E})$ , where the maximisation occurs over the convex set of  $\text{SU}(2)$ -covariant channels between spin- $j_A$  and spin- $j_B$  systems. Then, the maximal spin-amplification factor  $\kappa_+$  is given by:

$$\kappa_+ = \frac{j_B}{j_A} \quad \text{for } j_A \geq j_B, \quad (79a)$$

$$\kappa_+ = \frac{j_B + 1}{j_A + 1} \quad \text{for } j_A < j_B. \quad (79b)$$

#### 4.5.2 Optimal encoding of information into asymmetry

**Encodings into resources destroyed by  $G$ -twirling.** In Ref. [H13] a communication scenario was analysed, where the sender  $S$  and receiver  $R$  are connected via a noiseless channel, but the encoding ability of  $S$  is constrained. In particular, it is assumed that  $S$  does not have the ability to prepare arbitrary quantum states. Instead, she is given a quantum system in a state  $\rho$  that acts as an information carrier, and can encode a message  $m$  into it by applying a quantum channel  $\mathcal{E}_m$  from a constrained set of *encodings into resources destroyed by  $\mathcal{G}$*  that satisfy

$$\mathcal{E}_m \circ \mathcal{G} = \mathcal{G}, \quad (80a)$$

$$\mathcal{G} \circ \mathcal{E}_m = \mathcal{G}, \quad (80b)$$

Above,  $\mathcal{G}$  is the  $G$ -twirling channel over some subgroup  $G$  of unitary channels,

$$\mathcal{G}(\rho) := \frac{1}{|G|} \sum_{U_g \in G} U_g \rho U_g^\dagger, \quad (81)$$

where for continuous groups the above sum can be replaced by an integral  $\int d\mu(U_g)$  with respect to the Haar measure. To understand the meaning of such constraints, note that the channel  $\mathcal{G}$  is a projector onto symmetric states (i.e., states invariant under the action of all group elements), and so it erases all the asymmetry present in a state it acts upon. Since the application of  $\mathcal{G}$  to any state  $\rho$  renders it useless from the perspective of  $S$  (as  $\mathcal{G}(\rho)$  is invariant under  $\mathcal{E}_m$  through Eq. (80a)), and the application of  $\mathcal{G}$  to an encoded state  $\mathcal{E}_m(\rho)$  renders it useless from the perspective of  $R$  (as every  $\mathcal{E}_m(\rho)$  gets sent to a fixed state  $\mathcal{G}(\rho)$  according to Eq. (80b)), encodings  $\mathcal{E}_m$  into resources destroyed by  $\mathcal{G}$  correspond to sending information encoded in the resource of asymmetry [24], i.e., into the degrees of freedom that are not invariant under the group action. Importantly, unitary channels  $U_g(\cdot)U_g^\dagger$  belonging to  $G$  (i.e., the symmetry actions on the set of quantum states) satisfy conditions from Eq. (80a)-(80b).

The general communication setting described above allows one to study a variety of constrained communication scenarios. When  $G$  is a full unitary group,  $\mathcal{G}$  becomes the completely depolarizing channel, i.e.,  $\mathcal{G}(\rho) = \mathbb{1}/d$  for all  $\rho$ . Then, Eq. (80b) is satisfied automatically and Eq. (80a) constrains the encoding to unital channels. Physically, this case corresponds to the sender  $S$  being unable to decrease the entropy of the information carrier, and so the information is encoded into the resource of purity [15]. Moreover, if  $G$  is the unitary group on a subsystem  $S_1$  of a multipartite system  $S_{1\dots n}$ , the encodings are restricted to unital channels acting locally on  $S_1$ . This way one can study encoding information not only into a resource of local purity, but also in entanglement, allowing one to assess the capacity of the system for super-dense coding [109]. When  $G$  is a subgroup of all unitaries diagonal in a given basis  $\{|k\rangle\}$  (so it is a subgroup of commuting unitaries),  $\mathcal{G}$  becomes the completely dephasing map  $\mathcal{D}$  with respect to this basis, i.e.,  $\mathcal{D}(\rho) = \sum_k \langle k | \rho | k \rangle |k\rangle\langle k|$ . Equations (80a)-(80b) then constrain encoding maps  $\mathcal{E}_m$  to be Schur-product channels [110]. Since such channels do not modify populations (diagonal elements of  $\rho$  in the given basis), but only affect coherences (off-diagonal elements), investigating communication scenarios with this constraint corresponds to asking how much classical information can be encoded into the resource of quantum coherence [43].

**Optimal communication rate.** The main goal of Ref. [H13] was to find optimal ways to encode a message  $m$ , chosen uniformly at random from the set  $\mathcal{M} = \{1, \dots, M\}$ , using a  $d$ -dimensional quantum state  $\rho$  and a constrained set of quantum channels, described by Eqs. (80a)-(80b), so that this message can be faithfully recovered later up to average probability of error  $\epsilon$ . One is thus looking for an encoder in terms of a set of quantum channels  $\{\mathcal{E}_m\}_{m \in \mathcal{M}}$  that are encodings into resources destroyed  $\mathcal{G}$ ; and a decoder specified by a quantum measurement described by the POVM elements  $\{D_m\}_{m \in \mathcal{M}}$ , such that

$$\frac{1}{M} \sum_{m=1}^M \text{Tr}(\mathcal{E}_m(\rho)D_m) \geq 1 - \epsilon, \quad (82)$$

i.e., the average probability of incorrectly decoding the message is smaller than  $\epsilon$ . One is interested in the maximal allowed value of  $M$  for given  $\rho$  and  $\epsilon$ . Of special importance is the case when one deals with  $N$  independent and identically distributed copies of a state  $\rho$ , i.e., when one encodes into  $\rho^{\otimes N}$  using encodings into resources destroyed by  $\mathcal{G}^{\otimes N}$ . Then, the aim is to find the optimal rate  $R$  (in bits per resource use) for encoding information into asymmetry of quantum states,

$$R(\rho, N, \epsilon) := \sup \left\{ \frac{\log M}{N} \mid \text{Eq. (82) holds} \right\}, \quad (83)$$

and, in particular, to understand its asymptotic behavior as  $N \rightarrow \infty$ .

In Ref. [H13], it was proven that the maximum number of messages  $M(\rho, \epsilon)$  that can be encoded into resources of a quantum state  $\rho$  destroyed by the  $G$ -twirling channel  $\mathcal{G}$  over a unitary subgroup  $G$ , for an average decoding error at most  $\epsilon$ , is bounded by

$$\log M(\rho, \epsilon) \leq D_s^{\epsilon+\delta}(\rho \parallel \mathcal{G}(\rho)) + \log \frac{1}{\delta}, \quad (84a)$$

$$\log M(\rho, \epsilon) \geq D_s^{\epsilon-\delta}(\rho \parallel \mathcal{G}(\rho)) - \log \frac{2}{\delta}, \quad (84b)$$

for all  $\delta \in (0, \min\{\epsilon, 1 - \epsilon\})$  with  $D_s^\epsilon$  denoting the information spectrum relative entropy given by [111]

$$D_s^\delta(\rho \parallel \sigma) := \sup \{K \mid \text{Tr}(\rho \Pi_{\rho \leq 2^K \sigma}) \leq \delta\}, \quad (85)$$

where  $\Pi_{\rho \leq 2^K \sigma}$  is the orthogonal projection onto the subspace generated by eigenspaces of  $2^K \sigma - \rho$  with non-negative eigenvalues. Moreover, it was proven that  $M(\rho, \epsilon)$  can be attained using unitary encodings belonging to  $G$ . It was also proven that the optimal rate  $R(\rho, N, \epsilon)$  for encoding information into resources of a quantum state  $\rho^{\otimes N}$  destroyed by the  $G$ -twirling channel  $\mathcal{G}^{\otimes N}$  over a unitary subgroup  $G^{\times N}$ , for an average decoding error at most  $\epsilon$ , is governed by the following second-order asymptotic expansion

$$R(\rho, N, \epsilon) \simeq D(\rho \parallel \mathcal{G}(\rho)) + \frac{\Phi^{-1}(\epsilon)}{\sqrt{N}} \sqrt{V(\rho \parallel \mathcal{G}(\rho))}, \quad (86)$$

with  $\Phi^{-1}$  denoting the inverse function of the normal Gaussian cumulative distribution function  $\Phi$ ,  $D(\cdot \parallel \cdot)$  being the relative entropy,  $V(\cdot \parallel \cdot)$  being the relative entropy variance, and  $\simeq$  denoting equality up to terms of order  $o(1/\sqrt{N})$ . Again, the optimal rate is achieved using product unitary encodings belonging to  $G^{\times N}$ .

**Applications to super-dense coding and secure communication.** As already mentioned, the general results on optimal communication rate with encodings into resources destroyed by  $\mathcal{G}$  allow one to find optimal solutions for a variety of communication scenarios. Two important examples discussed in Ref. [H13] are as follows. First, consider encoding information into a state  $\rho_{AB}$  of a bipartite system  $AB$  (with local dimensions  $d_A$  and  $d_B$ ), using encodings into resources destroyed by the  $G$ -twirling channel  $\mathcal{G}$  over all unitaries on  $A$ . As shown in Ref. [H13], such encodings correspond to local unital channels on system  $A$ . Using Eq. (86), one can then find the number of approximately orthogonal states that the global state of  $AB$  can be steered to by operating only locally on  $A$ . In other words, one can study the optimal rate of unital super-dense coding. More precisely, one can show that product unitary encodings on subsystem  $A$  achieve (up to second order asymptotic terms) the same optimal super-dense coding rate  $R_{\text{loc}}(\rho_{AB}, N, \epsilon)$  as unital encodings on subsystem  $A$ :

$$R_{\text{loc}}(\rho_{AB}, N, \epsilon) \simeq R_{\text{loc}}(\rho_{AB}) + \frac{\Phi^{-1}(\epsilon)}{\sqrt{N}} \sqrt{V(A|B)}, \quad (87a)$$

$$R_{\text{loc}}(\rho_{AB}) := \log d_A - S(A|B), \quad (87b)$$

with  $S(A|B) = -D(\rho_{AB} \| \mathbb{1}_A \otimes \rho_B) = S(\rho_{AB}) - S(\rho_B)$  being the conditional entropy, and  $V(A|B) = V(\rho_{AB} \| \mathbb{1}_A \otimes \rho_B)$  being the corresponding variance [37].

Second, encodings into resources destroyed by  $\mathcal{G}$  are related to private classical communication scheme for a decohering superoperator  $\mathcal{G}$  [112], as introduced in the studies on quantum reference frames [25]. In this scenario there are three parties: beyond the sender  $S$  and the receiver  $R$ , there is also an eavesdropper  $E$ . The two communicating parties share a private reference frame for some degree of freedom, i.e., both  $S$  and  $R$  agree on the form of group representation  $U(g)$  given a classical label  $g$  describing it. As an example, consider a shared Cartesian frame of reference (given, e.g., by three mutually orthogonal rigid rods defining directions  $x, y, z$ ). Then, the classical description of an element of the rotation group can be given by three Euler angles with respect to the axes defined by the shared reference frame. Thus, if  $S$  tells  $R$  that she prepared a spin-1/2 particle along the positive  $z$  direction, and he wants to rotate it, so that it points in the opposite direction, he knows precisely which  $U(g)$  to perform. However,  $E$  may not have full access to that reference frame. If she does not have any information about the orientation of the reference frame, her description of the system is given by a uniform mixture (stemming from no knowledge about the orientation of the reference frame) over all possible rotations of the reference frame. This way a state  $\rho$  is described by  $E$  as  $\mathcal{G}(\rho)$ , where  $\mathcal{G}$  is the twirling over  $\text{SO}(3)$  group, and so any initial state of a spin-1/2 particle looks to  $E$  like a maximally mixed state. Of course, in a general case the twirling can happen over arbitrary group  $G$  corresponding to a shared reference frame between  $S$  and  $R$  that  $E$  has no access to. Now, following the definition given in Ref. [112],  $S$  and  $R$  have a private classical communication scheme employing a shared reference frame related to a group  $G$ , if  $S$  can prepare  $M$  orthogonal states  $\sigma_m$ , such that  $\mathcal{G}(\sigma_m) = \rho_0$  for all  $m$  and some fixed state  $\rho_0$ . This means that  $S$  can send one of  $M$  perfectly distinguishable messages to  $R$ , while at the same time for the eavesdropper  $E$  all these messages will be completely indistinguishable, and so the communication will be secure. Through Eq. (80b), it is then clear that if for a state  $\rho$  there exists  $M$  encodings into resources destroyed by  $\mathcal{G}$ , then  $S$  and  $R$  have a private classical communication scheme:  $S$  prepares one of the states  $\mathcal{E}_m(\rho)$  that are (almost) perfectly distinguishable by  $R$ , but for  $E$  they are all described by  $\mathcal{G}(\mathcal{E}_m(\rho)) = \mathcal{G}(\rho)$ . Thus, each state  $\rho$  specifies a private communication scheme allowing for the secure communication of  $\log M$  bits, and Eqs. (84a)-(84b) provide upper and lower bounds for  $\log M$  in the single-shot regime. Optimising the information spectrum relative entropy between  $\rho$  and  $\mathcal{G}(\rho)$  over all states  $\rho$  then yields the optimal scheme for secure communication.

## 4.6 Results on classicality constraints

### 4.6.1 Minimising irreversibility of a random process

**Classical and quantum randomness.** Consider a finite-dimensional physical system undergoing some unknown evolution. In order to characterize it, one first measures the system, finding it in some well-defined state  $j$ , e.g., an eigenstate of observable  $A$ . One then allows the system to evolve for time  $\tau$  and performs the same measurement again, this time finding the system in state  $i$ . By repeating this procedure many times and collecting the statistics of measurement outcomes, one can reconstruct the transition matrix  $T$ ,

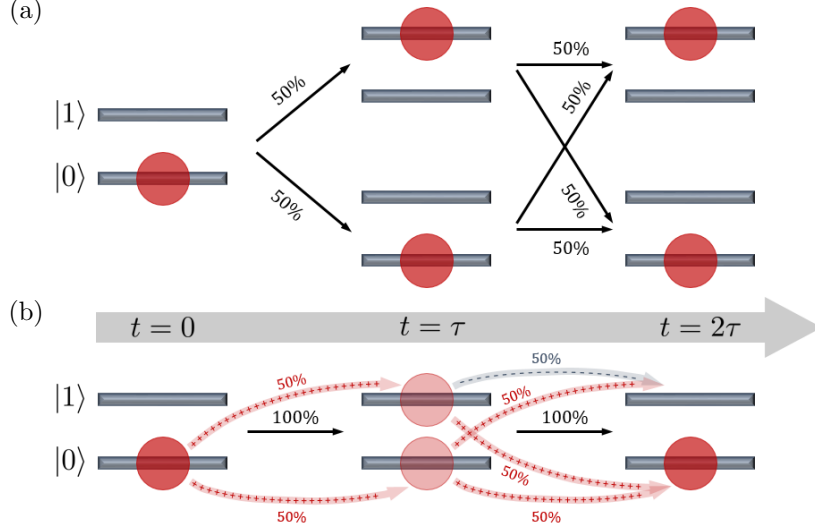


Figure 13: **Classical versus quantum randomness.** A two-dimensional system is initially prepared in a state  $|0\rangle\langle 0|$ . (a) The random classical evolution, running between times 0 and  $\tau$  and mapping between states  $|0\rangle\langle 0|$  and  $|1\rangle\langle 1|$ , is described by the transition matrix  $T$  with  $T_{ij} = 1/2$  for all  $i, j$ . The resulting state of the system at time  $\tau$  is maximally mixed,  $(|0\rangle\langle 0| + |1\rangle\langle 1|)/2$ . Further evolution between times  $\tau$  and  $2\tau$  is also described by  $T$ , leading to the total evolution being described by  $T^2$  and leaving the system in the maximally mixed state. (b) The quantum evolution between times 0 and  $\tau$  is described by a unitary operator  $U$  with  $U_{11} = -1/\sqrt{2}$  and  $U_{ij} = 1/\sqrt{2}$  otherwise (hence  $U$  is a normalized  $2 \times 2$  Hadamard matrix). The resulting state of the system at time  $\tau$  is  $|+\rangle\langle +|$ , with  $|+\rangle = (|0\rangle + |1\rangle)/\sqrt{2}$ . Note that if a measurement were performed at time  $\tau$ , one would recover transition probabilities  $T_{ij}$  as in (a). However, if the system evolves further between times  $\tau$  and  $2\tau$  according to  $U$ , due to interference of the paths, the state of the system becomes  $|0\rangle\langle 0|$ , and thus the total evolution is described by the identity matrix,  $U^2 = \mathbb{1}$ .

with entries  $T_{ij}$  describing transition probabilities between states  $j$  and  $i$ . Now, for a truly random classical process, repeating it (e.g., by letting the system evolve for  $2\tau$  instead of  $\tau$ ) leads to the evolution described by  $T^2$ . This is illustrated in Fig. 13a for an exemplary two-dimensional system. However, in quantum physics, different transitions (paths) of  $T$  can interfere with each other, so that the composition of two processes will generally not be described by a transition matrix  $T^2$ . In particular, the compound process can even become fully deterministic, leading to the complete disappearance of the observed randomness (see Fig. 13b). The question I investigated in Ref. [H3] was: how close to being deterministic (and thus reversible) can a random process be, while being constrained to induce a classical transition described by a matrix  $T$ ?

**Coherification.** To investigate this problem in a quantitative way, a notion of *coherification* of a random process was introduced in Ref. [H3]. To formally define it, one needs to recall a few concepts. First, for any quantum channel  $\mathcal{E}$ , one can define the associated *Jamiolkowski state* [113], as the image of the extended map acting on a maximally entangled state,

$$J_{\mathcal{E}} = \frac{1}{d}(\mathcal{E} \otimes \mathcal{I}) |\Omega\rangle\langle \Omega|, \quad (88)$$

with  $|\Omega\rangle = \sum_i |ii\rangle$  and  $\mathcal{I}$  denoting the identity channel. The condition of  $\mathcal{E}$  being a quantum channel (i.e., being completely positive and trace-preserving) is equivalent to [113]

$$J_{\mathcal{E}} \geq 0, \quad \text{Tr}_1(J_{\mathcal{E}}) = \frac{\mathbb{1}}{d}. \quad (89)$$

These conditions imply that diagonal elements (in the preferred basis) of the Jamiołkowski state correspond to the entries of a  $d \times d$  (column-stochastic) transition matrix  $T$ ,

$$\langle ij | J_{\mathcal{E}} | ij \rangle = \frac{1}{d} T_{ij}, \quad (90)$$

with  $T$  being precisely the classical action of  $\mathcal{E}$ , i.e., the transition matrix that describes how initial populations (occupations in the preferred basis) are transformed by  $\mathcal{E}$  to final populations,

$$T_{ij} = \langle i | \mathcal{E}(|j\rangle\langle j|) | i \rangle. \quad (91)$$

Thus, diagonal Jamiołkowski states (with the only non-zero entries on the diagonal) represent classical random processes described by stochastic matrices acting on probability vectors of size  $d$ . Now, given a fixed transition matrix  $T$ , coherification of  $T$  is any quantum channel  $\mathcal{E}$  with the classical action (the diagonal of  $J_{\mathcal{E}}$ ) given by  $T$ . In particular, for a given  $T$ , one is interested in finding the optimally coherified quantum map  $\mathcal{E}^{\mathcal{C}}$ , such that the coherence of the corresponding Jamiołkowski state  $J_{\mathcal{E}^{\mathcal{C}}}$  is the largest (or its mixedness is the smallest). Such optimally coherified maps are the answer to the central question studied in Ref. [H3], as they provide a quantum channel closest to being unitary (so deterministic and reversible), while inducing a random transition given by a stochastic matrix  $T$ . The following standard measures of mixedness and coherence were used: entropic coherence of a channel,

$$\mathcal{C}_e(\mathcal{E}) := S(\mathcal{D}(J_{\mathcal{E}})) - S(J_{\mathcal{E}}), \quad (92)$$

where  $S(\rho) := -\text{Tr}(\rho \log \rho)$  is the von Neumann entropy and  $\mathcal{D}$  is a decohering superoperator sending all off-diagonal elements to zero; and 2-norm coherence of a channel,

$$\mathcal{C}_2(\mathcal{E}) := \gamma(J_E) - \gamma(\mathcal{D}(J_E)), \quad (93)$$

where  $\gamma(\rho) = \text{Tr}(\rho^2)$  is the purity of a state  $\rho$ .

**Bounds on optimal coherifications.** First, it was proven in Ref. [H3] that a stochastic matrix  $T$  can be completely coherified (in the sense that the resulting channel  $\mathcal{E}^{\mathcal{C}}$  is reversible) if and only if it is unistochastic, meaning that there exists a unitary matrix  $U$  such that  $T_{ij} = |U_{ij}|^2$ . Next, for non-unistochastic  $T$  and employing majorization techniques, the following bounds for coherence and mixedness of the optimal coherification  $\mathcal{E}^{\mathcal{C}}$  of a stochastic matrix  $T$  were obtained:

$$H\left(\frac{1}{d}\mathbf{T}\right) - H(\boldsymbol{\mu}^{\prec}(T)) \leq \mathcal{C}_e(\mathcal{E}^{\mathcal{C}}) \leq H\left(\frac{1}{d}\mathbf{T}\right) - H(\boldsymbol{\mu}^{\succ}(T)), \quad (94a)$$

$$\boldsymbol{\mu}^{\prec}(T) \cdot \boldsymbol{\mu}^{\prec}(T) - \frac{1}{d^2}\mathbf{T} \cdot \mathbf{T} \leq \mathcal{C}_2(\mathcal{E}^{\mathcal{C}}) \leq \boldsymbol{\mu}^{\succ}(T) \cdot \boldsymbol{\mu}^{\succ}(T) - \frac{1}{d^2}\mathbf{T} \cdot \mathbf{T}. \quad (94b)$$

In the above,  $H(\mathbf{p}) := -\sum_i p_i \log p_i$  is the Shannon entropy,  $\mathbf{T}$  is a  $d^2$ -dimensional vector with the entries  $T_{ij}$ , whereas the vectors  $\boldsymbol{\mu}^{\prec}(T)$  and  $\boldsymbol{\mu}^{\succ}(T)$  are defined as follows. First, for every row of  $T$ , write the sum over its columns as  $\sum_j T_{ij} = n_i + a_i$ , with  $n_i$  being an integer and  $a_i \in [0, 1)$ . Then, using the following set of vectors:

$$\mathbf{s}^{(i)}(T) = \left[ \underbrace{1, 1, \dots, 1}_{n_i \text{ times}}, a_i, 0, \dots, 0 \right], \quad (95)$$

$\boldsymbol{\mu}^{\succ}(T)$  is defined as

$$\boldsymbol{\mu}^{\succ}(T) := \frac{1}{d} \sum_{i=1}^d \mathbf{s}^{(i)}(T). \quad (96)$$

To define  $\boldsymbol{\mu}^{\prec}(T)$ , one first introduces vectors  $\mathbf{r}^{(i)}$  given by the rows of  $T$  with entries arranged in a non-increasing order,

$$\mathbf{r}^{(i)} = [T_{i1}, \dots, T_{id}]^{\downarrow}. \quad (97)$$

Then,  $\mu^\prec(T)$  is given by

$$\mu^\prec(T) := \frac{1}{d} \sum_{i=1}^d r^{(i)}. \quad (98)$$

The bounds from Eqs. (94a)-(94b) provide limitations on how much a given  $T$  can be coherified, but also show to what extent a given  $T$  can be at least coherified. The upper bounds (i.e., the right hand sides of the above equations) trivialise when  $T$  is bistochastic, but this was remedied in Ref. [H3] by deriving more involved upper bounds on the purity of  $\mathcal{E}^C$  (see Fig. 14a for an example).

**Optimally coherified qubit and qutrit channels.** In Ref. [H3], coherifications of transition matrices for small dimension sizes  $d$  were also explicitly investigated. In particular, it was shown that the derived upper bounds on coherifications, Eqs. (94a)-(94b), can be saturated for  $d = 2$  and the form of the corresponding optimally coherified qubit channel  $\mathcal{E}^C$  was found. In that case, the classical action is given by a  $2 \times 2$  transition matrix  $T$  described by two real parameters,

$$T = \begin{bmatrix} a & 1-b \\ 1-a & b \end{bmatrix} =: \begin{bmatrix} a & \tilde{b} \\ \tilde{a} & b \end{bmatrix}, \quad (99)$$

with  $\tilde{x} := 1 - x$ . One can focus on the case when  $a \leq b$ , as the results for the case  $a > b$  are analogous. Namely, one only needs to exchange  $a$  with  $b$  in all expressions, and transform all matrices  $X$  by replacing  $X_{kl}$  with  $X_{\tilde{k}\tilde{l}}$ . To express the Kraus operators of the corresponding optimally coherified channel  $\mathcal{E}^C$ , first introduce a unitary

$$U = \frac{1}{\sqrt{a+\tilde{b}}} \begin{bmatrix} \sqrt{a} & -\sqrt{\tilde{b}} \\ \sqrt{\tilde{b}} & \sqrt{a} \end{bmatrix}, \quad (100)$$

and a decaying channel  $\Psi(\cdot) = L_1(\cdot)L_1^\dagger + L_2(\cdot)L_2^\dagger$  with

$$L_1 = \begin{bmatrix} \sqrt{a+\tilde{b}} & 0 \\ 0 & 1 \end{bmatrix}, \quad L_2 = \begin{bmatrix} 0 & 0 \\ \sqrt{b-a} & 0 \end{bmatrix}. \quad (101)$$

Then, the optimally coherified channel with a classical action  $T$  is given by  $\mathcal{E}^C(\cdot) = K_1(\cdot)K_1^\dagger + K_2(\cdot)K_2^\dagger$  with

$$K_1 = L_1 U^\dagger = \begin{bmatrix} \sqrt{a} & \sqrt{\tilde{b}} \\ -\sqrt{\frac{\tilde{b}}{a+\tilde{b}}} & \sqrt{\frac{a}{a+\tilde{b}}} \end{bmatrix}, \quad K_2 = L_2 U^\dagger = \begin{bmatrix} 0 & 0 \\ \sqrt{\tilde{a} - \frac{\tilde{b}}{a+\tilde{b}}} & \sqrt{b - \frac{a}{a+\tilde{b}}} \end{bmatrix}. \quad (102)$$

The action of  $\mathcal{E}^C$  a Bloch sphere for a particular choice of  $T$  is illustrated in Fig. 14b. Finally, optimal coherifications  $\mathcal{E}^C$  of  $3 \times 3$  stochastic matrices  $T$  belonging to one of the following three families,

$$T \in \left\{ \begin{bmatrix} 0 & a & b \\ c & 0 & \tilde{b} \\ \tilde{c} & \tilde{a} & 0 \end{bmatrix}, \begin{bmatrix} a & b & 0 \\ 0 & 0 & c \\ \tilde{a} & \tilde{b} & \tilde{c} \end{bmatrix}, \begin{bmatrix} a & b & c \\ \tilde{a} & \tilde{b} & \tilde{c} \\ 0 & 0 & 0 \end{bmatrix} \right\}, \quad (103)$$

were also found and proven to saturate the derived upper-bounds.

**Structure of unistochastic matrices.** As was discussed above and in Ref. [H3], investigating the problem of unistochasticity (i.e., which stochastic matrices are unistochastic) can provide insight into the nature of randomness, since unistochastic random processes can arise from fully deterministic and reversible dynamics. The problem of characterizing the set  $\mathcal{U}_d$  of unistochastic matrices of size  $d$  is also related to the issue of quantization of classical dynamical systems determined by a given bistochastic transition matrix [114, 115]. Moreover, unistochasticity is also linked to the problem of finding all discrete quantum walks on graphs with  $d$  vertices [116]. The main aim of the work [H11] was to contribute to the understanding of the structure of the set  $\mathcal{U}_d$ . This was achieved by introducing the set  $\mathcal{L}_d$  of *bracelet matrices* that includes the analyzed

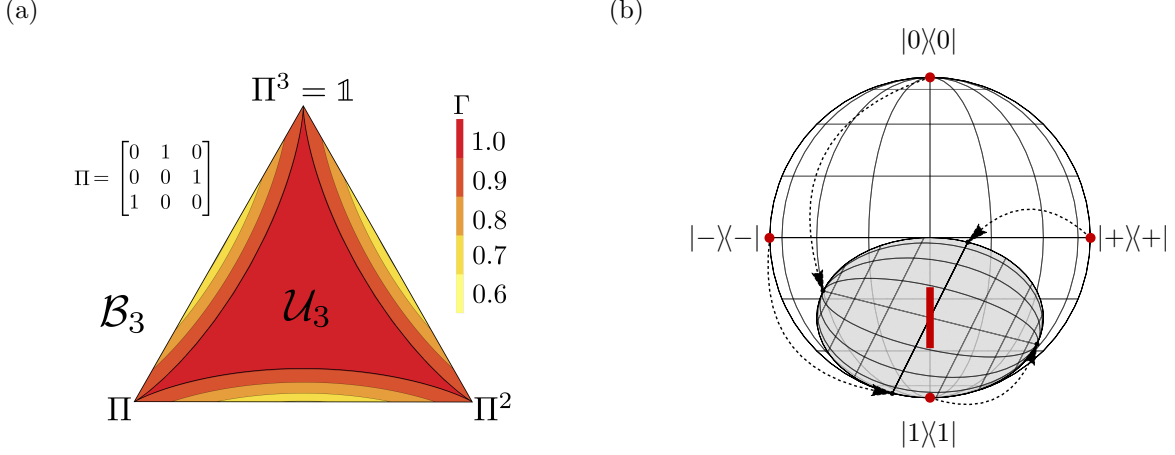


Figure 14: (a) **Purity bound.** The upper-bound on purity  $\gamma$  of the family of optimally coherified qutrit channels with the classical action given by a bistochastic transition matrix  $T = \sum_{i=1}^3 q_i \Pi^i$ , with  $\sum_i q_i = 1$  and  $\Pi$  being a cyclic permutation matrix. Any unistochastic matrix  $T \in \mathcal{U}_3$  can be completely coherified, so that  $\gamma = 1$ . (b) **Action of the optimally coherified qubit channel.** The image of the Bloch sphere under  $\mathcal{E}^{\mathcal{C}}$  (with classical action described by  $a = \frac{1}{3}$  and  $b = \frac{5}{6}$ ) is represented by the grey ellipsoid. The thick red line represents the action of the classical channel  $T$ , while dashed lines show transformations of significant points of the sphere.

set  $\mathcal{U}_d$  and approximates it from outside. The set  $\mathcal{L}_d$  consists of these bistochastic matrices  $B$  whose entries satisfy:

$$2 \max_j \sqrt{B_{jk} B_{jl}} \leq \sum_{j=1}^d \sqrt{B_{jk} B_{jl}}, \quad 2 \max_l \sqrt{B_{jl} B_{kl}} \leq \sum_{l=1}^d \sqrt{B_{jl} B_{kl}}, \quad (104)$$

and the name refers to the fact that when the above inequalities are satisfied, a certain sequence of segments with specified lengths can be closed to form a polygon (a “bracelet”) in the complex plane. The following important properties of  $\mathcal{L}_d$  were proven in Ref. [H11]. First, the set of bracelet matrices  $\mathcal{L}_d$  is closed under multiplication by factorizable matrices and, as a result, every factorizable bistochastic matrix is also bracelet (recall that a factorizable matrix is a matrix that can be expressed as a product of bistochastic matrices acting non-trivially on at most two levels [95]). Second, the set of bracelet matrices (and the set of factorizable matrices) are star-shaped with respect to the flat van der Waerden matrix  $W_d$  with all entries equal to  $1/d$ . Finally, if  $B_1 \in \mathcal{L}_{d_1}$  and  $B_2 \in \mathcal{L}_{d_2}$  then  $B = B_1 \otimes B_2$  belongs to  $\mathcal{L}_{d_1 d_2}$ . These properties of  $\mathcal{L}_d$  not only characterise the superset of unistochastic matrices, but also yield complete information in certain low-dimensional cases, as then the two sets coincide. More precisely, it has been established that  $\mathcal{U}_3 = \mathcal{L}_3$  [94], and so the results of Ref. [H11] also mean that the set of  $3 \times 3$  unistochastic matrices is closed under multiplication by factorizable matrices and is star-shaped with respect to the flat matrix  $W_3$ . Moreover, it was shown in Ref. [H11] that for  $d = 4$  the set of circulant unistochastic matrices coincides with the set of circulant bracelet matrices (recall that a circulant matrix is a square matrix in which all row vectors are composed of the same elements and each row vector is rotated one element to the right relative to the preceding row vector). Thus, the set of circulant unistochastic matrices is closed under multiplication by circulant factorizable matrices and is star-shaped with respect to the flat matrix  $W_4$ . Its geometric structure is illustrated in Fig. 15a. Finally, Ref. [H11] also investigated *doubly circulant* unistochastic matrices (i.e., these unistochastic matrices that arise from circulant unitary dynamics) and characterized their spectra. More precisely, it was proven that the eigenvalues of a  $d \times d$  doubly circulant unistochastic matrix  $B$  lie inside a unit  $d$ -hypocycloid  $H_d$  on a complex plane, i.e., inside the star-shaped region with the boundary parametrized by

$$x(\theta) = \frac{d-1}{d} \cos \theta + \frac{1}{d} \cos((d-1)\theta), \quad y(\theta) = \frac{d-1}{d} \sin \theta - \frac{1}{d} \sin((d-1)\theta), \quad (105)$$

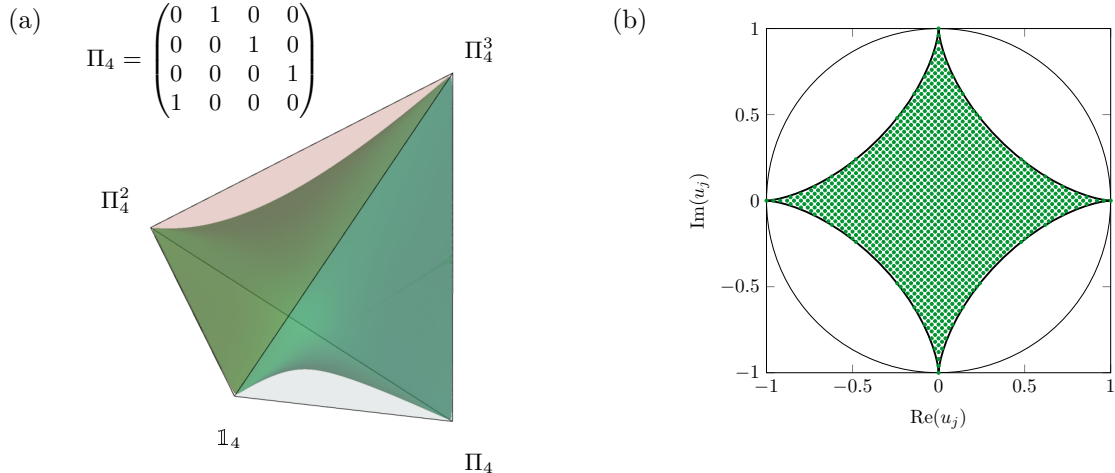


Figure 15: **(a) Circulant unistochastic matrices of size  $d = 4$ .** The set of  $4 \times 4$  circulant matrices can be represented by a tetrahedron with vertices corresponding to four circulant permutation matrices  $\Pi_4^n$ , and the points inside to convex combinations of these extremal matrices. The subset of circulant matrices that additionally satisfy the bracelet condition (so, according to the results of Ref. [H11], the set of circulant unistochastic matrices) is presented as the non-convex, green shape inside the tetrahedron. **(b) Eigenvalues of doubly circulant unistochastic matrices.** Eigenvalues of  $4 \times 4$  doubly circulant unistochastic matrices in the complex plane (green dots) together with the astroid, i.e. the 4-hypocycloid. The plotted set of matrices was obtained by discretizing 4-dimensional probability vectors describing a given circulant matrix using a grid of size 0.02, and verifying whether the resulting matrix is a bracelet matrix.

which is illustrated in Fig. 15b. What is more, it was shown that in dimensions  $d \leq 4$  the sets of circulant unistochastic matrices coincide with the sets of doubly circulant unistochastic matrices.

#### 4.6.2 Structural differences between classical and quantum randomness

**Classically indistinguishable channels and states.** The concept of coherification introduced in Ref. [H3] was employed in Ref. [H7] to investigate how much richer the structure of quantum randomness is compared to classical randomness. This richness comes from the fact that there may exist many distinct quantum coherifications of a given classical transition matrix  $T$ , and the question is, how to accurately quantify it? In Ref. [H7], I addressed this problem by introducing and studying the following two concepts: the *distinguishability number*  $M(T)$ , given by the maximal number of quantum channels that share the same classical action  $T$  and can be perfectly distinguished in an experiment; and the *restricted distinguishability number*  $\tilde{M}(T)$ , given by the maximal number of quantum channels with the same classical action  $T$  and perfectly distinguishable from each other without using entangled input states. Studying distinguishability numbers allows one to quantify distinct ways of processing information encoded in quantum coherence, since all coherifications of  $T$  are classically indistinguishable (i.e., classical degrees of freedom are transformed in the same way by  $T$ ), and so the only way to distinguish them is through the effect they have on quantum degrees of freedom. Moreover, in Ref. [H7], I also investigated the differences between classical and quantum randomness by extending the concept of coherification from channels to states: a quantum state  $\rho$  is said to be a coherification of a classical probability distribution  $\mathbf{p}$  if its occupations in the distinguished basis are described by  $\mathbf{p}$  (i.e.,  $\langle i | \rho | i \rangle = p_i$ ). A  $d$ -dimensional probability vector  $\mathbf{p}$  is then said to belong to  $M$ -*distinguishability region*  $\mathcal{A}_d^M$  of the probability simplex  $\Delta_d$ , if and only if there exist  $M$  perfectly distinguishable quantum states with the same classical version  $\mathbf{p}$  (i.e., classically indistinguishable).

**Number of distinct state coherifications.** The analysis in Ref. [H7] begins with looking for necessary conditions for  $M$ -distinguishability of states. Geometrically, this problem is equivalent to bounding  $M$ -distinguishability regions  $\mathcal{A}_d^M$  within the probability simplex  $\Delta_d$ . First, note that, by definition, one has

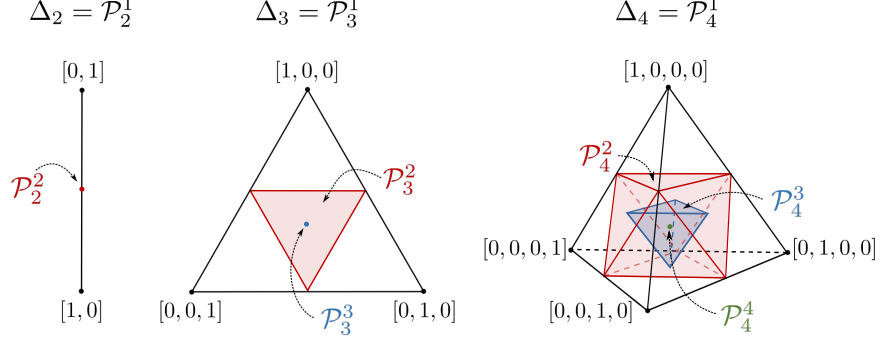


Figure 16: **Permutohedra.** Visualization of permutohedra  $\mathcal{P}_d^M$  for  $2 \leq d \leq 4$  and  $1 \leq M \leq d$ . Permutohedron  $\mathcal{P}_d^M$  has  $\binom{d}{M}$  vertices located at the centres of  $(M - 1)$ -faces of the probability simplex  $\Delta_d$ .

$\mathcal{A}_d^l \subset \mathcal{A}_d^k$  for  $1 \leq k < l \leq d$ , and  $\mathcal{A}_d^1 = \Delta_d$ . In order to find further non-trivial conditions, a concept of permutohedron [117] is needed. For every  $\mathbf{x} \in \mathbb{R}^d$ , the permutohedron  $\mathcal{P}_d(\mathbf{x})$  is the convex hull of all the permutations of  $\mathbf{x}$ ,

$$\mathbf{y} \in \mathcal{P}_d(\mathbf{x}) \iff \exists \boldsymbol{\lambda} : \mathbf{y} = \sum_k \lambda_k \Pi_k \mathbf{x}, \quad (106)$$

with  $\boldsymbol{\lambda}$  being  $d!$ -dimensional probability vector and  $\{\Pi_k\}$  denoting the set of  $d!$  permutation matrices acting on  $d$ -dimensional vectors. In particular, a shorthand notation  $\mathcal{P}_d^M$  will be used to denote a permutohedron for  $\mathbf{x}$  being a flat distribution with the first  $M$  entries equal to  $1/M$ . Permutohedra  $\mathcal{P}_d^M$  form nested convex polytopes in  $\mathbb{R}^{d-1}$  satisfying  $\mathcal{P}_d^{M+1} \subset \mathcal{P}_d^M$ ,  $\mathcal{P}_d^1 = \Delta_d$  and  $\mathcal{P}_d^d = \{\boldsymbol{\eta}\}$ , with  $\boldsymbol{\eta}$  denoting the uniform distribution  $[1/d, \dots, 1/d]$ . The first few of them are illustrated in Fig. 16. In Ref. [H7], it was proven that the  $M$ -distinguishability region  $\mathcal{A}_d^M$  lies inside a permutohedron  $\mathcal{P}_d^M$ , and this result was referred to as the *permutohedron bound*. This means that the necessary condition for  $M$ -distinguishability of a set of quantum states  $\{\rho^{(n)}\}_{n=1}^M$  with a fixed classical version  $\mathbf{p} = \max_k p_k \leq 1/M$ . Moreover, it was proven that this necessary condition for  $M$ -distinguishability is also sufficient for  $M = 2$  and  $M = d$  (i.e.,  $\mathcal{A}_d^2 = \mathcal{P}_d^2$  and  $\mathcal{A}_d^d = \mathcal{P}_d^d$ ), but is not sufficient for  $M = d - 1$  and even  $d > 2$  (i.e.,  $\mathcal{A}_d^{d-1} \neq \mathcal{P}_d^{d-1}$  for even  $d > 2$ ). Next, it was shown that for distributions lying at the boundary of permutohedron  $\mathcal{P}_d^M$ ,  $M$ -distinguishability of mixed states is equivalent to  $M$ -distinguishability of pure states, significantly simplifying the problem. Moreover, it was proven that  $M$ -distinguishability of a set of pure quantum states  $\{|\psi\rangle^{(n)}\}_{n=1}^M$  with a fixed classical version  $\mathbf{p}$  is equivalent to the existence of a unistochastic matrix  $T$  with first  $M$  columns equal to  $\mathbf{p}$ , thus relating the current subject of study to the well-known unistochasticity problem [93, 94]. For prime  $d$ , it was demonstrated that there exists  $d - 1$  perfectly distinguishable states with classical version  $\mathbf{p}$  if  $\mathbf{p}$  is close enough to a maximally mixed distribution, i.e.,

$$\exists \epsilon > 0 : \mathcal{B}(\boldsymbol{\eta}, \epsilon) \subseteq \mathcal{A}_d^{d-1}, \quad (107)$$

where  $\mathcal{B}(\boldsymbol{\eta}, \epsilon)$  denotes a ball of radius  $\epsilon$  centred at  $\boldsymbol{\eta}$ . Finally, it was proven that if there exist  $M$  perfectly distinguishable pure states with a classical version  $\mathbf{q}$  given by coarse-graining of  $\mathbf{p}$ , i.e.,  $\mathbf{q} = G\mathbf{p}$  with  $G$  being a stochastic matrices with entries in  $\{0, 1\}$ , then there exists  $M$  perfectly distinguishable pure states with a classical version  $\mathbf{p}$ .

**Relation to energy-time uncertainty relation.** In Ref. [H7], a strong link between the problem of  $M$ -distinguishability of states and energy-time uncertainty relation was pointed out. To understand this, consider the distinguished basis to be given by the eigenstates of Hamiltonian  $H$ ,  $\{|E_k\rangle\}$ , so that  $\mathbf{p}$  is given by energy occupations  $p_k = \langle E_k | \rho | E_k \rangle$ . Although an observable for time does not exist, there is nevertheless the expectation that time and energy should be complementary variables, resulting in a version of uncertainty relation between them. Non-rigorously, it should state that if a given state  $\rho$  has a well-defined energy then it is a bad clock, i.e., it does not significantly change in time (in the limit of  $\rho$  being a sharp energy eigenstate,

$\rho$  becomes stationary and does not evolve in time at all); and if a state  $\rho$  allows one to distinguish different moments of time with high precision, then the energy of  $\rho$  cannot be well-defined. Of course, there are many ways to quantify both the sharpness of energy of  $\rho$  and the quality of  $\rho$  as a clock. For example, in the most traditional formulation by Mandelstam and Tamm [118], the uncertainty of energy is quantified by the variance of  $\mathbf{p}$ , and the timing quality of  $\rho$  is given by the minimal time needed for  $\rho$  to evolve to another distinguishable state (clearly, if such time is long, then the time resolution is low, meaning the quality of  $\rho$  as a clock is low). Alternatively, given a state with energy distribution  $\mathbf{p}$ , its timing quality can be measured by  $M$ , which tells one how many different moments in time can be distinguished unambiguously (i.e, with no uncertainty) using  $\rho$ . The  $M$ -distinguishability regions  $\mathcal{A}_d^M$  provide then a geometric way to visualize energy-time uncertainty relation: the closer one gets to the centre of the probability simplex (the uniform distribution), the more uncertain the energy outcomes become, but the better potential timing quality of the state becomes. Direct application of the derived permutohedron bound then leads to the following statement: a state that is able to distinguish  $M$  different moments in time satisfies the inequality for min-entropy  $H_\infty(\mathbf{p}) \geq \log M$ , with  $\mathbf{p}$  denoting its distribution over energy. Note that this coincides with the particular version of the recent result presented in Ref. [119], where the authors studied entropic formulations of energy-time uncertainty relation. Thus, any improvements over the permutohedron bound could also tighten inequalities derived there.

**Number of distinct channel coherifications.** Concerning distinguishability numbers, the following results were obtained in Ref. [H7]. First, for every unistochastic  $T$  the restricted distinguishability number  $\tilde{\mathcal{M}}(T)$  was proven to be maximal,  $\tilde{\mathcal{M}}(T) = d$ . Analogous result was proven for all circulant stochastic matrices. Distinguishability numbers for the identity and van den Waerdan matrix were also found to be given by  $\mathcal{M}(\mathbb{1}) = d$  and  $\mathcal{M}(W) = d^2$ , showing that unrestricted distinguishability numbers for unistochastic matrices can take extremal allowed values. It also proved that the maximal number of perfectly distinguishable generalised dephasing channels  $\mathcal{D}_C$ , introduced in Ref. [120] and defined through a correlation matrix  $C$  by

$$\langle i | \mathcal{D}_C(\rho) | j \rangle = \rho_{ij} C_{ij}, \quad (108)$$

is equal to  $d$ . Moreover, it was shown in Ref. [H7] that for every bistochastic matrix  $T$  one has  $\mathcal{M}(T) \geq 2$ . The restricted distinguishability numbers  $\tilde{\mathcal{M}}(T)$  were related to distinguishability regions  $\mathcal{A}_d^M$ : if a probability distribution given by a column of  $T$  belongs to  $\mathcal{A}_d^M$ , then  $\tilde{\mathcal{M}}(T) \geq M$ . Also, if the entries of at least one column of the stochastic matrix  $T$  satisfy the generalised triangle inequality, then  $\tilde{\mathcal{M}}(T) \geq 2$ . Finally, the problem of distinguishability numbers was fully solved for a two-level system:  $\tilde{\mathcal{M}}(T)$  for a qubit classical action  $T$  parametrized as in Eq. (99) was shown to be given by

$$\tilde{\mathcal{M}}(T) = \begin{cases} 1 & : \text{ for } \frac{1}{2} < |a - b| \leq 1, \\ 2 & : \text{ for } 0 \leq |a - b| \leq \frac{1}{2}, \end{cases} \quad (109)$$

whereas  $\mathcal{M}(T)$  was shown to satisfy

$$\mathcal{M}(T) = \begin{cases} 2 & : \text{ for } 0 < |a - b| \leq \frac{1}{2}, \\ 3 & : \text{ for } a = b \text{ and } a \in \left[ \frac{1}{3}, \frac{2}{3} \right] \setminus \left\{ \frac{1}{2} \right\}, \\ 4 & : \text{ for } a = b = \frac{1}{2}. \end{cases} \quad (110)$$

**Dephasing superchannels.** In Ref. [H10], I introduced and investigated a class of environmental noises that leave invariant the classical transitions induced by a quantum channel  $\mathcal{E}$  in the distinguished basis, but non-trivially affect its quantum properties. This provides yet another perspective to study the structural differences between classical and quantum processes – while these *dephasing superchannels* have no effect on classical dynamics, they have a rich structure affecting the coherence dynamics. More formally, a mathematical concept that can capture a general effect of noise is a quantum superchannel [121], which is a linear

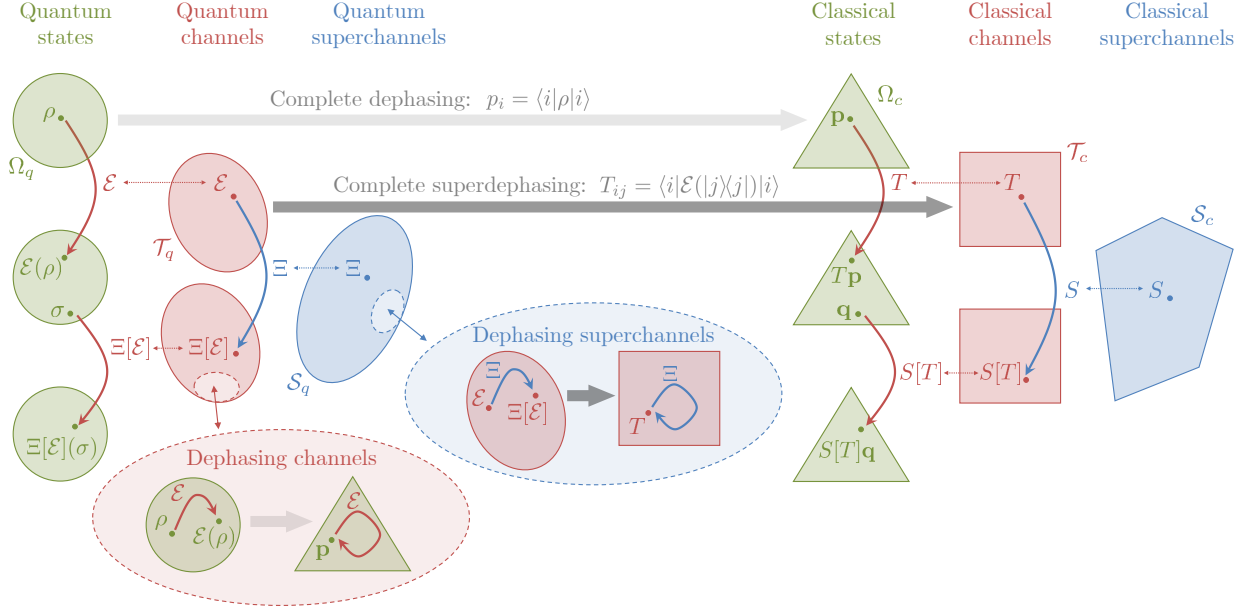


Figure 17: **Dephasing channels and superchannels.** The set of quantum states  $\Omega_q$  (density matrices) is projected onto the set of classical states  $\Omega_c$  (probability distributions) via the completely dephasing channel that removes all coherences in the distinguished basis, but keeps the occupations unchanged. General dephasing channels are those maps between quantum states that affect coherences, but do not change occupations, i.e., they keep the classical (completely dephased) version of the state invariant. Analogously, the set of quantum channels  $\mathcal{T}_q$  (completely positive trace-preserving maps) is projected onto the set of classical channels  $\mathcal{T}_c$  (stochastic matrices) via a completely dephasing superchannel that removes all coherent properties of the channel, but keeps the transition probabilities in the distinguished basis unchanged. General dephasing superchannels form the subset of quantum superchannels  $\mathcal{S}_q$  that affect coherent properties of the channel, but do not change transition probabilities, i.e., they keep the classical (completely superdephased) version of the channel invariant.

transformation  $\Xi$  mapping between quantum channels. It has a standard physical realization in terms of pre- and post-processing by channels  $\mathcal{N}_1$  and  $\mathcal{N}_2$  with a memory system:

$$\Xi[\mathcal{E}] = \begin{array}{c} \text{---} \boxed{\Xi[\mathcal{E}]} \text{---} \\ = \\ \begin{array}{c} \text{---} \boxed{\mathcal{N}_1} \text{---} \boxed{\mathcal{E}} \text{---} \boxed{\mathcal{N}_2} \text{---} \\ |0\rangle\langle 0| \text{---} \text{---} \text{---} \text{---} \text{---} \\ \text{discard} \end{array} \end{array} \quad (111)$$

Now, a quantum superchannel  $\Xi$  is called a dephasing superchannel if the transition probabilities in the distinguished basis are invariant under  $\Xi$ :

$$\forall \mathcal{E}, |i\rangle, |j\rangle : \quad \langle i | \Xi[\mathcal{E}] (|j\rangle\langle j|) | i \rangle = \langle i | \mathcal{E} (|j\rangle\langle j|) | i \rangle. \quad (112)$$

The concept of a dephasing superchannel and its relation to dephasing channels is illustrated in Fig. 17.

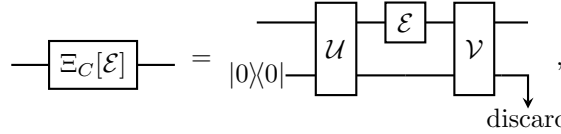
First, dephasing superchannels were mathematically characterized in Ref. [H10] by establishing a one-to-one correspondence between dephasing superchannels and a particular subclass of Schur-product supermaps that act on the Jamiłkowski state  $J(\mathcal{E})$  of a channel  $\mathcal{E}$ . More precisely, a linear transformation  $\Xi$  was proven to be a dephasing superchannel if and only if it transforms the Jamiłkowski state in the following way:

$$J(\Xi[\mathcal{E}]) = \sum_{ijkl} J(\mathcal{E})_{ij,kl} C_{ij,kl} |ij\rangle\langle kl| = J(\mathcal{E}) \circ C, \quad (113)$$

where  $\{|ij\rangle\}$  is the distinguished basis,  $\circ$  denotes Schur (entry-wise) product in that basis, and  $C$  is a correlation matrix (positive matrix with all diagonal entries equal to 1) of size  $d^2$  and the following form

$$C = \begin{bmatrix} C_{11} & C_{12} & \dots & C_{1N} \\ C_{21} & C_{11} & \dots & C_{2N} \\ \vdots & \vdots & \ddots & \vdots \\ C_{N1} & C_{N2} & \dots & C_{11} \end{bmatrix}, \quad (114)$$

where  $C_{ij}$  are  $d \times d$  matrices and  $C_{11}$  is a correlation matrix. A physical realization of general dephasing superchannel  $\Xi$  was also found as a unitary pre- and post-processing with an ancillary system of dimension  $d^2$  and of the following form:



$$\Xi_C[\mathcal{E}] = |0\rangle\langle 0| \text{---} \mathcal{U} \text{---} \mathcal{E} \text{---} \mathcal{V} \text{---} \text{discard}, \quad (115)$$

where

$$\mathcal{U}(\cdot) = U(\cdot)U^\dagger, \quad U = \sum_{i=1}^d |i\rangle\langle i| \otimes U_i, \quad (116a)$$

$$\mathcal{V}(\cdot) = V(\cdot)V^\dagger, \quad V = \sum_{i=1}^d |i\rangle\langle i| \otimes V_i, \quad (116b)$$

with  $\{U_i\}, \{V_i\}$  being arbitrary unitaries of size  $d^2$ . The relation between  $C$  and these unitaries is given by

$$C_{ik,jl} = \langle 0| U_l^\dagger V_j^\dagger V_i U_k |0\rangle. \quad (117)$$

The above physical realisation was also directly related to pre- and post-processing employing generalised dephasing channels with memory, and it was explicitly demonstrated that for system's dimension  $d \geq 3$  this memory effect extends the set of possible dephasing noises. Moreover, it was proven in Ref. [H10] that coherence generating power [122] of a general quantum channel is monotonically decreasing under dephasing superchannels. Finally, the effect that dephasing noise can have on a quantum channel  $\mathcal{E}$  was analysed by investigating the number  $M(\mathcal{E}, \epsilon)$  of  $\epsilon$ -distinguishable (i.e., distinguishable with probability  $1 - \epsilon$ ) channels that  $\mathcal{E}$  can be mapped to by a family of dephasing superchannels. It was shown that the number  $M(\mathcal{E}, \epsilon)$  is upper-bounded by

$$M(\mathcal{E}, \epsilon) \leq 2^{\mathcal{C}_{D_H}^\epsilon(\mathcal{E}||\mathcal{E}_\Delta)}, \quad (118)$$

where  $\mathcal{E}_\Delta$  is a classical (completely dephased) version of  $\mathcal{E}$  and  $\mathcal{C}_{D_H}^\epsilon$  is the channel coherence measure based on a channel divergence related to hypothesis testing relative entropy [123],

$$\mathcal{C}_{D_H}^\epsilon(\mathcal{E}_1||\mathcal{E}_2) := \sup_{\rho^{AB}} D_H^\epsilon((\mathcal{E}_1^A \otimes \mathcal{I}^B)(\rho^{AB})||(\mathcal{E}_2^A \otimes \mathcal{I}^B)(\rho^{AB})), \quad (119)$$

with

$$D_H^\epsilon(\rho||\sigma) := -\log \inf \{ \text{Tr}(Q\sigma) \mid 0 \leq Q \leq \mathbb{1}, \text{Tr}(Q\rho) \geq 1 - \epsilon \}. \quad (120)$$

A complementary perspective on that problem was also presented, where coherence of a channel  $\mathcal{E}$  can be seen as a resource for distinguishing between various dephasing superchannels.

## 5 Presentation of significant scientific activity

### 5.1 Scientific activity at academic institutions

During my scientific career, I have performed research at 5 different academic institutions, including 2 foreign ones in Australia and the United Kingdom.

#### Research performed at academic institutions after obtaining the PhD degree:

1. **Jagiellonian University, Poland** – October, 2019 – present  
10 published papers: [H8–H15] and [KK14, KK15]  
1 invited conference talk, 6 contributed conference talks and 8 seminar talks
2. **University of Gdańsk, Poland** – June, 2019 - December, 2019  
3 published papers: [H8, H9, H13]  
1 invited conference talk
3. **University of Sydney, Australia** – January, 2017 - May, 2019  
8 published papers: [H1–H8]  
5 contributed conference talks and 8 seminar talks

#### Research performed at academic institutions before obtaining the PhD degree:

4. **Imperial College London, UK** – March, 2013 - October, 2016  
9 published papers: [KK5, KK7–KK12] and [H1, H2]  
5 contributed conference and 7 seminar talks
5. **Wrocław University of Science and Technology, Poland** – October, 2009 - July 2012  
5 published papers: [KK1–KK3, KK5, KK7]  
1 contributed conference talk and 2 seminar talks

### 5.2 Scientific papers not included in the habilitation series

During my scientific career, I have published 12 scientific papers in renowned journals that are not included in the habilitation series.

#### Papers outside the habilitation series after obtaining the PhD degree:

1. [KK15] *Fast estimation of outcome probabilities for quantum circuits*  
Hakop Pashayan, Oliver Reardon-Smith, Kamil Korzekwa, Stephen D. Bartlett  
[PRX Quantum](#) **3**, 020361 (2022) [arXiv:2101.12223]  
Pages: 29+13, No ministerial points yet (journal established in 2020), Impact factor: 7.514
2. [KK14] *Work fluctuations due to partial thermalizations in two-level systems*  
Maria Quadeer, Kamil Korzekwa, Marco Tomamichel  
[Phys. Rev. E](#) **103**, 042141 (2021) [arXiv:2101.01330]  
Pages: 16, Points awarded by Ministry of Science and Education: 140, Impact factor: 2.296

#### Papers outside the habilitation series before obtaining the PhD degree:

3. [KK12] *Classical noise and the structure of minimal uncertainty states*  
Kamil Korzekwa, Matteo Lostaglio  
[Phys. Rev. A](#) **93**, 062347 (2016) [arXiv:1602.01850]  
Pages: 14, Points awarded by Ministry of Science and Education: 100, Impact factor: 2.777
4. [KK11] *The extraction of work from quantum coherence*  
Kamil Korzekwa, Matteo Lostaglio, Jonathan Oppenheim, David Jennings  
[New J. Phys.](#) **18**, 023045 (2016) [arXiv:1506.07875]  
Pages: 18, Points awarded by Ministry of Science and Education: 140, Impact factor: 3.539

5. [KK10] *Quantum Coherence, Time-Translation Symmetry, and Thermodynamics*  
Matteo Lostaglio, Kamil Korzekwa, David Jennings, Terry Rudolph  
[Phys. Rev. X \*\*5\*\*, 021001 \(2015\) \[arXiv:1410.4572\]](#)  
Pages: 11, Points awarded by Ministry of Science and Education: 200, Impact factor: 12.577
6. [KK9] *Operational constraints on state-dependent formulations of quantum error-disturbance trade-off relations*  
Kamil Korzekwa, David Jennings, Terry Rudolph  
[Phys. Rev. A \*\*89\*\*, 052108 \(2014\) \[arXiv:1311.5506\]](#)  
Pages: 6, Points awarded by Ministry of Science and Education: 100, Impact factor: 2.777
7. [KK8] *Quantum and classical entropic uncertainty relations*  
Kamil Korzekwa, Matteo Lostaglio, David Jennings, Terry Rudolph  
[Phys. Rev. A \*\*89\*\*, 042122 \(2014\) \[arXiv:1402.1143\]](#)  
Pages: 9, Points awarded by Ministry of Science and Education: 100, Impact factor: 2.777
8. [KK7] *Quantum-state transfer in spin chains via isolated resonance of terminal spins*  
Kamil Korzekwa, Paweł Machnikowski, Paweł Horodecki  
[Phys. Rev. A \*\*89\*\*, 062301 \(2014\) \[arXiv:1403.7359\]](#)  
Pages: 6, Points awarded by Ministry of Science and Education: 100, Impact factor: 2.777
9. [KK5] *Spin dynamics in p-doped semiconductor nanostructures subject to a magnetic field tilted from the Voigt geometry*  
K. Korzekwa, C. Gradl, M. Kugler, S. Furthmeier, M. Griesbeck, M. Hirmer, D. Schuh, W. Wegscheider, T. Kuhn, C. Schüller, T. Korn, P. Machnikowski  
[Phys. Rev. B \*\*88\*\*, 155303 \(2013\) \[arXiv:1306.6363\]](#)  
Pages: 8, Points awarded by Ministry of Science and Education: 140, Impact factor: 3.575
10. [KK3] *Spin dynamics in two-dimensional electron and hole systems revealed by resonant spin amplification*  
T. Korn, M. Griesbeck, M. Kugler, S. Furthmeier, C. Gradl, M. Hirmer, D. Schuh, W. Wegscheider, K. Korzekwa, P. Machnikowski, T. Kuhn, M.M. Glazov, E.Ya. Sherman, C. Schüller  
[Proc. SPIE 8461, Spintronics V, 84610O \(2012\)](#)  
Pages: 12
11. [KK2] *Decoherence-assisted initialization of a resident hole spin polarization in a pp-doped semiconductor quantum well*  
M. Kugler, K. Korzekwa, P. Machnikowski, C. Gradl, S. Furthmeier, M. Griesbeck, M. Hirmer, D. Schuh, W. Wegscheider, T. Kuhn, C. Schüller, T. Korn  
[Phys. Rev. B \*\*84\*\*, 085327 \(2011\) \[arXiv:1105.1338\]](#)  
Pages: 9, Points awarded by Ministry of Science and Education: 140, Impact factor: 3.575
12. [KK1] *Tunneling transfer protocol in a quantum dot chain immune to inhomogeneity*  
Kamil Korzekwa, Paweł Machnikowski  
[Acta Phys. Pol. A, \*\*120\*\*, 859-861 \(2011\) \[arXiv:1108.5749\]](#)  
Pages: 3, Points awarded by Ministry of Science and Education: 40, Impact factor: 0.857

### 5.3 Local and international collaborations

During my scientific career, I have fruitfully collaborated with many researchers from 16 different academic institutions around the world. The list below contains all these institutions and researchers the collaboration with whom resulted in at least one scientific paper published.

#### Collaboration after obtaining the PhD degree:

1. ICFO, The Barcelona Institute of Science and Technology, Barcelona, Spain
  - Dr Matteo Lostaglio: [H2]

2. University of Technology Sydney, Sydney, Australia
    - Prof. Marco Tomamichel: [H4–H6]
    - Dr Maria Quadeer: [KK14]
  3. University of Sydney, Sydney, Australia
    - Prof. Stephen Bartlett: [KK15]
    - Dr Christopher T. Chubb: [H4–H6]
  4. Jagiellonian University, Kraków, Poland
    - Prof. Karol Życzkowski: [H3, H7, H10, H11, H13]
    - Dr Stanisław Czachórski: [H3, H7]
    - Dr Roberto Salazar: [H10]
    - Dr Oliver Reardon-Smith: [KK15]
    - Mr Alexssandre de Oliveira Junior: [H12]
  5. Polish Academy of Sciences
    - Prof. Zbigniew Puchała: [H3, H7, H10, H11, H13]
    - Dr Grzegorz Rajchel-Mieldzióć: [H11]
  6. University of Oxford, Oxford, UK
    - Dr David Jennings: [H8]
    - Dr Cristina Cîrstoiu: [H8]
  7. Delft University of Technology, Delft, Netherlands
    - Dr Matteo Lostaglio: [H9]
  8. University of Gdańsk, Gdańsk, Poland
    - Prof. Paweł Horodecki: [H10]
    - Prof. Michał Horodecki: [H12]
    - Mr Tanmoy Biswas: [H12]
  9. National University of Singapore, Singapore
    - Prof. Marco Tomamichel: [KK14] and [H13]
  10. Perimeter Institute for Theoretical Physics, Waterloo, Canada
    - Dr Hakop Pashayan: [KK15]
  11. University of Amsterdam, Amsterdam, Netherlands
    - Dr Matteo Lostaglio: [H14, H15]
  - 12a. Imperial College London, London, UK
    - Dr Antony Milne: [H2]
- Collaboration before obtaining the PhD degree:**
- 12b. Imperial College London, London, UK
    - Prof. Terry Rudolph: [KK8–KK10]

- Dr David Jennings: [KK8–KK11]
  - Dr Matteo Lostaglio: [KK8–KK12]
13. University College London, London, UK
- Prof. Jonathan Oppenheim: [KK11]
14. Technical University of Gdańsk, Gdańsk, Poland
- Prof. Paweł Horodecki: [KK7]
15. Universität Regensburg, Regensburg, Germany
- Prof. Tobias Korn: [KK2, KK3, KK5]
  - Dr Michael Kugler: [KK2, KK3, KK5]
16. Wrocław University of Science and Technology, Wrocław, Poland
- Prof. Paweł Machnikowski: [KK1–KK3, KK5, KK7]

## 5.4 Talks at conferences and seminars

During my scientific career, I have delivered 44 conference and seminar talks concerning my research in academic institutions in 12 countries.

### Talks after obtaining the PhD degree:

1. *Optimizing thermalizations*

- Conference talk at Quantum Thermodynamics Conference 2022, Belfast, UK (2022)
- Conference talk at 25th Annual Conference on Quantum Information Processing, Pasadena, USA (2022)

2. *Fundamental constraints of quantum thermodynamics in the Markovian regime*

- Invited conference talk at Quantum Optics X, Toruń, Poland (2021)
- Invited seminar talk at UTS Centre for Quantum Software and Information Seminar, Sydney, Australia (2021)

3. *Fast estimation of outcome probabilities for quantum circuits*

- Invited seminar talk at Terhal Group Seminar, QuTech, Delft, Netherlands (2021)

4. *Quantum advantage in simulating stochastic processes*

- Distinguished conference talk at the Annual Ingarden session on Quantum Information, Sopot, Poland (2020)
- Seminar talk at Quantum Information & Chaos Seminar, Jagiellonian University, Kraków, Poland (2020)
- Invited seminar talk at The Quantum and Complexity Science Initiative Seminar, Nanyang Technological University, Singapore (2020)

5. *Encoding classical information in quantum resources*

- Conference talk at CTP Quantum Information Days, Warsaw, Poland (2021)
- Conference talk at Beyond IID in Information Theory 8, Palo Alto, USA (2020)
- Conference talk at 15th Conference on the Theory of Quantum Computation, Communication and Cryptography, Riga, Latvia (2020)

- Seminar talk at Quantum Information & Chaos Seminar, Jagiellonian University, Kraków, Poland (2020)

6. *Classical simulations of quantum circuits*

- Invited seminar talk at International Centre for Theory of Quantum Technologies Seminar, University of Gdańsk, Gdańsk, Poland (2020)
- Seminar talk at Quantum Information & Chaos Seminar, Jagiellonian University, Kraków, Poland (2020)
- Invited seminar talk at Krakow Quantum Informatics Seminar, Krakow, Poland (2020)

7. *Resource-theoretic approach to the thermodynamic arrow of time*

- Invited conference talk at Quantum Information Theory and Mathematical Physics Workshop, Budapest, Hungary (2019)

8. *Avoiding irreversibility: lossless interconversion of quantum resources*

- Invited conference talk at X Jubilee Symposium KCIK, Sopot, Poland (2019)
- Invited seminar talk at Quantum Information & Chaos seminar, Jagiellonian University, Kraków, Poland (2018)
- Conference talk at AIP Congress, Perth, Australia (2018)
- Conference talk at Island Physics Conference, Magnetic Island, Australia (2018)

9. *Beyond the thermodynamic limit*

- Conference talk at Asian Quantum Information Science Conference, Nagoya University, Japan (2018)
- Invited seminar talk at Center for Theoretical Physics seminar, Polish Academy of Sciences, Poland (2017)
- Invited seminar talk at Quantum Information & Chaos seminar, Jagiellonian University, Poland (2017)
- Invited conference talk at Quantum Foundations and Beyond symposium, National Quantum Information Centre, Sopot, Poland (2017)
- Seminar talk at Quantum Science Group seminar, University of Sydney, Australia (2017)

10. *Coherifying quantum states and channels*

- Invited seminar talk at Centre for Quantum Software and Information seminar, University of Technology Sydney, Sydney, Australia (2018)
- Invited seminar talk at Monash Quantum Information Science seminar, Monash University, Melbourne Australia (2018)
- Invited seminar talk at QSciTech Research Group seminar, Macquarie University, Sydney, Australia (2018)

11. *On time evolution of coherences and populations*

- Invited seminar talk at Quantum Information & Chaos seminar, Jagiellonian University, Kraków, Poland (2016)

**Talks before obtaining the PhD degree:**

12. *The extraction of work from quantum coherence*

- Conference talk at Scientific meeting of PhD students, Wrocław University of Science and Technology, Poland (2016)

13. *Quantum information and thermodynamics: a resource-theoretic approach*

- Seminar talk at Quantum Optics and Laser Science Group seminar, Imperial College London, United Kingdom (2016)
- Invited seminar talk at Takahiro Sagawa's Group seminar, University of Tokyo, Japan (2016)
- Invited seminar talk at Quantum Science Group seminar, University of Sydney, Australia (2016)
- Invited seminar talk at Coherence-Correlations-Complexity seminar, Wrocław University of Science and Technology, Poland (2015)

14. *Quantum Coherence, Time-Translation Symmetry, and Thermodynamics*

- Conference talk at APS March Meeting, Baltimore, USA (2016)
- Conference talk at 4th International Workshop on the Optical Properties of Nanostructures, Wrocław, Poland (2016)
- Invited seminar talk at Quantum Information Theory seminar, ICFO Barcelona, Spain (2016)
- Conference talk at Symposium on Quantum Coherence, University of Ulm, Germany (2015)
- Invited seminar talk at Quantum Information Theory seminar, ETH Zurich, Switzerland (2015)
- Conference talk at 7th Colleges of London Quantum Information Meeting, Imperial College London, United Kingdom (2014)

15. *Quantum state transfer via spin chains*

- Invited seminar talk at Coherence-Correlations-Complexity seminar, Wrocław University of Science and Technology, Poland (2013)

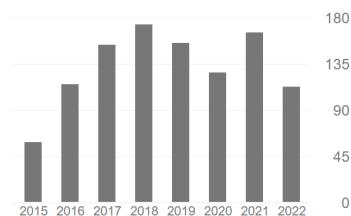
16. *Decoherence-driven mechanism for initialization of hole spins in a p-doped semiconductor quantum well*

- Conference talk at 41st "Jaszowiec" International School & Conference on the Physics of Semiconductors, Krynica-Zdrój, Poland (2012)
- Invited seminar talk at Optical Spectroscopy of Semiconductor Quantum Structures seminar, Universität Regensburg, Germany (2011)
- Seminar talk at Coherence-Correlations-Complexity seminar, Wrocław University of Science and Technology, Poland (2011)

## 5.5 Bibliometric data

Google Scholar (21 July 2022):

- Total number of citations: 1100
- H-index: 12
- Citations over the years:



Web of Science (21 July 2022):

- Total number of citations: 722 (689 excluding self-citations)
- H-index: 10

## 6 Teaching, organizational and ‘popularization of science’ achievements

### 6.1 Teaching achievements

#### Academic teaching:

- **Teaching assistant, University of Sydney** – January, 2018 - February 2018  
Short lecture series on: *Quantum Spookiness* (2nd year undergraduate course)
- **Teaching assistant, Imperial College London** – October, 2014 - December 2014  
Tutorials on: *Mathematics: Functions* (1st year undergraduate course)

#### Invited lectures:

- **University of Wrocław** – November, 2016  
Short lecture series on: *Introduction to Quantum Information Theory* (for graduate students)

#### Supervision:

- **Supervision of an intern student** – August, 2021 - September, 2021  
Student: Michał Piotrak  
University: Imperial College London  
Project title: *Optimal quantum protractor*
- **Co-supervision of a PhD student** – November, 2020 - present  
PhD student: Tanmoy Biswas  
University: University of Gdańsk  
PhD thesis: *Finite-size effects in quantum thermodynamics*
- **Co-supervision of a PhD student** – March, 2020 - present  
PhD student: Alexssandre de Oliveira Junior  
University: Jagiellonian University  
PhD thesis: *Geometric and information-theoretic aspects of quantum thermodynamics*
- **Supervision of a Bachelor’s student** – October, 2020 - present  
Student: Piotr Przedwojski  
University: Jagiellonian University  
Bachelor’s thesis: *Asymmetrising quantum states and channels*
- **Co-supervision of an Honours student** – February, 2017 - October, 2017  
Student: Taiga Adair  
University: University of Sydney  
Honours thesis: *Measurement-Based Quantum Computation with a Foliated Colour Code*
- **Supervision of a Bachelor’s student** – March, 2017 - June, 2017  
Student: Matthew Winnel  
University: University of Sydney  
Senior’s project: *Exploring the thermodynamic arrow of time for low-dimensional quantum systems*
- **Co-supervision of a Master’s student** – November, 2014 - May, 2015  
Student: Sofia Qvarfort  
University: Imperial College London  
MSc Thesis: *A Resource-Theoretical Approach to Time-Energy Measurements in Quantum Mechanics*

## 6.2 Organisational achievements

- **Organiser of the weekly JQI Team arXiv Review seminars** – March, 2022 - June, 2022
- **Co-organiser of the JQI Team Gorce Workshop** – July, 2021
- **Organiser of the weekly JQI Team Meeting seminars** – February, 2021 - June, 2021
- **Referee of the PhD thesis and PhD examiner** – September, 2020  
Title of the PhD thesis: *The Structure and Manipulation of Resources in Quantum Information Theory*  
PhD student: Thomas Hebdige  
University: Imperial College London, London, United Kingdom
- **Head of the Quantum Resources research group** – October, 2019 - present  
Leading the research group consisting of 3 post-doctoral researchers and 1 PhD student
- **Evaluation Expert for the National Science Centre** – March, 2018  
Assessed the application for *Preludium* grant.
- **Active referee for conference submissions** – 2017 - present  
Refereed for:
  - Quantum Information Processing (4 reviews)
  - Theory of Quantum Computation, Communication and Cryptography (4 reviews)
  - IEEE Information Theory Workshop (1 review)
- **Active referee for multiple journals** – 2014 - present  
Refereed for:
  - Physical Review A (17 reviews)
  - Physical Review E (1 review)
  - Physical Review Letters (5 reviews)
  - PRX Quantum (2 reviews)
  - Nature Physics (1 review)
  - Journal of Physics A (1 review)
  - New Journal of Physics (1 review)
  - Entropy (1 review)
  - Quantum (8 reviews)
  - IEEE Transactions on Information Theory (1 review)All reviews can be verified at <https://publons.com/researcher/1425073/kamil-korzekwa>
- **Co-organiser of the QUICC Summer School** – August, 2013

## 6.3 Popularisation of science achievements

- **Article covered in the *Physics Viewpoint*** – July, 2022  
Results from [H15] described for a broader audience in a magazine from the American Physical Society focusing on important results from the Physical Review journals
- **Featured in the national newspaper *The Sydney Morning Herald*** – December, 2017  
Article promoting the activities of Quantum Science Research Group at the University of Sydney
- **Article covered in the *Physics Viewpoint*** – November, 2015  
Results from [KK10] described for a broader audience in a magazine from the American Physical Society focusing on important results from the Physical Review journals
- **Outreach activities during *The Imperial Festival*** – May, 2014
- **Outreach activities during *The Amazing Quantum World* show** – May, 2013

## 7 Other scientific achievements

### 7.1 Awards and scholarships

- Scholarship of the Polish Ministry of Science and Higher Education for outstanding young scientists – September, 2020
- Wrocław University of Science and Technology Medal for best graduate student – July, 2012
- Engineering and Physical Sciences Research Council MRes and PhD scholarship – April, 2012
- Scottish Universities Physics Alliance Prize PhD scholarship – April, 2012 (declined)
- Diamond Grant PhD scholarship – March, 2012 (declined)
- Polish Ministry of Science and Higher Education scholarship – October, 2011 - June, 2012
- Foundation for Polish Science TEAM programme MSc scholarship – October, 2010 - June 2012

### 7.2 Distinguished papers

- Presentation of the results from papers [H14, H15] given the Best Early-Career Researcher Talk Prize at the Quantum Thermodynamics 2022 Conference.
- Paper [H15] selected by the editors of Physical Review Letters to be an Editors' Suggestion and featured in Physics Viewpoint
- Paper [H14] selected by the editors of Physical Review A to be an Editors' Suggestion
- Paper [H10] selected by the editors of Physical Review A to be an Editors' Suggestion
- Paper [KK11] chosen by the editors of New Journal of Physics to be among the Highlights of 2016
- Paper [KK10] chosen as a seminal paper ten years after establishing Physical Review X, and also featured in Physics Viewpoint
- Paper [KK5] selected by the editors of Physical Review B to be an Editors' Suggestion

## References: Papers in the applicant's series

- [H1] K. Korzekwa, “Structure of the thermodynamic arrow of time in classical and quantum theories,” *Phys. Rev. A* **95**, 052318 (2017).
- [H2] M. Lostaglio, K. Korzekwa, and A. Milne, “Markovian evolution of quantum coherence under symmetric dynamics,” *Phys. Rev. A* **96**, 032109 (2017).
- [H3] K. Korzekwa, S. Czachórski, Z. Puchała, and K. Życzkowski, “Coherifying quantum channels,” *New J. Phys.* **20**, 043028 (2018).
- [H4] C. T. Chubb, M. Tomamichel, and K. Korzekwa, “Beyond the thermodynamic limit: finite-size corrections to state interconversion rates,” *Quantum* **2**, 108 (2018).
- [H5] C. T. Chubb, M. Tomamichel, and K. Korzekwa, “Moderate deviation analysis of majorization-based resource interconversion,” *Phys. Rev. A* **99**, 032332 (2019).
- [H6] K. Korzekwa, C. T. Chubb, and M. Tomamichel, “Avoiding irreversibility: Engineering resonant conversions of quantum resources,” *Phys. Rev. Lett.* **122**, 110403 (2019).
- [H7] K. Korzekwa, S. Czachórski, Z. Puchała, and K. Życzkowski, “Distinguishing classically indistinguishable states and channels,” *J. Phys. A: Math. Theor.* **52**, 475303 (2019).
- [H8] C. Cirstoiu, K. Korzekwa, and D. Jennings, “Robustness of Noether’s principle: Maximal disconnects between conservation laws and symmetries in quantum theory,” *Phys. Rev. X* **10**, 041035 (2020).
- [H9] K. Korzekwa and M. Lostaglio, “Quantum advantage in simulating stochastic processes,” *Phys. Rev. X* **11**, 021019 (2021).
- [H10] Z. Puchała, K. Korzekwa, R. Salazar, P. Horodecki, and K. Życzkowski, “Dephasing superchannels,” *Phys. Rev. A* **104**, 052611 (2021).
- [H11] G. Rajchel-Międzyoć, K. Korzekwa, Z. Puchała, and K. Życzkowski, “Algebraic and geometric structures inside the Birkhoff polytope,” *J. Math. Phys.* **63**, 012202 (2022).
- [H12] T. Biswas, A. Junior, M. Horodecki, and K. Korzekwa, “Fluctuation-dissipation relations for thermodynamic distillation processes,” *Phys. Rev. E* **105**, 054127 (2022).
- [H13] K. Korzekwa, Z. Puchała, M. Tomamichel, and K. Życzkowski, “Encoding classical information into quantum resources,” *IEEE Trans. Inf. Theory* **68**, 4518 (2022).
- [H14] M. Lostaglio and K. Korzekwa, “Continuous thermomajorization and a complete set of laws for Markovian thermal processes,” *Phys. Rev. A* **106**, 012426 (2022).
- [H15] K. Korzekwa and M. Lostaglio, “Optimizing thermalizations,” *Phys. Rev. Lett.* **129**, 040602 (2022)

## References: Papers by the applicant not in the series

- [KK1] K. Korzekwa and P. Machnikowski, “Tunneling transfer protocol in a quantum dot chain immune to inhomogeneity,” *Acta Phys. Pol. A* **120**, 859–861 (2011).
- [KK2] M. Kugler, K. Korzekwa, P. Machnikowski, C. Gradl, S. Furthmeier, M. Griesbeck, M. Hirmer, D. Schuh, W. Wegscheider, T. Kuhn, *et al.*, “Decoherence-assisted initialization of a resident hole spin polarization in a p-doped semiconductor quantum well,” *Phys. Rev. B* **84**, 085327 (2011).
- [KK3] T. Korn, M. Griesbeck, M. Kugler, S. Furthmeier, C. Gradl, M. Hirmer, D. Schuh, W. Wegscheider, K. Korzekwa, P. Machnikowski, *et al.*, “Spin dynamics in two-dimensional electron and hole systems revealed by resonant spin amplification,” in *Spintronics V*, Vol. 8461 (International Society for Optics and Photonics, 2012) p. 84610O.

- [KK4] K. Korzekwa, *Magneto-optical Kerr effect and resonant spin amplification*, [Master's thesis](#), Wrocław University of Technology (2012).
- [KK5] K. Korzekwa, C. Gradl, M. Kugler, S. Furthmeier, M. Griesbeck, M. Hirmer, D. Schuh, W. Wegscheider, T. Kuhn, C. Schueller, *et al.*, “Spin dynamics in p-doped semiconductor nanostructures subject to a magnetic field tilted from the Voigt geometry,” [Phys. Rev. B](#) **88**, 155303 (2013).
- [KK6] K. Korzekwa, *Resource theory of asymmetry*, [Master's thesis](#), Imperial College London (2013).
- [KK7] K. Korzekwa, P. Machnikowski, and P. Horodecki, “Quantum-state transfer in spin chains via isolated resonance of terminal spins,” [Physical Review A](#) **89**, 062301 (2014).
- [KK8] K. Korzekwa, M. Lostaglio, D. Jennings, and T. Rudolph, “Quantum and classical entropic uncertainty relations,” [Phys. Rev. A](#) **89**, 042122 (2014).
- [KK9] K. Korzekwa, D. Jennings, and T. Rudolph, “Operational constraints on state-dependent formulations of quantum error-disturbance trade-off relations,” [Phys. Rev. A](#) **89**, 052108 (2014).
- [KK10] M. Lostaglio, K. Korzekwa, D. Jennings, and T. Rudolph, “Quantum coherence, time-translation symmetry, and thermodynamics,” [Phys. Rev. X](#) **5**, 021001 (2015).
- [KK11] K. Korzekwa, M. Lostaglio, J. Oppenheim, and D. Jennings, “The extraction of work from quantum coherence,” [New J. Phys.](#) **18**, 023045 (2016).
- [KK12] K. Korzekwa and M. Lostaglio, “Classical noise and the structure of minimum uncertainty states,” [Phys. Rev. A](#) **93**, 062347 (2016).
- [KK13] K. Korzekwa, *Coherence, thermodynamics and uncertainty relations*, [Ph.D. thesis](#), Imperial College London (2016).
- [KK14] M. Quadeer, K. Korzekwa, and M. Tomamichel, “Work fluctuations due to partial thermalizations in two-level systems,” [Phys. Rev. E](#) **103**, 042141 (2021).
- [KK15] H. Pashayan, O. Reardon-Smith, K. Korzekwa, and S. D. Bartlett, “Fast estimation of outcome probabilities for quantum circuits,” [PRX Quantum](#) **xxx**, xxx (2022)

## References: External

- [1] A. Eddington, *The nature of the physical world: The Gifford lectures 1927* (Cambridge University Press, 1930).
- [2] K. Huang, *Statistical Mechanics* (John Wiley & Sons, 2008).
- [3] R. Horodecki, P. Horodecki, M. Horodecki, and K. Horodecki, [Rev. Mod. Phys.](#) **81**, 865 (2009).
- [4] C. H. Bennett, H. J. Bernstein, S. Popescu, and B. Schumacher, [Phys. Rev. A](#) **53**, 2046 (1996).
- [5] M. A. Nielsen, [Phys. Rev. Lett.](#) **83**, 436 (1999).
- [6] C. H. Bennett, G. Brassard, C. Crépeau, R. Jozsa, A. Peres, and W. K. Wootters, [Phys. Rev. Lett.](#) **70**, 1895 (1993).
- [7] C. H. Bennett, G. Brassard, S. Popescu, B. Schumacher, J. A. Smolin, and W. K. Wootters, [Phys. Rev. Lett.](#) **76**, 722 (1996).
- [8] J. C. Maxwell, *Theory of Heat* (Longmans, Green and Co., 1873).
- [9] L. Szilard, [Z. Phys.](#) **53**, 840 (1929).
- [10] R. Landauer, [IBM J. Res. Dev.](#) **5**, 183 (1961).

- [11] C. H. Bennett and G. Brassard, in *Proceedings of IEEE International Conference on Computers, Systems and Signal Processing*, Vol. 175 (1984) p. 8.
- [12] A. Ekert, *Phys. Rev. Lett.* **67**, 661 (1991).
- [13] P. W. Shor, in *Proceedings 35th annual symposium on foundations of computer science* (IEEE, 1994) pp. 124–134.
- [14] L. K. Grover, in *Proceedings of the twenty-eighth annual ACM symposium on Theory of computing* (1996) pp. 212–219.
- [15] M. Horodecki and J. Oppenheim, *Int. J. Mod. Phys. B* **27**, 1345019 (2013).
- [16] E. Chitambar and G. Gour, *Rev. Mod. Phys.* **91**, 025001 (2019).
- [17] M. Horodecki and J. Oppenheim, *Nat. Commun.* **4**, 2059 (2013).
- [18] F. G. S. L. Brandão, M. Horodecki, J. Oppenheim, J. M. Renes, and R. W. Spekkens, *Phys. Rev. Lett.* **111**, 250404 (2013).
- [19] V. Gorini, A. Kossakowski, and E. C. G. Sudarshan, *J. Math. Phys.* **17**, 821 (1976).
- [20] G. Lindblad, *Commun. Math. Phys.* **48**, 119 (1976).
- [21] H.-P. Breuer and F. Petruccione, *The theory of open quantum systems* (Oxford University Press, 2002).
- [22] F. G. S. L. Brandão, M. Horodecki, N. H. Y. Ng, J. Oppenheim, and S. Wehner, *Proc. Natl. Acad. Sci. U.S.A.* **112**, 3275 (2015).
- [23] E. Noether, Nachrichten von der Gesellschaft der Wissenschaften zu Göttingen, Mathematisch-Physikalische Klasse **1918**, 235 (1918).
- [24] I. Marvian, *Symmetry, Asymmetry and Quantum Information*, Ph.D. thesis, University of Waterloo. (2012).
- [25] S. D. Bartlett, T. Rudolph, and R. W. Spekkens, *Rev. Mod. Phys.* **79**, 555 (2007).
- [26] J. Goold, M. Huber, A. Riera, L. del Rio, and P. Skrzypczyk, *J. Phys. A* **49**, 143001 (2016).
- [27] D. Janzing, P. Wocjan, R. Zeier, R. Geiss, and T. Beth, *Int. J. Theor. Phys.* **39**, 2717 (2000).
- [28] J. Åberg, *Phys. Rev. Lett.* **113**, 150402 (2014).
- [29] M. Lostaglio, D. Jennings, and T. Rudolph, *Nat. Commun.* **6**, 6383 (2015).
- [30] P. Ćwikliński, M. Studziński, M. Horodecki, and J. Oppenheim, *Phys. Rev. Lett.* **115**, 210403 (2015).
- [31] R. Uzdin, A. Levy, and R. Kosloff, *Phys. Rev. X* **5**, 031044 (2015).
- [32] R. Alicki and M. Fannes, *Phys. Rev. E* **87**, 042123 (2013).
- [33] M. Perarnau-Llobet, K. V. Hovhannisyanyan, M. Huber, P. Skrzypczyk, N. Brunner, and A. Acín, *Phys. Rev. X* **5**, 041011 (2015).
- [34] J. B. Brask, G. Haack, N. Brunner, and M. Huber, *New J. Phys.* **17**, 113029 (2015).
- [35] A. Uhlmann, *Ann. Phys. (N. Y.)* **497**, 524 (1985).
- [36] H. Umegaki, *Kodai Math. Sem. Rep.* **14**, 59 (1962).
- [37] M. Tomamichel and M. Hayashi, *IEEE Trans. Inf. Theory* **59**, 7693 (2013).
- [38] K. Li, *Ann. Stat.* **42**, 171 (2014).

- [39] W. Kumagai and M. Hayashi, *IEEE Trans. Inf. Theory* **63**, 1829 (2017).
- [40] G. Vidal, D. Jonathan, and M. Nielsen, *Phys. Rev. A* **62**, 012304 (2000).
- [41] V. Strassen, in *Trans. Third Prague Conf. Inf. Theory* (Prague, 1962) pp. 689–723.
- [42] Y. Altug and A. B. Wagner, *IEEE Trans. Inf. Theory* **60**, 4417 (2014).
- [43] T. Baumgratz, M. Cramer, and M. Plenio, *Phys. Rev. Lett.* **113**, 140401 (2014).
- [44] S. Du, Z. Bai, and Y. Guo, *Phys. Rev. A* **91**, 052120 (2015).
- [45] M. Hayashi, *IEEE Trans. Inf. Theory* **54**, 4619 (2008).
- [46] J. Åberg, *Nat. Commun.* **4**, 1925 (2013).
- [47] N. H. Y. Ng, M. P. Woods, and S. Wehner, *New J. Phys.* **19**, 113005 (2017).
- [48] R. Kubo, *Rep. Prog. Phys.* **29**, 255 (1966).
- [49] M. V. S. Bonança, *Phys. Rev. E* **78**, 031107 (2008).
- [50] A. Einstein, *Ann. Phys.* **324**, 371 (1906).
- [51] M. von Smoluchowski, *Ann. Phys.* **326**, 756 (1906).
- [52] B. A. Davey and H. A. Priestley, *Introduction to lattices and order* (Cambridge university press, 2002).
- [53] R. Kosloff, *Entropy* **15**, 2100 (2013).
- [54] R. Alicki and R. Kosloff, “Introduction to quantum thermodynamics: History and prospects,” in *Thermodynamics in the Quantum Regime: Fundamental Aspects and New Directions*, edited by F. Binder, L. A. Correa, C. Gogolin, J. Anders, and G. Adesso (Springer International Publishing, Cham, 2018) pp. 1–33.
- [55] E. T. Campbell, B. M. Terhal, and C. Vuillot, *Nature* **549**, 172 (2017).
- [56] J. Klatzow, J. N. Becker, P. M. Ledingham, C. Weinzetl, K. T. Kaczmarek, D. J. Saunders, J. Nunn, I. A. Walmsley, R. Uzdin, and E. Poem, *Phys. Rev. Lett.* **122**, 110601 (2019).
- [57] E. B. Davies, *Commun. Math. Phys.* **39**, 91 (1974).
- [58] W. Roga, M. Fannes, and K. Życzkowski, *Rep. Math. Phys.* **66**, 311 (2010).
- [59] V. Scarani, M. Ziman, P. Štelmachovič, N. Gisin, and V. Bužek, *Phys. Rev. Lett.* **88**, 097905 (2002).
- [60] C. Perry, P. Źwikliński, J. Anders, M. Horodecki, and J. Oppenheim, *Phys. Rev. X* **8**, 041049 (2018).
- [61] E. Bäumer, M. Perarnau-Llobet, P. Kammerlander, H. Wilming, and R. Renner, *Quantum* **3**, 153 (2019).
- [62] H. J. Miller, M. Scandi, J. Anders, and M. Perarnau-Llobet, *Phys. Rev. Lett.* **123**, 230603 (2019).
- [63] K. Korzekwa, *Continuous thermomajorisation* (2021), [github.com/KorzekwaKamil/continuous\\_thermomajorisation](https://github.com/KorzekwaKamil/continuous_thermomajorisation).
- [64] L. J. Schulman and U. V. Vazirani, in *Proceedings of the thirty-first annual ACM symposium on Theory of computing* (ACM, 1999) pp. 322–329.
- [65] P. O. Boykin, T. Mor, V. Roychowdhury, F. Vatan, and R. Vrijen, *Proc. Natl. Acad. Sci. U.S.A* **99**, 3388 (2002).
- [66] N. A. Rodríguez-Briones and R. Laflamme, *Phys. Rev. Lett.* **116**, 170501 (2016).
- [67] S. Raeisi and M. Mosca, *Phys. Rev. Lett.* **114**, 100404 (2015).

- [68] N. A. Rodríguez-Briones, *Novel Heat-Bath Algorithmic Cooling methods*, Ph.D. thesis, University of Waterloo (2020).
- [69] L. J. Schulman, T. Mor, and Y. Weinstein, *Phys. Rev. Lett.* **94**, 120501 (2005).
- [70] N. A. Rodríguez-Briones, J. Li, X. Peng, T. Mor, Y. Weinstein, and R. Laflamme, *New J. Phys.* **19**, 113047 (2017).
- [71] J. G. Richens and L. Masanes, *Nat. Commun.* **7**, 1 (2016).
- [72] M. Perarnau-Llobet and R. Uzdin, *New J. Phys.* **21**, 083023 (2019).
- [73] F. G. S. L. Brandão, M. Horodecki, N. H. Y. Ng, J. Oppenheim, and S. Wehner, *Proc. Natl. Acad. Sci. U.S.A.* **112**, 3275 (2015).
- [74] N. H. Y. Ng, L. Mančinska, C. Cirstoiu, J. Eisert, and S. Wehner, *New J. Phys.* **17**, 085004 (2015).
- [75] P. Lipka-Bartosik and P. Skrzypczyk, *Phys. Rev. X* **11**, 011061 (2021).
- [76] Á. M. Alhambra, M. Lostaglio, and C. Perry, *Quantum* **3**, 188 (2019).
- [77] H. Wilming, R. Gallego, and J. Eisert, *Phys. Rev. E* **93**, 042126 (2016).
- [78] A. Polkovnikov, *Ann. Phys.* **326**, 486 (2011).
- [79] J. P. Santos, L. C. Céleri, G. T. Landi, and M. Paternostro, *npj Quantum Inf.* **5**, 1 (2019).
- [80] A. Rényi, in *Fourth Berkeley Symposium on Mathematical Statistics and Probability* (1961) pp. 547–561.
- [81] C. Tsallis, *J. Stat. Phys.* **52**, 479 (1988).
- [82] S. Abe, *Phys. Lett. A* **271**, 74 (2000).
- [83] C. Tsallis, *Introduction to nonextensive statistical mechanics: approaching a complex world* (Springer Science & Business Media, 2009).
- [84] A. M. Mariz, *Phys. Lett. A* **165**, 409 (1992).
- [85] H. Wilming and R. Gallego, *Phys. Rev. X* **7**, 041033 (2017).
- [86] E. B. Davies, *Electron. J. Probab.* **15**, 1474 (2010).
- [87] G. Elfving, *Acta Soc. Sci. Fennicae, n. Ser. A2* **8**, 1 (1937).
- [88] J. F. C. Kingman, *Probab. Theory Relat. Fields* **1**, 14 (1962).
- [89] J. T. Runnenburg, *P. K. Ned. Akad. A Math* **65**, 536 (1962).
- [90] G. S. Goodman, *Probab. Theory Relat. Fields* **16**, 165 (1970).
- [91] P. Carette, *New York J. Math* **1**, 129 (1995).
- [92] M. M. Wolf, J. Eisert, T. S. Cubitt, and J. I. Cirac, *Phys. Rev. Lett.* **101**, 150402 (2008).
- [93] I. Bengtsson, *arXiv quant-ph/0403088* (2004).
- [94] I. Bengtsson, Å. Ericsson, M. Kuś, W. Tadej, and K. Życzkowski, *Commun. Math. Phys.* **259**, 307 (2005).
- [95] Y.-T. Poon and N.-K. Tsing, *Linear Multilinear A.* **21**, 253 (1987).
- [96] P. Lencastre, F. Rauschel, T. Rogers, and P. G. Lind, *Phys. Rev. E* **93**, 032135 (2016).
- [97] D. H. Wolpert, A. Kolchinsky, and J. A. Owen, *Nat. Commun.* **10**, 1 (2019).

- [98] P. Taranto, F. Bakhshinezhad, P. Schüttelkopf, F. Clivaz, and M. Huber, *Phys. Rev. Appl.* **14**, 054005 (2020).
- [99] G. Gour and R. W. Spekkens, *New J. Phys.* **10**, 033023 (2008).
- [100] I. Marvian and R. W. Spekkens, *Phys. Rev. A* **94**, 052324 (2016).
- [101] I. Marvian and R. W. Spekkens, *Phys. Rev. A* **90**, 062110 (2014).
- [102] C. Fleming, N. I. Cummings, C. Anastopoulos, and B. L. Hu, *J. Phys. A* **43**, 405304 (2010).
- [103] M. Keyl and R. F. Werner, *J. Math. Phys.* **40**, 3283 (1999).
- [104] T. R. Bromley, M. Cianciaruso, and G. Adesso, *Phys. Rev. Lett.* **114**, 210401 (2015).
- [105] I. A. Silva, A. M. Souza, T. R. Bromley, M. Cianciaruso, R. Marx, R. S. Sarthour, I. S. Oliveira, R. Lo Franco, S. J. Glaser, E. R. deAzevedo, D. O. Soares-Pinto, and G. Adesso, *Phys. Rev. Lett.* **117**, 160402 (2016).
- [106] J. C. Baez and B. Fong, *J. Math. Phys.* **54**, 013301 (2013).
- [107] J. E. Gough, T. S. Ratiu, and O. G. Smolyanov, *J. Math. Phys.* **56**, 022108 (2015).
- [108] J. Wallman, C. Granade, R. Harper, and S. T. Flammia, *New J. Phys.* **17**, 113020 (2015).
- [109] C. H. Bennett and S. J. Wiesner, *Phys. Rev. Lett.* **69**, 2881 (1992).
- [110] S.-H. Kye, *Linear Algebra Appl.* **216**, 239 (1995).
- [111] M. Hayashi and H. Nagaoka, *IEEE Trans. Inf. Theory* **49**, 1753 (2003).
- [112] S. D. Bartlett, T. Rudolph, and R. W. Spekkens, *Phys. Rev. A* **70**, 032307 (2004).
- [113] A. Jamiołkowski, *Rep. Math. Phys.* **3**, 275 (1972).
- [114] P. Pakoński, K. Życzkowski, and M. Kuś, *J. Phys. A* **34**, 9303 (2001).
- [115] P. Pakoński, G. Tanner, and K. Życzkowski, *J. Stat. Phys.* **111**, 1331 (2003).
- [116] A. Ambainis, *Int. J. Quantum Inf* **01**, 507 (2003).
- [117] A. Postnikov, *Int. Math. Res. Notices* **2009**, 1026 (2009).
- [118] L. Mandelstam and I. G. Tamm, in *Selected Papers* (Springer, 1991) pp. 115–123.
- [119] P. J. Coles, V. Katariya, S. Lloyd, I. Marvian, and M. M. Wilde, *Phys. Rev. Lett.* **122**, 100401 (2019).
- [120] I. Devetak and P. W. Shor, *Commun. Math. Phys.* **256**, 287 (2005).
- [121] G. Chiribella, G. M. D’Ariano, and P. Perinotti, *EPL* **83**, 30004 (2008).
- [122] A. Mani and V. Karimipour, *Phys. Rev. A* **92**, 032331 (2015).
- [123] G. Gour, *IEEE Trans. Inf. Theory* **65**, 5880 (2019)